

Université Pierre et Marie Curie

École Doctorale Cerveau Cognition et Comportement  
Inserm-CEA Unicog, NeuroSpin

---

# CHARACTERIZING THE NEUROCOGNITIVE MECHANISMS OF ARITHMETIC

---

Pedro PINHEIRO-CHAGAS

Dissertation submitted for the degree of  
Doctor of Philosophy

Supervised by Stanislas DEHAENE  
Co-supervised by Manuela PIAZZA

Publicly defended on the 29<sup>th</sup> of November 2017

Jury:

Wim FIAS	Ghent University	Reviewer
Christian BÉNAR	Aix-Marseille University	Reviewer
Lionel NACCACHE	Pierre et Marie Curie University	Examiner
Elizabeth SPELKE	Harvard University	Examiner
Manuela PIAZZA	Trento University	Co-supervisor
Stanislas DEHAENE	Collège de France	Supervisor



## ACKNOWLEDGMENTS

---

I had the great fortune to work with Stanislas Dehaene. His brilliant, creative and extremely precise thinking were invaluable to help me sculpting my ideas and translating them into experiments or data analyses. He gave me all the resources I needed to use any method I wanted, with virtually unlimited funding - also thanks to the remarkable infra-structure of NeuroSpin. By observing his passion in producing cutting-edge science, I learned several key aspects of scientific writing and management. Most of all, I thank him for our thrilling weekly meetings, during which he shared with me his vast knowledge and translucent introspection: the necessary building blocks to create a science of mental life.

I also warmly thank my co-supervisor Manuela Piazza for receiving me in the lab. Her exigence and sharpness guided my first steps towards finding original research questions. She gave me important opportunities to develop my scientific skills, notably reviewing articles and teaching at the University of Trento.

Working with a very close friend is simply delightful. Thanks to Dror Dotan, I had the chance to enjoy this experience during my entire PhD. With his extraordinary generosity, methodic reasoning and constant support, he showed me how to express my thoughts into lines of code and helped me coping with some of the critical stages of my scientific development.

I am profoundly honored to have a group of such brilliant scientists who accepted to read, review and discuss my dissertation. Wim Fias, Christian Bénar, Lionel Naccache and Elizabeth Spelke: you have my eternal gratitude.

A PhD requires a great deal of administration and logistics. I thank the witty Vanna Santoro for artistically managing my unusual working contracts and Laurence Labruna for organizing my trips. I also thank the NeuroSpin nurses and Isabelle Brunet from the École Normale Supériore for helping me recruiting and preparing the volunteers, as well as Marco Buiatti and Leila Azizi for the MEG technical support.

I had the privilege to work in a very intellectually stimulant environment, where I met a group of exceptional scientists, who became close friends and colleagues. Special thanks to Fosca Al Roumi for our beautiful friendship, for blossoming the lab, organizing epic barbecue parties and driving me around on her powerful BMW; Valentina Borghesani for her admirable

philanthropism and for bringing me to her tasty San Giovanni in Persiceto; Lola de Hevia for sharing my obsessions with food and cinema; Yi-Chen Lin for her gentleness, delicious cooking and precious *oolong*; Aina Frau for the companionship and impeccable *sobrassada*; Liping Wang for the double spicy dinners and for having the happiest smile on Earth; Ramon Guevara for mastering the art of storytelling; Michael Eickenberg for the brewing and the stimulating discussions about virtually everything; Fabian Pedregosa for the *jamón de bellota* and scikit-learn; Pablo Barttfeld for his kindness, Matlab support and for the bike; Maxime Maheu for his magnificent scientific art and precocious knowledge; Lucie Berkovitch for always end up discussing about the greatest thing in life; Darinka Trübutschek for sharing so many codes and always be willing to listen; Elisa Castaldi for teaching me all about mushrooms; Evelyn Eger for her precise feedback and love of Brazilian music; François Leroy for making the RER B a better place; Mainak Jas and Yousra Bekhti for the MNE-Python and machine learning support; Marco Buiatti and Sébastien Marti for teaching me so many things about MEG; Benoît Larrat for the late night rides; Chantal Ginisty for being magnetically adorable; Isabelle Denghien for helping me boosting the speed of my data analyses with the cluster; Marie Almaric for the future jam sessions; Andrés Hoyos Idrobo and Elvis Dohmatob for being great ping-pong apprentices and Python gurus; Timo van Kerkoerle for his enthusiasm; Ana Fló for her calm; Milad Ekramnia for his passion; Lina Teichmann who came all the way from Australia just to cheer me up; and to all the other members of the Unicog and Parietal teams at NeuroSpin.

Half away through my PhD, Stan introduced me to the unique Josef Parvizi and we started an amazing and successful collaboration that fortunately is going to continue during my postdoc. I thank Josef for receiving me in his lab at Stanford University in such an enthusiastic way and for giving me complete freedom to explore the incredible universe of intracranial recordings in humans. I also thank his postdoc and now my friend and collaborator Amy Daitch for her support and for teaching me the *crème de la crème* of the American slangs. I cannot wait to join their lab!

Science is a fundamentally social activity, in which debate plays a central role. I was lucky to be selected to attend for three times the coolest possible scientific area: the Latin American School for Education, Cognitive and Neural Sciences. I thank John Bruer and Susan Fitzpatrick from the James S. McDonnell Foundation and the organizers Sidarta Ribeiro, Marcela Peña and Mariano Sigman for making this event possible. It was during my first school, when it was held in the astonishing Patagonia, that I met Stan, and one year later I joined his lab. In the beaches

of Punta del Este and around the geysers of the Atacama Desert, I met a group of incredible scientists who instantly became very good friends and helped me never forgetting the lyrics of my favorite Brazilian songs as well as the bigger picture of my research program. Special thanks to Marcela Perrone-Bertolotti and our *casita*; Marie Lallier for being so lovely; Justin Halberda, Mitch Nathan and Mariano for the guitar; Camila Zugarramurdi and Sidarta for the voice; Natália Mota for the pandeiro; and the amazing Julia Leonard. Julia, thank you for all the beautiful moments that we spent together all over the world. I grew so much around you. Your intelligence, unlimited energy and humor keep blowing my mind.

Investment in science should be a priority in all countries. Thanks to the innovative program *Science Without Borders* launched by Dilma Rousseff and now sadly extinguished by her illegitimate successor, me and thousands of young Brazilian scientists were awarded with a full PhD scholarship to study abroad. I thank the CNPq for flawlessly implementing and managing my contract. I would also like to express my gratitude to the following institutions that funded my research: Inserm, CEA, Bettencourt Schueller Foundation, Collège de France, Stanford University and the NIMH, as well as all the volunteers who participated in my experiments.

Nobody can properly work with hunger and thirst. For feeding my body and soul, I thank Patrick Roger pour son Equateur 85%; Axelle de *La Felicité*, Thomas de *L'établi* et Marina de *Paris Terroirs* pour m'avoir ouvert l'univers du *vin nature*; Cécile de *Brewberry* pour avoir apporté des bières artisanales scandinaves dans le 5ème; Hugo Desnoyer pour ses *ris de veau* exquis et sa *côte de boeuf* maturée; Androuet pour leur *vacherin fribourgeois*; Maison Morange pour leur baguette sortie du four; les producteurs du Marché Monge pour leurs légumes et leurs huîtres fraîches; l'équipe de l'Abri pour leurs chaleureux sourire et *soba*, et tant d'autres...

Many thanks to my dearest friends Ricardo Lins Horta, Júlia Goyatá, Lucas Cunha, Luisa Reis Castro, Daniel Gonzaga, Gabriel Malheiros, Maria Chiaretti, Alesia and Valentina Giura, Júlia D'Almeida, Thiago Pedroso, Mariana Camargo, Fernando Mistura, Los Amigos...

Bruno, Laure, Edith, Inès, Guy, Henri and the Sá Moreiras: thank you for everything.

My dearest thanks to my parents, grandparents, Pat, Mateus and Régis for their unconditional support and enthusiasm.

Milena, merci por seu amor absoluto, pela paciência, compreensão e apoio nesses últimos meses de escrita, por compartilhar seus incríveis e inúmeros talentos, pelos belíssimos recitais particulares, pelo gamão, pour l'Alain Rey, pour Morgat e pelo nosso querido gorila Kundurwanda!

*To my parents,*



## ABSTRACT

---

How are two numbers combined into a third? Arithmetic is one of the most important cultural inventions of humanity, however we still lack a comprehensive understanding of how the brain computes additions and subtractions. The main goal of my dissertation is to better understand the temporal and spatial dynamics of the neurocognitive mechanisms underlying mental calculation. In the first study, I used a novel behavioral method based on trajectory tracking capable of dissecting the succession of processing stages involved in arithmetic computations. Results supported a model whereby single-digit arithmetic is computed by a stepwise displacement on a spatially organized mental number line, starting with the larger operand and incrementally adding or subtracting the smaller operand. In a second study, I analyzed electrophysiological signals recorded directly from the human cortex while subjects solved addition problems. I found that the overall activity in the intraparietal sulcus monotonically increased as the operands got larger, providing evidence for its involvement in arithmetic computation and decision-making. Surprisingly, sites within the posterior inferior temporal gyrus showed an initial burst of activity that monotonically decreased as a function of problem-size, suggesting that the ventral temporal cortex contain neuronal populations specifically involved in arithmetic processing, possibly engaged in the early identification of the difficulty or amount of evidence available for a calculation. In the last study, I recorded magnetoencephalography signals while subjects verified simple additions and subtractions in the form of  $3+2=9$ , with each successive symbol presented sequentially. By applying machine learning techniques, I investigated the temporal evolution of the representational codes of the operands and provided a first comprehensive picture of a cascade of unfolding processing stages underlying arithmetic calculation and decision-making at a single-trial level. Overall, this dissertation provides several contributions to our knowledge about how elementary mathematical concepts are implemented in the brain and shows that a multimethod approach including continuous behavioral measures and time-resolved neuroimaging can help us identify and characterize the mental processes of high-level symbolic cognition.

# TABLE OF CONTENTS

---

Acknowledgments .....	3
Abstract.....	8
Table of Contents .....	9
List of Figures.....	11
List of Tables.....	13
Publications by the author .....	14
<b>Chapter 1. General Introduction.....</b>	<b>17</b>
1.1 Paleolithic arithmetic .....	17
1.2 The origins of numerical abilities .....	19
1.3 Cognitive mechanisms of arithmetic calculations .....	26
1.4 Brain networks for arithmetic processing .....	32
1.5 Introduction to the experimental contributions .....	38
<b>Chapter 2. Finger-tracking reveals the covert stages of mental arithmetic.....</b>	<b>45</b>
2.1 Motivation.....	45
2.2 Abstract .....	46
2.3 Introduction .....	47
2.4 Methods .....	49
2.5 Results .....	51
2.6 Discussion.....	58
2.7 Acknowledgments.....	62
2.8 Supplementary Materials .....	63
<b>Chapter 3. Brain mechanisms of arithmetic: a crucial role for ventral temporal cortex .....</b>	<b>67</b>
3.1 Motivation.....	67
3.2 Abstract .....	68
3.3 Introduction .....	69
3.4 Methods .....	70
3.5 Results .....	74
3.6 Discussion.....	83
3.7 Acknowledgments.....	88
3.8 Supplementary Materials .....	89
<b>Chapter 4. Decoding the processing stages of mental arithmetic with MEG .....</b>	<b>95</b>
4.1 Motivation.....	95

4.2 Abstract .....	96
4.3 Introduction .....	97
4.4 Methods .....	100
4.5 Results .....	105
4.6 Discussion.....	118
4.7 Acknowledgments.....	127
4.8 Supplementary Materials .....	128
<b>Chapter 5. General Discussion .....</b>	<b>133</b>
5.1 Simple additions and subtractions rely on quantity manipulation.....	133
5.2 Arithmetic processing is implemented in the dorsal and ventral pathways .....	136
5.3 Decoding the processing stages of mental calculations.....	139
5.4 Searching for neural signatures of the internally computed result .....	140
5.5 Beyond numbers: the syntactic structure of arithmetic expressions .....	142
5.6 Conclusion.....	144
<b>References.....</b>	<b>145</b>

## LIST OF FIGURES

---

Figure 1.1 Examples of Artifical Memory System artifacts .....	18
Figure 1.2 Number-selective neurons in the monkey lateral and prefrontal cortices .....	21
Figure 1.3 Number representation in the human lateral parietal cortex .....	23
Figure 1.4 The min counting model by Groen and Parkman (1972) .....	27
Figure 1.5 Brain networks for arithmetic processing .....	33
Figure 1.6 Arithmetic processing in the ventral temporal cortex .....	37
Figure 2.1 Finger-tracking task and screen layout.....	49
Figure 2.2 Reconstructed trajectories averaged across subjects.....	53
Figure 2.3 Time course of the regression effects for additions per condition .....	54
Figure 2.4 Stepwise-displacement during additions and subtractions.....	56
Figure 2.5 Time course of the Operational Momentum effect .....	57
Figure 2.6 Time course for the regression effects of the predictors R-1 and SRP.....	63
Figure 2.7 Comparison of the time course of the regression effects .....	65
Figure 2.8 Operational Momentum effect in zero-problems relative to single-digits.....	66
Figure 3.1 Anatomical subdivisions, task, recording sites, and behavioral problem-size effect....	76
Figure 3.2 Exemplar sites whose activity was modulated by the min operand .....	78
Figure 3.3 Anatomical and functional specificity of the HFB activity modulation in the VTC ..	80
Figure 3.4 Separating the effects of number and reaction time .....	82
Figure 3.5 Anatomical and functional specificity of the HFB activity modulation in the LPC...	90
Figure 4.1 Sustained activity and signal propagation from posterior to anterior sensors .....	106
Figure 4.2 Decoding the time course of the processing stages underlying calculation .....	108
Figure 4.3 Cross-decoding from operation to operands.....	110
Figure 4.4 Theoretical predictors of dissimilarity matrices.....	112
Figure 4.5 Representational geometries of the operands.....	114
Figure 4.6 Attempting to decode the internally computed result .....	116

Figure 4.7 Generalization across time matrices during calculation.....	128
Figure 4.8 Matrix structure used for the RSA.....	129
Figure 4.9 Decoding the calculation features using regression.....	130
Figure 4.10 Searchlight decoding in time, sensor space and frequency .....	131
Figure 4.11 Decoding calculation features with Riemannian geometry .....	132
Figure 5.1 Time course of the regression effects for each type of expression .....	143

## LIST OF TABLES

---

Table 3.1 Subject demographics and behavioral performance .....	75
Table 3.2 Selectivity and modulation related to the recognition of Arabic numerals in the VTC channels that showed decreased initial activity as a function of min operand.....	81
Table 3.3 Arithmetic problem-size effect by subject.....	89
Table 3.4 Number of electrodes showing <i>math</i> selectivity and modulation by the min operand, by subject/anatomical region.....	91
Table 3.5 Number of electrodes showing <i>memory</i> selectivity and modulation by the min operand, by subject/anatomical region.....	92
Table 3.6 Number of electrodes showing modulation by the min operand by subject in other anatomical regions .....	93
Table 3.7 Stimuli list for the Math task .....	94

## PUBLICATIONS BY THE AUTHOR

---

### Articles included in the dissertation

**Chapter 2.** Pinheiro-Chagas, P., Dotan, D., Piazza, M., Dehaene, S. (2017). Finger tracking reveals the covert stages of mental arithmetic. *Open Mind: Discoveries in Cognitive Science*, 1(1), 30-41.

**Chapter 3.** Pinheiro-Chagas, P.\*, Daitch, A.\*, Parvizi, J., Dehaene, S. (*under review*). Brain mechanisms of arithmetic: a crucial role for ventral temporal cortex.

**Chapter 4.** Pinheiro-Chagas, P., Piazza, M., Dehaene, S. (*under review*). Decoding the processing stages of mental arithmetic with magnetoencephalography.

### Other articles produced during the dissertation

Pinheiro-Chagas, P., Dotan, D., Piazza, M., Dehaene, S. (*in preparation*). Decomposing the syntactic structure of arithmetic expressions.

Dotan, D., Pinheiro-Chagas, P., Dehaene, S. (*in preparation*) Track it to crack it: revealing the succession of processing stages with pointing trajectories.

Baek, S., Daitch, A., Pinheiro-Chagas, P., Parvizi, J. (*in preparation*). Neuronal population responses in the human ventral temporal and lateral parietal cortex during arithmetic processing with digits and number words.

Pinheiro-Chagas, P.\*, Dinino, D.\*, Haase, V. G., Wood, G., Knops, A. (*in preparation*) The developmental trajectory of the operational momentum effect.

Dresler, T., Bugden, S., Gouet, C., Lallier, M., Oliveira, D., **Pinheiro-Chagas, P.**, Pires, A., Wang, Y., Zugarramurdi, C., Weissheimer, J. (*under review*). Translational research in learning disabilities: the place of neuroimaging.

Borghesani\*, V., de Hevia\*, L., Viarouge\*, A., **Pinheiro-Chagas, P.**, Eger, E., Piazza, M. (2016). Comparing magnitudes across dimensions: a univariate and multivariate approach. International Workshop on Pattern Recognition in Neuroimaging, 1-4.

**Pinheiro-Chagas, P.** Wood, G., Knops, A., Krinzinger, H., Lonnemann, J., Starling-Alves, I., Willmes, K., Haase, V. G. (2014). In how many ways is the approximate number system associated with exact calculation? *PLoS One*, 19, 9(11), e111155.

Carvalho, M. R., Vianna, G., Oliveira, L., Costa, A. J., **Pinheiro-Chagas, P.**, Sturzenecker, R., Zen, P. R., Rosa, R. F., de Aguiar, M. J., Haase, V. G. (2014). Are 22q11.2 distal deletions associated with math difficulties? *American Journal of Medical Genetics Part A*, 164A(9), 2256-62.

Haase, V. G., Júlio-Costa, A., Lopes-Silva, J. B., Starling-Alves, I., Antunes, A. M., **Pinheiro-Chagas, P.**, Wood, G. (2014). Contributions from specific and general factors to unique deficits: two cases of mathematics learning difficulties. *Frontiers in Psychology*, 13, 5-102.

Moura, R., Wood, G., **Pinheiro-Chagas, P.**, Lonnemann, J., Krinzinger, H., Willmes, K., Haase, V. G. (2013). Transcoding abilities in typical and atypical mathematics achievers: the role of working memory and procedural and lexical competencies. *Journal of Experimental Child Psychology*, 116(3), 707-27

\* The authors equally contributed to the work



# **Chapter 1. GENERAL INTRODUCTION**

---

Revolutionary cultural inventions such as mathematics are unique to the human species and radically enhances our native cognitive competence. In fact, mathematics proved to be so powerful that it became the fundamental language of science, which we use to understand ourselves and everything else. In increasingly technological societies, revealing how mathematics is implemented in the brain is an extremely important and fascinating research program.

Arithmetic is the most elementary branch of mathematics and consists of the study of numbers and the operations between them. Despite decades of research, it is still largely unknown how the brain solves a simple calculation such as  $3+5=8$ . Although seemingly simple for educated adults, exact arithmetic involves highly sophisticated abstract concepts and operations, result of thousands of years of evolution, and engages a complex network comprising several brain regions (Arsalidou & Taylor, 2011; Dehaene, 1999; Menon, 2014).

How are two numbers combined into a third? This is the foundational question that guides my dissertation. I approached it by conducting a series of studies with the goal of better understanding the neurocognitive mechanisms of arithmetic calculations and characterizing their temporal and spatial dynamics in the human brain.

## **1.1 Paleolithic arithmetic**

Humans have been actively using numbers at least since the Upper Paleolithic (40,000-10,000 years BP). Archeological research has revealed the existence of several objects, usually animal bones, that contain well organized sets or carved notches, commonly known as *tally sticks*. Although still subject of debate, abundant evidence suggests that these objects were simple exosomatic devices or Artificial Memory Systems that employed a unary notation system to create, store, process and transmit numerical and temporal information central to these societies, such as keeping record of objects and cattle, representing the lunar calendar, etc. This evidence comes

from the careful examination of several characteristics of the marks, namely their number, morphology, accumulation over time and spatial distribution (d'Errico, 1998).

The oldest object of this class is the Lebombo Bone (Figure 1.1a), a baboon fibula found in the Border Cave in the Lebombo Mountains (South Africa), dating to 44,000 years BP. It contains 29 notches, divided in groups produced with different tools. Thus, it is considered to be the first record of counting or addition (d'Errico et al., 2012).

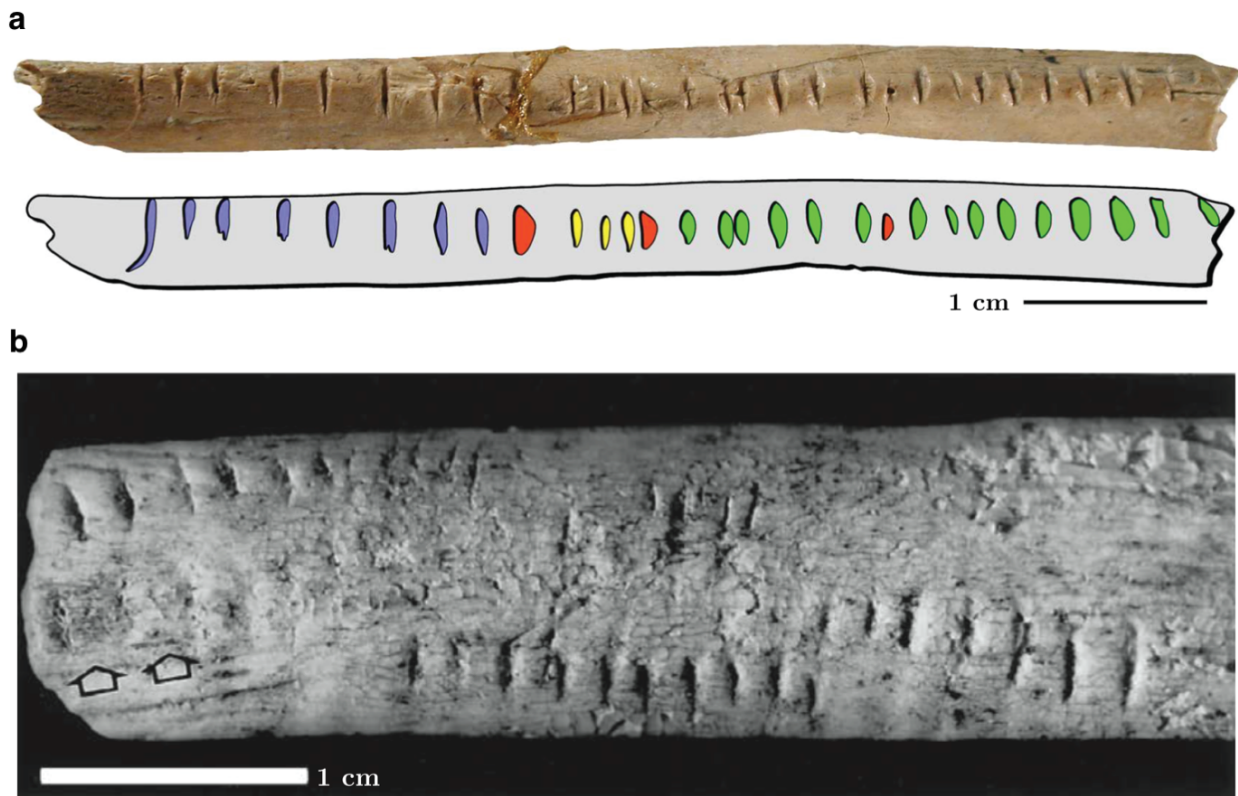


**Figure 1.1 Examples of Artificial Memory System artifacts**

a) Lebombo Bone. The different colors represent notches made by different tools. Adapted from d'Errico et al. (2012). b) Spatula made of a rib. Arrows indicate the areas that were scraped/subtracted. Adapted from d'Errico (1998).

Another interesting object is a spatula made from a rib (Figure 1.1b), found in the Magdalenian (17,000 - 12,000 BP) levels of Laugerie-Basse (Dordogne, France), which contains more than 150 marks, grouped in at least 17 different sets and made by different tools. This object contains the earliest known evidence of a subtraction, since one of the sets appears to have

been deliberatively erased by scraping (d'Errico, 1998).

The evolution of these devices is thought to have culminated on the development of a variety of more elaborated numerical systems and symbolic notations found in several ancient societies (d'Errico, 1998; d'Errico et al., 2012), most notably the Babylonians, Mayans, Greeks and Egyptians, which formed the basis for the way we represent and operate with numbers today.

## 1.2 The origins of numerical abilities

### 1.2.1 The *number sense*

The ability to instantly grasp the approximate number of objects in a scene and to compare abstract quantities, known as the '*number sense*' (Dantzig, 1967), is a cognitive capacity already present in human newborns (de Hevia, Izard, Coubart, Spelke, & Streri, 2014; Izard, Sann, Spelke, & Streri, 2009) and possibly even in fetuses during the last three months of pregnancy (Schleger et al., 2014). It has been extensively shown that humans share this *approximate number system* (ANS) (Feigenson, Dehaene, & Spelke, 2004) with a variety of other animal species, from beetles (Carazo, Font, Forteza-Behrendt, & Desfilis, 2009) to monkeys (Piantadosi & Cantlon, 2017). Therefore, the dominant view is that the ANS was selected during evolution as a highly advantageous function serving several vital behaviors, such as protecting cubs (McComb, Packer, & Pusey, 1994), selecting preys (Krause & Godin, 1995), mating (Carazo et al., 2009) and making collective decisions (Piantadosi & Cantlon, 2017).

The ANS is thought to represent numbers as analog magnitudes (Gallistel, 1990), similarly to ways we represent space and time (Dehaene & Brannon, 2010; Walsh, 2003). Importantly, the psychophysics Weber-Fechner law<sup>1</sup> that characterizes the perception of stimuli in several basic sensory modalities can also be applied to describe approximate number comparison and estimation

---

<sup>1</sup> According to Weber's law, a variation that can be discriminated in the stimulus intensity ( $\Delta\phi$ ) is a constant fraction ( $c$ ) of the stimulus initial value ( $\phi$ ). Mathematically:  $\Delta\psi = c \frac{\Delta\phi}{\phi}$ , where ( $\Delta\psi$ ) is the variation in the perception. According to Fechner's law, the perceived magnitude of a stimulus is equal to the natural logarithm of the stimulus multiplied by a given constant ( $k$ ), which varies with the particular dimensions of the stimuli. Mathematically:  $\psi = k \log \phi$ .

in both human and other animal species (Cantlon & Brannon, 2006; Dehaene, Dehaene-Lambertz, & Cohen, 1998; Jevons, 1871). More specifically, the Weber-Fechner law can account for two behavior effects commonly found, namely the *distance effect*: it is easier and faster to discriminate between pairs of quantities as their numerical distance increases (Moyer & Landauer, 1967); *size effect*: the discrimination of pair of quantities with a fixed numerical distance becomes less accurate and slower as the quantities increase (scalar variability or ratio-dependency) (Dehaene, 2007).

### 1.2.2 The neural basis of the *approximate number system*

Pioneering electrophysiological work revealed the existence of neurons tuned to specific numerosities (the cardinality of a set of objects) in the monkey ventral intraparietal area (VIP) and lateral prefrontal cortex (LPFC) (Nieder & Miller, 2004). In a typical setting, monkeys are trained to perform a delayed match-to-numerosity task, in which they must compare two sequentially presented sets of dots, controlled for basic visual features of the stimuli, such as dot size and total area occupied (Figure 1.2a). Figure 1.2c shows an exemplar VIP neuron which responds more strongly to the number 6 as compared to other numbers. These neurons were also found in monkeys that were completely naïve to the task and did not receive any explicit numerical training (Viswanathan & Nieder, 2013). The responses of some of these neurons were also found to be supramodal, that is, independent of the stimulus modality: auditory or visual (Nieder, 2012, Figure 1.2d). Finally, the activity pattern observed in these neurons can be modeled by the Weber-Fecher law: the standard deviation of the Gaussian tuning curves increases as a function of numerosity, a pattern that is mathematically equivalent to fixed standard deviation in a log-compressed scaled (Nieder, 2016).

Additionally to the number-selective neurons found in VIP, Roitman, Brannon and Platt (2007) reported neurons in the lateral intraparietal area (LIP), whose discharge rate monotonically increased or decreased as a function of numerosity. Therefore, the interactions between LIP-VIP neurons could be the neurophysiological implementation of an early neural-network model: numerosity detection may arise by a combination of a first layer containing “summation” units (possibly in LIP) with a second layer composed by selective units (possibly in LIP) (Dehaene & 20

Changeux, 1993, see also Stoianov & Zorzi, 2012; and Verguts & Fias, 2004).

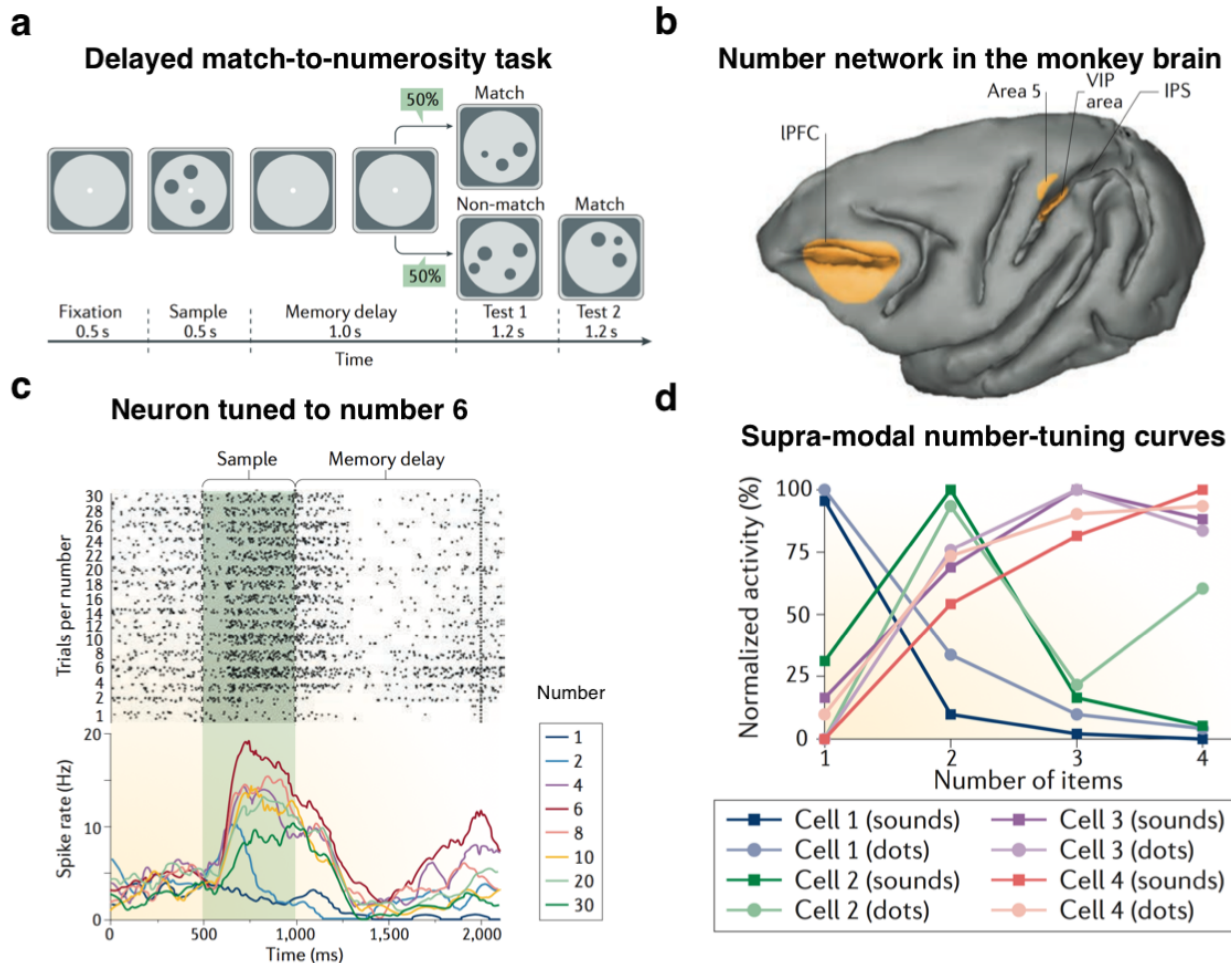


**Figure 1.2 Number-selective neurons in the monkey lateral and prefrontal cortices**

a) Experimental design. Monkeys are trained in a task in which they must judge whether two sequentially presented collection of dots are the same or different. b) Recording sites: ventral parietal area (VIP) and lateral prefrontal cortex (IPFC). c) An exemplar neuron that shows higher spiking rate for the number 6 during the sample period. d) Tuning curves for number selective neurons that show a modality-independent (auditory vs. visual) stimuli response. Adapted from Nieder (2016).

A series of functional magnetic resonance imaging (fMRI) confirmed the selective engagement of the lateral parietal cortex (LPC) in number processing in humans adults and children (Cantlon, Brannon, Carter, & Pelpfrey, 2006). Piazza, Izard, Pinel, Le Bihan and Dehaene (2004) asked adult subjects to passively attend to a rapid stream of sets of dots that had

a constant numerosity, but varied in their basic visual properties, such as dot size and occupied area. After a habituation period, in which the fMRI activity dropped, a deviant number was presented, causing a rebound effect. By systematically varying the distance between the adapted and deviant stimuli, the authors modeled the fMRI activity evoked by the deviant number and revealed the existence of tuning curves in the bilateral intraparietal sulcus (IPS). Remarkably, these tuning curves at the population level were similar to the ones found in single cells of nonhuman primates (Figure 1.3b). Subsequent studies revealed that the IPS responses to numbers are independent of the stimulus format (i.e., non-symbolic sets of dots, Arabic numerals and number words), suggesting that the IPS hosts a common code for abstract quantities. (Fias, Lammertyn, Reynvoet, Dupont, & Orban, 2003; Piazza, Pinel, Le Bihan, & Dehaene, 2007, Figure 1.3a,b,c; but see Cohen Kadosh & Walsh, 2009). Furthermore, using multivariate pattern analysis (MVPA), Eger et al., 2009 showed that the identity of individual numbers can be decoded from the fMRI activity in the IPS. Importantly, a decoder trained to classify digits significantly generalized to discriminate dots (Figure 1.3d). More recently, studies using ultra-high-field fMRI (7T) reported a topographical organization of numerosity in the superior parietal lobe (SPL) (Harvey, Klein, Petridou, & Dumoulin, 2013), subsequently also observed in other associative areas along the temporal-occipital cortex and precentral sulcus (Harvey & Dumoulin, 2017; Harvey, Ferri, & Orban, 2017, Figure 1.3e).

### 1.2.3 The *mental number line*

Numbers seem to be represented in a spatially organized form, like a *mental number line*. This idea dates to the late 19<sup>th</sup> century, when Sir Francis Galton qualitatively examined several drawings reflecting subject's introspection on how they visualized numbers in their mind (Galton, 1881).

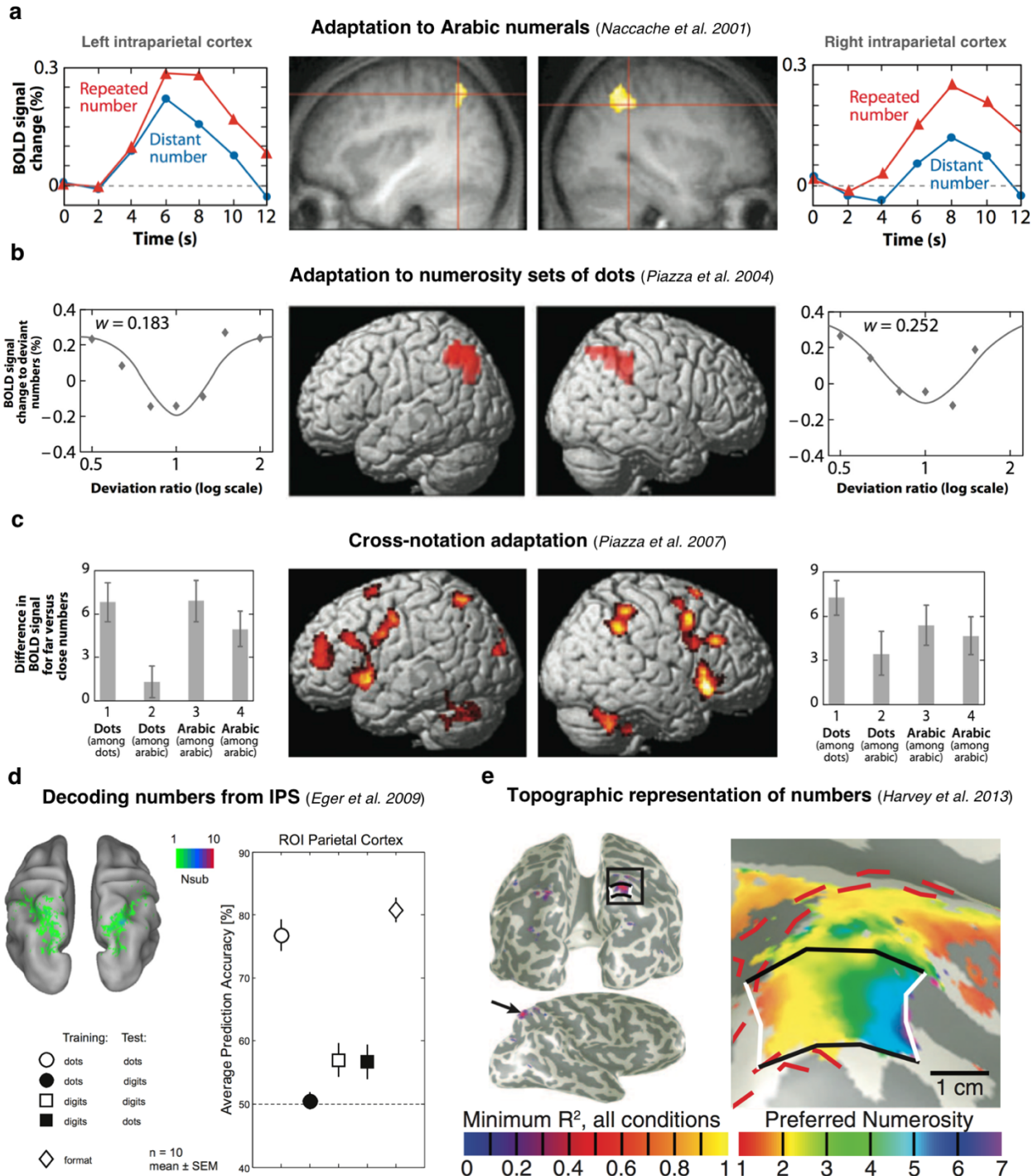


**Figure 1.3 Number representation in the human lateral parietal cortex**

a) fMRI Subliminal priming study showing left and right intraparietal response to numerical novelty for both Arabic numerals and number words. Adapted from (Naccache & Dehaene, 2001). b) fMRI adaptation study using non-symbolic numbers (sets of dots), showing tuning curves for numbers at the bilateral intraparietal sulcus (IPS). Adapted from (Piazza et al., 2004). c) fMRI adaptation study showing that the distance effect observed in the bilateral IPS also occurs across

notation: Arabic numerals vs. sets of dots. Adapted from (Piazza et al., 2007). d) fMRI multivariate decoding study showing that the identity of both Arabic numerals and non-symbolic numbers can be decoded from IPS activity. Adapted from (Eger et al., 2009). e) Ultra-high field fMRI at 7T revealed a topographic organization of non-symbolic numbers in the human SPL. Adapted from (Harvey et al., 2013).

A century later, Dehaene, Bossini and Giraux (1993) tested and presented convincing evidence supporting this hypothesis. The authors observed that, in a parity judgment tasks, subjects were faster to respond to smaller numbers when pressing a button with the left hand and faster for larger numbers with the right hand. This ‘spatial-numerical association of response codes’ (SNARC) effect has been extensively replicated using a variety of tasks (Nuerk, Wood, & Willmes, 2005) and it was even found in other species such as monkeys (Drucker & Brannon, 2014) and even in newborn chicks (Rugani, Vallortigara, Priftis, & Regolin, 2015). An interesting attentional variation of this effect was found using a modified Posner Cueing Task (Posner, 1980): cueing human subjects with small vs. large numbers caused shifts in the covert attention to the left vs. right side of the screen, respectively, thus facilitating target detection (Fischer, Castel, Dodd, & Pratt, 2003). Complementarily, it has been found that patients suffering from hemispatial neglect, a neuropsychological syndrome that causes systematic failure in attending to one side of the space (usually the left), show a bias towards higher numbers when asked to bisect a numerical interval (e.g., they would respond that the middle of 11–19 is 17, instead of 15), as if they were also neglecting the left side of the mental number line (Zorzi, Priftis, & Umiltà, 2002). Although the orientation of the mental number line can be at least partially driven by cultural factors, such as writing direction (Dehaene et al., 1993), a robust body of evidence suggests that the numerical–spatial interactions are innate (Rugani & de Hevia, 2017) and, in the human brain, share a common parietal circuit for attention to external space and internal approximate number representation (Hubbard, Piazza, Pinel, & Dehaene, 2005; for a alternative and potentially complementary working memory account, see van Dijck & Fias, 2011).

#### **1.2.4 From approximate quantities to exact symbols**

In addition to the ANS, humans (Feigenson et al., 2004) and other animals (Agrillo, Piffer,

Bisazza, & Butterworth, 2012; Tomonaga & Matsuzawa, 2002) also share a core system for representing objects, based on spatial-temporal features, such as cohesion (objects move as bounded wholes), continuity (objects move on connected, unobstructed paths), and contact (objects do not interact at a distance) (Spelke & Kinzler, 2007). Differently from the ANS, this ‘object tracking system’ (OTS) allows to instantly grasp the exact number of small sets containing up to four items (a process also known as *subitizing*). *Subitizing* does not follow Weber’s law, that is, subject’s error rates and RTs do not increase as a function of magnitude from 1 to 4 (Anobile, Cicchini, & Burr, 2016; Jevons, 1871).

Unlike the ANS and OTS, number symbols and number words are uniquely human inventions, which are used to represent, manipulate and combine exact quantities (Dehaene, 1992). Since both the ANS and OTS are found to be present in pre-verbal infants and interact during development, they are generally considered to be, with the mediation of language, complementary core neurocognitive ‘start-up tools’ from which symbolic arithmetic is built (Piazza, 2010). In fact, it has been extensively shown that the acuity of the ANS is an important predictor of mathematical achievement (Halberda, Mazzocco, & Feigenson, 2008; Piazza et al., 2010; Pinheiro-Chagas et al., 2014; Starr, Libertus, & Brannon, 2013). However, the precise developmental mechanism underlying the acquisition of exact number representation is still subject to debate (see Carey, 2009; and Dehaene, 1999).

At the neurophysiological level, a computational model provided evidence for the hypothesis that the higher precision in symbolic number representation could be achieved by a progressive narrowing of the Gaussian tuning curves of number-selective neurons, in a way that, at least part of the population, would become precisely tuned to specific quantities and not respond to its neighboring ones (Verguts & Fias, 2004). It is important to note that, although symbolic numbers convey exact meaning, they seem to be grounded on a quantity-based representation, with similar properties as the ones of the ANS. For example, in symbolic number comparison tasks, behavior performance is also explained by Weber-Fechner’s law, that is, it becomes increasingly faster and accurate to discriminate pairs of Arabic numerals as their numerical distance increases (Dehaene, 2007; Moyer & Landauer, 1967).

## 1.3 Cognitive mechanisms of arithmetic calculations

Although great progress has been made in understanding how the brain represent numbers, much less is known about the neurocognitive mechanisms underlying exact number manipulation in the form of arithmetic calculations, such as additions and subtractions. In the past 40 years, researchers have been using *mental chronometry* (Donders, 1969; Sternberg, 1969) to measure behavioral performance in several arithmetic tasks. Despite the variety of chronometric findings, one particular effect has been widely replicated in virtually all studies that investigated mental arithmetic, namely the *problem-size effect*: reaction times (RTs) increases as a function of the size of the operands to be added, subtracted or multiplied (Zbrodoff & Logan, 2005; Zimmerman et al., 2016). The aim to find the origins of problem-size effect became a central topic in the literature and, by investigating its properties across operations and during development, researchers have come to propose different cognitive models of arithmetic.

### 1.3.1 The *min* model

Thomas (1963) was the first to propose an information-processing account for mental arithmetic, suggesting that the time needed to perform a given calculation should be strictly proportional to the amount of information that must be handled by the system. Inspired by this idea, Groen and Parkman conducted a series of mental calculation experiments measuring RTs in both children and adults. In their seminal study, Groen and Parkman (1972) presented first-graders with several single-digit additions and asked them to press one out of ten buttons corresponding to the results 0 to 10. They found that the best predictor of RTs was the smaller of the two operands (*min*), with a slope of 410 ms per unit. Therefore, they proposed a model based on a counter device, which starts by setting its value to the larger of the two operands and then increments it with a number of units corresponding to the *min* operand in steps of one, with each step taking 410 ms (Figure 1.4a,b). As the 410 ms step is within the implicit speech rates, ~150 ms (Landauer, 1962), Groen and Parkman (1972) proposed that children could be actually performing silent counting. Using a verification task with adults, Parkman and Groen (1971) also

found that the *min* operand was the best predictor of RT, but with a much steeper slope of only 20 ms per unit, which is way faster than the implicit speech rates (Figure 1.4c).

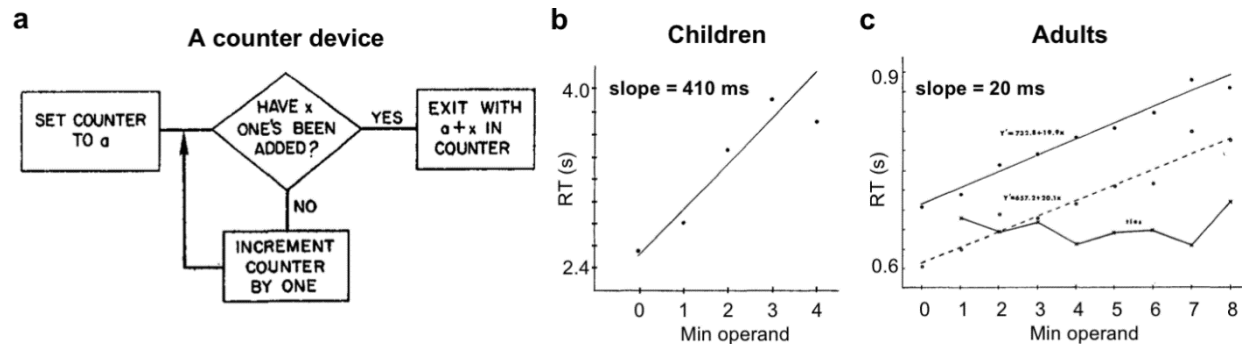


**Figure 1.4 The min counting model by Groen and Parkman (1972)**

a) A device which sets the counter to  $a$  and adds  $x$  to  $a$  by increments of one. Based on the results,  $a = \max$  operand and the number of increments =  $\min$  operand. b) Mean RTs as a function of  $\min$  operand in children using a production task (children had to press one out of ten buttons representing the results 0-10). c) Mean RTs as a function of  $\min$  operand in adults using a verification task. The two upper parallel lines represent the regression fit for non-tie problems (filled line indicate incorrect problems, which were slower than correct ones - dotted line). Bottom line represent tie problems, in which the min model was not significant. Adapted from Groen and Parkman (1972).

Importantly, no problem-size effect was found for tie problems (e.g.,  $3+3$ ), which were all solved within  $\sim 650$  ms, suggesting that the result could be accessed through direct retrieval from long-term memory. Because the slope of the *min* effect for non-tie problems was found to be too fast for an explicit counting procedure, the authors proposed that, in most cases, adults can also solve single-digit non-tie additions by direct retrieval from long-term memory, due to the effect of overlearning the arithmetic table in the first years of formal schooling. Therefore, the reduced problem-size effect observed would, arise from a small percentage of the cases ( $\sim 5\%$ ) in which the retrieval strategy fails, requiring adults to use the backup counting strategy.

### 1.3.1.1 Fact-retrieval models of elementary arithmetic

The idea of occasional failure of direct retrieval was further corroborated by LeFevre et al. (1996) who asked subjects to introspect about their strategies while solving additions problems.

The authors showed that in more than 80% of the small problems ( $\text{sum} \leq 10$ ), but only in 47% of the large problems ( $10 < \text{sum} < 18$ ), adults reported the use of a retrieval strategy. Surprisingly, even in the small problems that were classified as retrieval, a problem-size effect was observed, which was incompatible with the idea of direct retrieval as a sole strategy. The authors interpreted this result in light of other retrieval-based models (Ashcraft, 1992; Campbell, 1987; Siegler & Shrager, 1984). For example, Siegler and collaborators attributed the difference in retrieval latencies to the acquisition history of each problem (Siegler & Jenkins, 1989; Siegler & Shrager, 1984). More specifically, each single addition is associate initially with both correct and incorrect results and, during learning, the correct results are straightened, therefore producing a more peaked distribution, centered on the correct result. Because the frequency of numbers (Dehaene & Mehler, 1992) and operations (Hamann & Ashcraft, 1986) decreases as a function of magnitude, smaller problems are more likely to have a peaked distribution and consequently be solved by direct retrieval (due to higher confidence associated with the retrieved result), whereas larger problems presumably have flatter distributions and therefore are more likely to be solved by counting or other reconstructive strategies. However, this model does not fully explain the problem-size effect in calculations solved by supposedly direct retrieval. An alternative model by Ashcraft and colleagues (Ashcraft, 1992; Ashcraft & Battaglia, 1978) proposed that the 100 single-digit additions are stored as a tabular representation in the memory network, where rows and columns represent the operands, and cells represent the sum. When presented with a problem such as  $4+3=7$ , subjects adopt a strategy of systematic search along the mental table, beginning at 0,0 and progressing outward until the intersection is reached. The authors found that the best predictor of subjects' RT was the square of the sum, which violated the linear relationship between the problem-size and RT assumed by the previous counting models. Therefore, they suggested that there could be a progressive "stretching" of the mental table as the operands increase, produce a non-linear slowdown of the continuous search, thus explaining the presence of a problem-size effect in the context of a retrieval strategy.

It is important to note that retrieval-based models suggest that adults also use supplementary strategies (Lefevre & Kulak, 1994; Siegler, 1987; Zbrodoff & Logan, 2005) to solve

simple arithmetic problems. For instance, Butterworth, Zorzi, Girelli, & Jonckheere and (2001) proposed that, given the commutativity of addition, only half of the table has to be stored in long-term memory (problems in which the first operand is larger than the second, which could be progressively committed to memory, as a result using the *min* counting strategy at a younger age). To solve problems presented in the opposite order (e.g., 2+7), subjects would reorder the operands prior to retrieval. In accord with this notion of reordering, they showed that adults' RTs for additions were indeed found to be higher when the first operand was smaller.

In summary, it has been historically agreed that educated adults solve elementary arithmetic problems primarily by direct fact retrieval and that the problem-size arises from structural and functional features of the long-term memory network (Ashcraft, 1992; Ashcraft & Battaglia, 1978; Campbell, 1987; LeFevre, Sadesky, & Bisanz, 1996; Siegler & Shrager, 1984; Stazyk, Ashcraft, & Hamann, 1982); which are potentially linked to a more latent variable of *problem-difficulty*, that would be coincidentally associated with the size of the operands (Ashcraft, 1992).

### **1.3.1.2 Calculation as movement along the mental number line**

A series of recent findings have begun to challenge the retrieval-based account for additions and subtractions in favor of a model that relies on quantity manipulation, possibly on a *mental number line* (Barrouillet & Thevenot, 2013; Dehaene & Changeux, 1993; Fayol & Thevenot, 2012; Knops, Viarouge, Dehaene, et al., 2009; Knops, Thirion, Hubbard, Michel, & Dehaene, 2009; Mathieu, Epinat-duclos, Sigovan, et al., 2017; Mathieu, Gourjon, Couderc, Thevenot, & Prado, 2016; McCrink, Dehaene, & Dehaene-Lambertz, 2007; Restle, 1970; Uittenhove, Thevenot, & Barrouillet, 2016). This model can be conceptualized as refinements of the simple counting/summation based models.

Fayol and Thevenot (2012) designed a task in which subjects had to solve additions, subtractions and multiplications. In some of the trials, the operation sign was presented 150 ms before the operands. Results showed a significant priming effect of the operation sign on RTs, but only for additions and subtractions. This effect was present even in single-digit additions, but

absent in tie problems. The authors suggested that differently from multiplications and tie problems, which are probably solved by direct fact retrieval, the abstract procedures underlying additions and subtractions can be pre-activated by the operation sign and therefore facilitate subsequent computation. Because of the effect of practice, these procedures could increasingly become automatized and be even faster than direct retrieval. This hypothesis was originally suggested by Baroody (1983), but did not achieve much acceptance when the retrieval-based models were dominant, probably because no precise mechanism was specified. More recently, using a large sample of subjects, Barrouillet and Thevenot (2013) and Uittenove, Thevenot and Barrouillet (2016) reported an almost perfect monotonic increase of RT as a function of problem-size in small additions ( $\text{sum} \leq 10$ ), with a slope of 20 ms per unit. These results pose a serious challenge for retrieval-based models, even when considering possible effects of frequency of exposure. As noted by Barrouillet and Thevenot (2013), during lexical decision task, dramatic differences in word frequency (from about 3,000 to 60 per million) give rise to only very small differences in RTs ( $\sim 15$  ms) (Ferrand et al., 2011). In contrast, different addition problems can have much larger RT differences, even when they probably have much smaller differences in frequency: for example, the authors observed a difference of  $\sim 90$  ms between the problems  $2+1$  and  $2+4$ . Therefore, in line with Baroody's hypothesis, they proposed that simple additions are solved through a mechanism of fast automated procedures that could take a form of compiled programs (Anderson, 1983) of scrolling on an ordered representation, such as the *mental number line*.

The ANS allows not only to instantly grasp the approximate number of objects present in a scene and compare them, but also to perform approximate additions and subtractions, which are also found to be present in human infants (McCrink & Wynn, 2004; Wynn, 1992) and can be trained in nonhuman primates (Cantlon & Brannon, 2007; Cantlon, Merritt, & Brannon, 2016; Livingstone et al., 2014). Importantly, like basic numerical processing, behavioral performance in approximate calculation with both non-symbolic and symbolic formats can be described by Weber-Fechner's law (Barth et al., 2006; Dehaene, 2007). To investigate the approximate calculation in adults more precisely, McCrink et al. (2007) presented subjects with short movies, in which a first

30

set of dots ( $n1$ ) flowed behind an occluder, followed by a second set of dots ( $n2$ ) that flowed either behind the occluder like the first one (representing additions) or out from the occluder (representing subtraction). The dots moved relatively fast to prevent exact counting. The occluder then shrank and disappeared to reveal a proposed outcome set ( $n3$ ), which subject had to judge if it was correct or incorrect. By continuously varying the magnitude of  $n3$ , the authors could model the behavioral responses with psychophysics. In line with Weber's law, they indeed found that the standard deviation of  $n3s$  judged as correct increased as a function of the sum. Surprisingly, although the mean also increased with the sum, it was systematically biased towards larger results in additions and towards smaller results in subtractions. This so-called *operational momentum* effect (OM) resembles a previously described *representational momentum*, observed when subjects estimate the position where a moving object stops - estimations are biased towards the direction of the movement (Freyd & Finke, 1984) - which was also found in other internal continua, such as action (Ashida, 2004) and sound pitch (Freyd, Kelly, & DeKay, 1990). Therefore, McCrink et al. (2007) suggested that additions and subtractions are performed by respectively rightward or leftward displacement on the spatially-organized mental representation of numbers.

Furthermore, the neural circuitry underlying mental calculation tightly overlaps with LPC regions involved in the control of attention and saccadic eye movements, possibly by a mechanism that implements a form of vector addition between eye-centered (retinotopic) and eye-position information (Pouget, Deneve, & Duhamel, 2002). Knops, Thirion, et al. (2009) reasoned that a similar mechanism could have been co-opted during evolution to perform arithmetic calculations. Corroborating this hypothesis, they showed that a classifier trained to discriminate left vs. right saccadic eye movements based on human fMRI activity in the superior parietal lobe (SPL) could significantly generalize to classify approximate subtractions vs. additions, respectively (Knops, Thirion, et al., 2009) (Figure 1.5f). Interestingly, a recent study showed that merely perceiving a “+” sign can elicit activity in brain regions engaged in the orienting of spatial attention (Mathieu, Epinat-duclos, Sigovan, et al., 2017).

Although the OM effect was first observed in non-symbolic arithmetic, subsequent studies showed that it is also present in symbolic arithmetic (Knops, Viarouge, Dehaene, et al., 2009)

even in small single-digit problems (Pinhas & Fischer, 2008), suggesting that exact and approximate additions and subtractions could rely on a shared fundamental mechanism of movement along the *mental number line*. This hypothesis, which resonates with Restle (1970), is appealing and compatible with other models based on counting/summation (Groen & Parkman, 1972), fast automated procedures (Barrouillet & Thevenot, 2013; Uittenhove et al., 2016), and even with the retrieval through a tabular search model by Ashcraft and Battaglia (1978). However, it still needs to be thoroughly tested and specified in both behavioral and neural levels.

## 1.4 Brain networks for arithmetic processing

### 1.4.1 The Triple-Code model

The classical Triple-Code model of numerical cognition (Dehaene, 1992), which was initially proposed based on converging evidence from human and animal behavioral studies together with neuropsychological case studies, proposes the existence of three interactive and partially independent codes for representing numbers, namely analog (correspondent to the ANS), symbolic (exact representation, i.e., Arabic numerals) and verbal (exact representation rooted in language processing i.e., number words). The analog code allows for approximate calculations, the verbal code for fact-retrieval based calculations (e.g., the multiplication table), and the symbolic code for procedure-based multi-digit calculations. In light of a series of subsequent double-dissociations found in brain-damaged patients and interpreted according to the Triple-Code model, Dehaene and Cohen (1995) proposed putative brain networks for arithmetic processing (Figure 1.5a). The main network comprised the lateral parietal cortex (LPC), engaged in numerosity representation and the ventral temporal cortex (VTC), involved in the recognition of numerical symbols (including a possible selective region to Arabic numerals; the ‘number form area’). Arithmetic calculations would therefore be performed by an interplay between these main hubs and auxiliary brain regions associated with executive functions and working memory (basal ganglia and dorsolateral prefrontal cortex, DLPFC), declarative and semantic memory formation (medial

and lateral temporal cortex), and allocation of attentional resources for goal-directed problem solving (PFC).

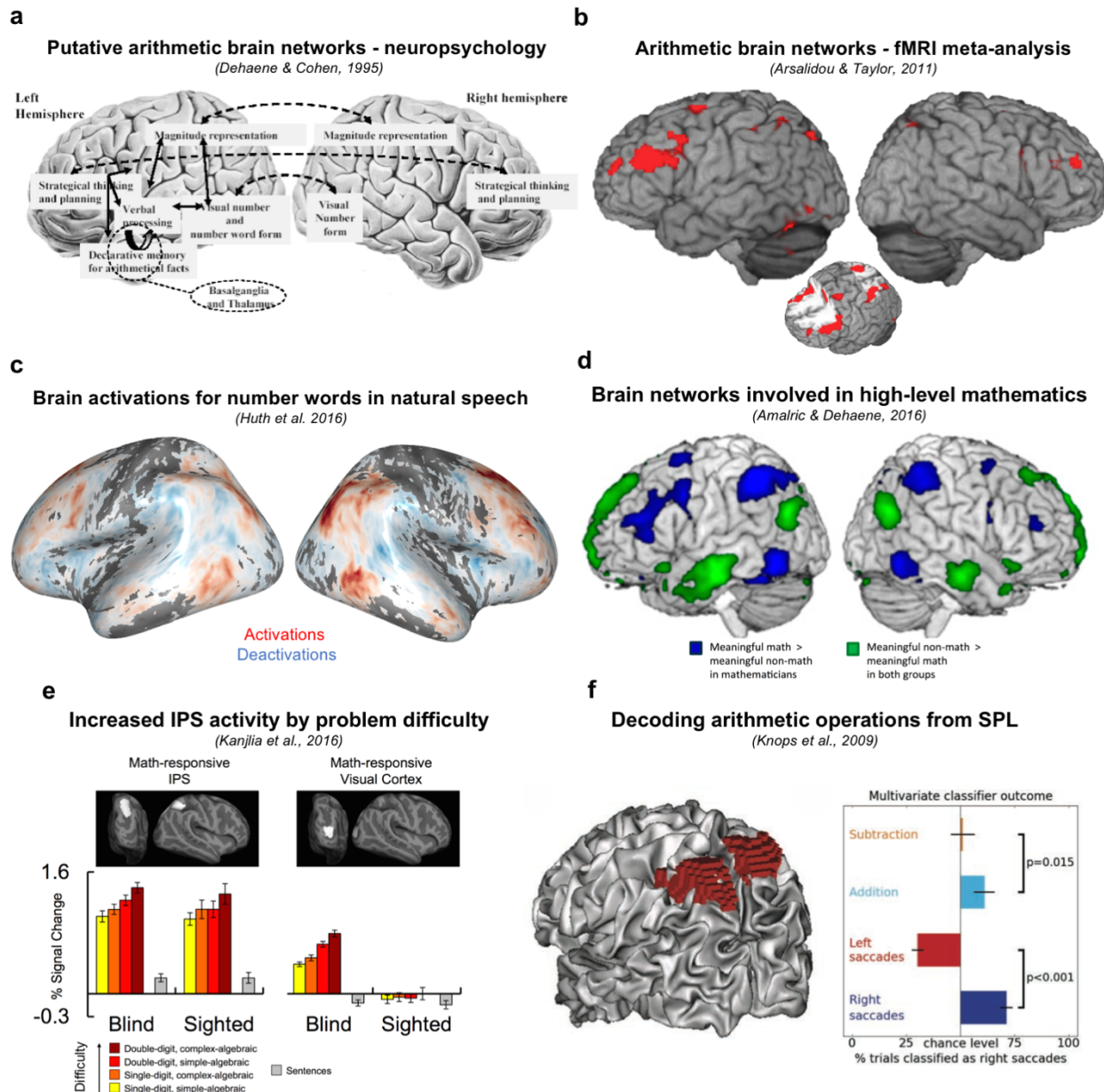


**Figure 1.5 Brain networks for arithmetic processing**

A) Putative brain networks involved in arithmetic, predicted by the Triple-Code Model (Dehaene, 1992) and inferred from a series of double dissociations found in neuropsychological patients (Dehaene & Cohen, 1995). B) An ALE meta-analysis with fMRI studies showing brain regions involved in arithmetic processing, confirming the neuropsychological predictions. Note that the networks largely overlap with the neuropsychological predictions. Adapted from Arsalidou and Taylor (2011). C) Univariate contrast between number words and baseline, generated with the

open source platform from Jack Gallant's lab, which uses fMRI data collected from subjects while listening to natural speech narratives (Huth, de Heer, Griffiths, Theunissen, & Gallant, 2016) <https://boldpredictions.gallantlab.org/>. The networks overlap with the ones showed in A and B. D) Results from an fMRI study showing brain regions engaged when professional mathematicians evaluate auditory presented math statements involving high-level concepts (blue) largely overlapping with the networks showed in A and B and dissociating from regions engaged by the evaluation of non-math domain-general statements (green). The math networks again largely overlap with the ones from A and B. Adapted from (Amalric & Dehaene, 2016). E) Results showing increasing BOLD activity in the IPS as a function of arithmetic problem-difficulty in both congenitally blind and sighted subjects. Interestingly, a similar parametric modulation was found in the visual cortex of congenitally blind subjects. Adapted from Kanjlia, Lane, Feigenson, & Bedny (2016). F) fMRI decoding study, showing that a classifier trained on discriminating left vs. right saccadic eye movements from the activity in the SPL significantly generalized to classify non-symbolic subtractions vs. additions, respectively. Adapted from (Knops, Thirion, et al., 2009).

Remarkably, this canonical brain network for arithmetic processing predicted by Dehaene and Cohen (1995) was largely confirmed by several subsequent fMRI studies (Chochon, Cohen, van de Moortele, & Dehaene, 1999; Dehaene, Spelke, Pinel, Stanescu, & Tsivkin, 1999; Menon, Rivera, White, Glover, & Reiss, 2000; Rickard et al., 2000; see Menon, 2014 for a recent review). The results were summarized in an activation likelihood estimation (ALE) meta-analysis (Laird et al., 2005), using 52 studies with a variety of calculation tasks (Arsalidou & Taylor, 2011, Figure 1.5b). The LPC network was later proposed to be subdivided in three circuits, namely the horizontal portion of the IPS (selectively associate with number comparison and calculation); the superior parietal lobe (SPL), engaged in visual-spatial processing and orienting of attention during calculation; see Knops, Thirion, et al., 2009) and the left angular gyrus (lAG), supposedly involved in verbal number processing such as fact-retrieval (Dehaene, Piazza, Pinel, & Cohen, 2003).

Furthermore, the main regions associated with arithmetic processing were also recently found to be active when subjects passively listened to number words from narratives (Huth, de Heer, Griffiths, Theunissen, & Gallant, 2016, Figure 1.5c) and when patients communicated numerical information with their doctors though natural speech (Dastjerdi, Ozker, Foster, Rangarajan, & Parvizi, 2013). More impressively, a recent study found a large overlap between regions engaged in basic arithmetic processing (symbolic numeral identification and calculation) and regions activated when professional mathematicians reflected upon high-level mathematical

concepts (Amalric & Dehaene, 2016): professional mathematicians and equally educated controls (humanities) were asked to judge the correctness of a series of auditory presented statements involving either high-level mathematical concepts from several fields (analysis, algebra, topology, and geometry; e.g., “A smooth function whose derivatives are all non-negative is analytic”) or non-math domain-general knowledge (e.g., “In Ancient Greece, a citizen who could not pay his debts was made a slave.”). The brain networks found in professional mathematicians during high-level mathematics largely overlapped with the one elicited by basic number processing (comprising the VTC, IPS and DLPFC) and almost perfectly dissociated from brain regions activated during non-math statements evaluation, which involved semantic-related language areas in the inferior parietal and anterior temporal cortices (Figure 1.5d). Therefore, Amalric & Dehaene (2016) suggested that high-level mathematics could have recycled (Dehaene & Cohen, 2007) brain regions that were originally selected during evolution to perform elementary arithmetic.

#### **1.4.2 Arithmetic processing in the dorsal and ventral pathways**

The original hypothesis postulated by the Triple-Code model, which has been dominant in the field, is that the IPS and SPL are the main hubs for the calculation mechanisms *per se* and that the VTC has a specific role in the visual recognition of numerical symbols (Dehaene & Cohen, 1995; Menon, 2014). Accordingly, it has been found that the activity in the IPS monotonically increases as problems become bigger/harder, reflecting the classical behavioral problem-size effect. (De Smedt, Holloway, & Ansari, 2011; Dehaene et al., 1999; Kanjlia, Lane, Feigenson, & Bedny, 2016; Molko et al., 2003; Visscher et al., 2015, Figure 1.5e). Additionally, as mentioned in the previous section, arithmetic operation types (additions vs. subtractions) could be decoded from SPL activity (Knops, Thirion, et al., 2009). As far as the VTC is concerned, a recent study using electrocorticography (ECoG) have confirmed the existence of neuronal populations in the bilateral posterior inferior temporal gyrus (pITG) that selectively activate during visual identification of Arabic numerals (the ‘number form area’, NFA), as compared to other similar morphometric symbols such as letters (Shum et al., 2013, Figure 1.6a). Follow-up fMRI studies reported similar selectivity to Arabic numerals in the VTC (Yeo, Wilkey, & Price, 2017).

However, the activity pattern observed in the pITG during arithmetic processing seems to be much richer than what has been proposed. First, Abboud et al. (2015) trained congenitally blind subjects to recognize the symbols I, V and X which were transformed into sound using a visual-to-music sensory-substitution device. The transformed symbols also carried color information (blue, red and white). Next, the authors measured fMRI activity from trained subjects while they were asked to identify the identity either the Number (Roman numerals), Letter or Color of the stimuli. The contrast between Number vs. Letter and Color revealed a significant activity in the right pITG, largely overlapping with the ECoG sites reported by Shum et al. (2013), thereby showing that the number-related activity in the pITG is not exclusively visual (Figure 1.6b). Secondly, in the study of Amalric and Dehaene (2016), the authors observed that the contrast between math and non-math statements in mathematicians activated the bilateral pITG, which intersected with the several contrasts involving arithmetic processing from a visual localizer task (number vs. other pictures and calculation vs. sentence processing). Critically, the math statements were presented in the auditory modality and did not contain any number words, again indicating that the pITG is not merely a visual processor. Last, a recent ECoG study have teased apart the responses to arithmetic processing of two different neuronal populations just a few centimeters apart from each other, within the pITG. Daitch et al. (2016) asked participants to solve three tasks: symbol identification (Arabic numerals, letter from the Latin alphabet and letters from foreign alphabets), additions vs. memory verification ( $15+3=17$  vs. ‘I ate fruit yesterday’), and single-digit additions in which the elements were sequentially presented (Figure 1.6d). They first observed some VTC sites that were selective to Arabic numerals in the symbol identification task (the NFA). However, adjacent sites that did not show any significant response to isolated Arabic numerals, were highly selective to addition problems, as compared to memory statements in the second task. Crucially, during sequentially presented additions, the same sites responded stronger and in some cases exclusively to the second operand and the proposed result, which are critical periods when number manipulation is required (see also Hermes et al., 2015). The authors also observed a high functional connectivity between the pITG calculation-selective sites and sites in the anterior IPS that were also selective to calculation (Figure 1.6e).

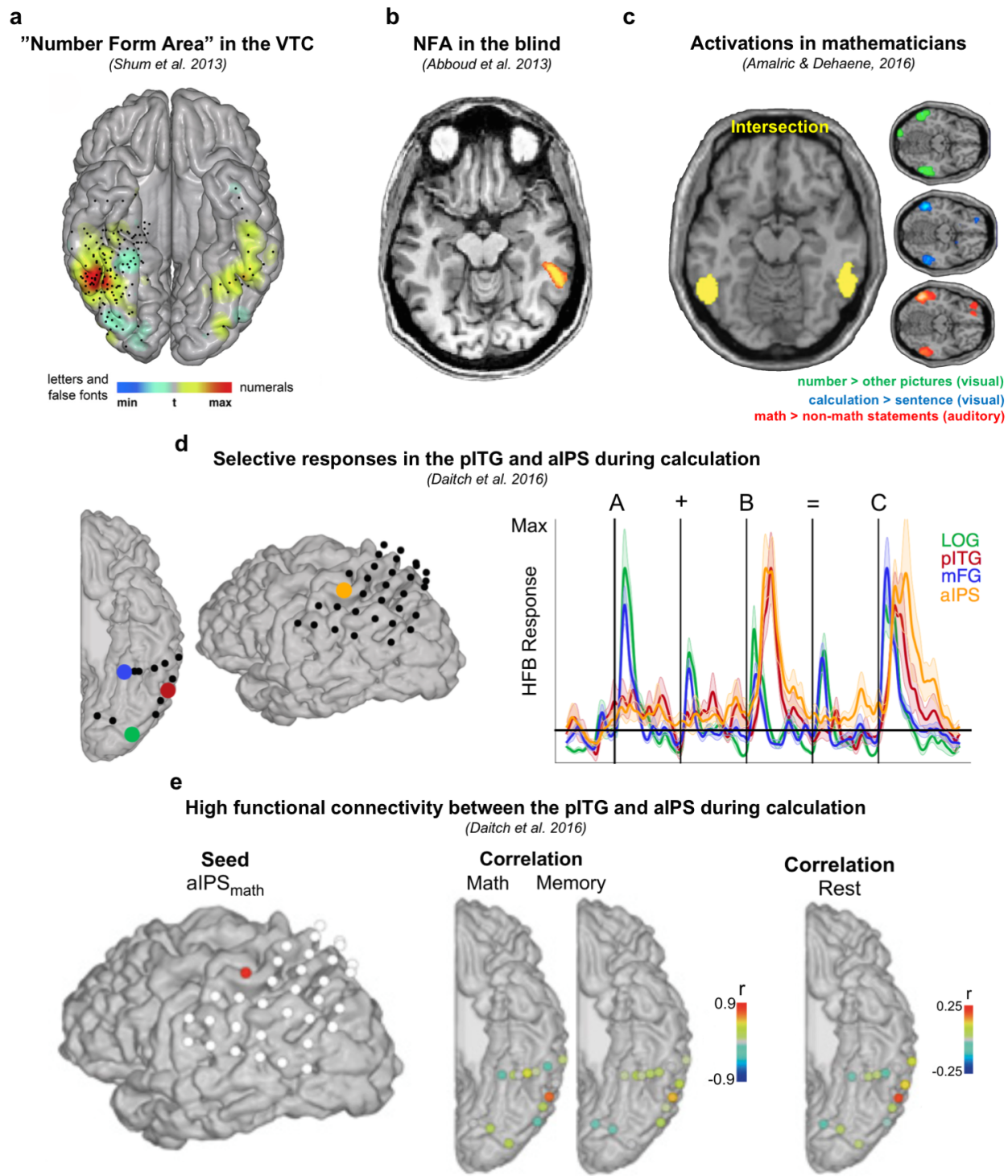


**Figure 1.6 Arithmetic processing in the ventral temporal cortex**

A) Selective ECoG responses for Arabic numerals as compared to other morphometric similar objects in the human pITG. Adapted from (Shum et al., 2013). B) fMRI study with congenitally blind subjects. The task required subjects to name either the Number, Letter or Color of the symbols I, V and X, which were transformed into sound using a visual-to-music sensory-

substitution device. The activation in the pITG represents the contrast of Roman numerals vs. Letter and Colors. Adapted from (Abboud et al., 2015)C) Results from an fMRI study showing an overlap (yellow) between regions more activated for number vs. other pictures (green; mathematicians and controls in a visual localizer task), calculation vs. sentence processing (blue; mathematicians and controls in a visual localizer task) and math vs. non-math statements (red; statements where presented in the auditory modality). Adapted from (Amalric & Dehaene, 2016). D) ECoG responses in an exemplar subject with coverage in both VTC and LPC. The HFB activity in adjacent neuronal populations to the NFA - also within the pITG – and in the anterior IPS is selective to the second operand and proposed result in a sequentially presented single-digit addition task. In contrast, control regions in the lateral occipital gyrus (LOG) and medial fusiform gyrus (mFG) respond to all elements of the calculation. E) The same exemplar subject as in D, showing higher correlations of HFB activity between the aIPS and the calculation selective site in the pITG, during calculation (math) and rest vs. sentence comprehension (memory) conditions. D and E are adapted from (Daitch et al., 2016).

In summary, these results suggest that pITG might be involved in mathematical processing beyond visual recognition of numbers, which is not predicted by current neurocognitive models of arithmetic and surprising given the traditional view of the VTC as the last stage of the ventral ‘what’ visual pathway, associated with object categorization (Grill-Spector & Weiner, 2014). However, all the studies that investigated the role of pITG in arithmetic processing so far were restricted to either contrasts between numerals and similar morphometric symbols or between calculation and other tasks (e.g., memory/sentence comprehension), thus never testing if, how and when the activity in pITG is modulated by numerical features of calculations. Consequently, the precise role of VTC in mathematical cognition remains largely elusive.

## 1.5 Introduction to the experimental contributions

One of the most fundamental problems in psychology is to characterize the series of successive processing stages underlying a given cognitive task. The traditional approach, which dates to Donders in the late 19th century (Donders, 1969), is *mental chronometry*. This approach uses RTs to infer the dynamics of mental operations. The core assumption is that RT indexes the duration of the operations, and in turn their complexity. If the operations are serial, RT would reflect the sum of their durations, and if they run in parallel, RT would reflect the duration of the

slower operation. Therefore, by manipulating experimental factors that would affect the processing time of specific operations, one can examine whether they unfold serially or in parallel (Dehaene, 1996; Sternberg, 1969, 2013). RTs can also reveal more specific patterns – for example, the psychological refractory period effect, PRP (Pashler, 1984; Sigman & Dehaene, 2005) is typical to situations where two tasks have initial stages that can run in parallel followed by a central bottleneck process.

Nevertheless, reaction time is only a *summary measure*: it reflects aggregate, thus indirect, information about the nature of the underlying operations. It can only be used to indirectly inform about serial vs. parallel implementation and the relative durations of each stage, but it is completely blind to the order in which the operations were executed and their absolute timing.

Since my goal in the present dissertation was to investigate the neurocognitive mechanisms of arithmetic calculations and how they unfold over time and across the brain, I chose a multimethod approach that combined continuous measurement of behavior, intracranial electroencephalography (iEEG), and machine learning applied to magnetoencephalography (MEG) signals. In following section, I briefly introduce the main advantages and limitations of each method and finally I provide an overview of how they helped me examine the specific questions that guided this work.

## 1.5.1 Methodology

### 1.5.1.1 Trajectory tracking

Recently, a new continuous behavior method was introduced, potentially offering a more direct solution to the problem of parsing the processing stages involved in cognitive tasks: *trajectory tracking*. In a typical setting, subjects respond by pointing from a fixed ‘start’ point to a given target location, either with their finger or with the mouse, and the full pointing trajectory is recorded as a series of time stamped *x* and *y* (and sometimes *z*) coordinates (Buc Calderon, Verguts, & Gevers, 2015; Dotan & Dehaene, 2013; Finkbeiner, Song, Nakayama, & Caramazza, 2008; Freeman & Ambady, 2010; Resulaj, Kiani, Wolpert, & Shadlen, 2009; Santens, Goossens,

& Verguts, 2011; Song & Nakayama, 2009). The core assumption is that the pointing trajectory reflects the ongoing cognitive activity. Therefore, analyzing the trajectories during the evolution of the trial can inform about the cognitive states at each time point, thus revealing the succession of processing stages (Berthier, 1996; Dotan & Dehaene, 2016; Dotan, Meyniel, & Dehaene, 2017; Erb, Moher, Sobel, & Song, 2016; Fitts, 1954; Friedman, Brown, & Finkbeiner, 2013; Resulaj et al., 2009). Indeed, trajectory tracking has proved to be a powerful method to investigate covert stages involved in decision-making (Buc Calderon, Dewulf, Gevers, & Verguts, 2017; Dotan, Meyniel, et al., 2017; Friedman et al., 2013; Lepora & Pezzulo, 2015; Scherbaum, Dshemuchadse, Fischer, & Goschke, 2010; Zgonnikov, Aleni, Piironen, O'Hora, & di Bernardo, 2017), subjective confidence estimation (Dotan, Meyniel, et al., 2017; Van Den Berg et al., 2016), cognitive control (Erb et al., 2016), number processing (Dotan & Dehaene, 2013, 2016; Dotan, Friedmann, & Dehaene, 2014; Faulkenberry, Cruise, Lavro, & Shaki, 2016; Marghetis, Núñez, & Bergen, 2014; Santens et al., 2011; Song & Nakayama, 2008), and syntactic processing (Al-Roumi, Dotan, Yang, Wang, & Dehaene, 2017).

Although very promising, the specific methods to maximally and unambiguously extract information from trajectory tracking are still under development. Current approaches rely on several assumptions that need to be carefully verified and potential biases related to motor activity and geometric factors must be taken into account. In collaboration with Dror Dotan and Stanislas Dehaene, I am working on a methodological paper (Dotan, Pinheiro-Chagas, & Dehaene, 2017) in which we describe the methods that we have been using (and critically compare to alternative approaches), which are implemented in an open source Matlab Toolbox ‘TrajTracker’, specifically developed to analyze trajectory tracking data (<http://trajtracker.com>).

### 1.5.1.2 Electrocorticography

The advent of neuroimaging methods, combined with behavioral measures, contributed to a remarkable improvement in our understanding of human cognition (Krakauer, Ghazanfar, Gomez-Marin, MacIver, & Poeppel, 2017). Typically, neuroimaging studies either use fMRI to investigate the functional maps or EEG/MEG to characterize the brain dynamics of cognitive

functions. However, the poor temporal resolution (and centimeter-scale spatial resolution) of fMRI and the poor spatial resolution of EEG/MEG impose a critical barrier to examine human cognition at a fine-grained level. Recently, this barrier started to be partially overcome by the blossoming of intracranial EEG or ECoG in cognitive neuroscience. The implantation of intracranial electrodes in human subjects occurs for medical proposes exclusively, in order to precisely localize and subsequently remove the source of seizures in the brain of patients suffering from medication-resistant forms of epilepsy. After implantation, these patients stay approximatively 6 to 10 days in the hospital with their brain activity constantly monitored. During this period, they are invited to participate in several cognitive experiments, which last about 2 to 3 hours per day and they typically report enjoying the interactions. Invasive recordings provide a unique opportunity to directly measure human brain activity with high signal-to-noise ratio, in a wide range of frequencies and with combined high temporal and spatial resolution (millimeter scale). ECoG has provided major advances in several fields, such as face processing (Parvizi et al., 2012), memory (Foster, Dastjerdi, & Parvizi, 2012), speech perception and production (Riès et al., 2017; Tang, Hamilton, & Chang, 2017), syntactic processing (Ding, Melloni, Zhang, Tian, & Poeppel, 2015), executive functions (Fonken et al., 2016; Voytek et al., 2015), attention (Daitch et al., 2013), arithmetic (Daitch et al., 2016; Hermes et al., 2015; Shum et al., 2013), etc.

Although ECoG solves the spatial vs. temporal tradeoff problem, it is also important to note several of its limitations. Since it is used for medical purposes, the scientist cannot choose how many and which sites to record from. Furthermore, it is often the case that the electrodes' coverage is sparse and restricted to a given brain region, thus making difficult to reproduce the results across many subjects. Finally, since the volunteers are in the process of preparing themselves for a brain surgery, the experimental designs must be simplified and the number of trials greatly reduced.

#### **1.5.1.3 Time-resolved multivariate pattern analysis**

Machine learning is flourishing in all domains of science and technology because of its exceptional predictive power. When applied to time-resolved brain signals in the framework of

decoding (King & Dehaene, 2014) and representational similarity analysis (RSA) (Kriegeskorte & Kievit, 2013), multivariate pattern analysis (MVPA) can be used to characterize the series of processing stages and mental transformations during cognitive tasks. Decoding analysis is typically implemented as a series of multivariate estimators aimed at predicting a vector of labels ( $y$ ) from a matrix of features composed by single-trial EEG/MEG amplitude signals ( $X$ , shape =  $n_{trials} \times n_{sensors} \times 1_{time\ sample}$ ). This procedure is then repeated for each time sample separately. One can also test if an estimator fitted across trials at time  $t$  can accurately predict the  $y$  value at time  $t'$ , therefore probing whether the coding pattern is similar between times  $t$  and  $t'$ . This procedure is known as the ‘temporal generalization method’ (King & Dehaene, 2014). RSA analysis are typically implemented by (1) calculating a dissimilarity matrix based on the pairwise correlation between experimental conditions across EEG/MEG sensors and (2) correlating the observed matrix with theoretical dissimilarity matrices derived from the stimuli features. This procedure can also be repeated for each time sample separately. By testing the precise times in which a given mental content becomes decodable from or correlates with brain activity, these methods can shed light on the temporal evolution of the underlying neural codes. Time-resolved MVPA has been successfully applied to characterize the spatial-temporal dynamics of several cognitive functions, such dual-task interference (Marti, King, & Dehaene, 2015), attention (Brandman & Peelen, 2017; Kaiser, Azzalini, & Peelen, 2016), working memory (King et al., 2016; Trübtschek et al., 2017; Wolff, Jochim, Akyürek, & Stokes, 2017), reward value (Bach, Symmonds, Barnes, & Dolan, 2017), taste perception (Crouzet, Busch, & Ohla, 2015), object processing (Carlson, Hogendoorn, Kanai, Mesik, & Turret, 2011; Carlson, Tovar, Alink, & Kriegeskorte, 2013; Cichy, Pantazis, & Oliva, 2014; Isik, Meyers, Leibo, & Poggio, 2014), written and spoken language (Chan, Halgren, Marinkovic, & Cash, 2011; Kocagoncu, Clarke, Devereux, & Tyler, 2017), etc. It has recently been shown that MVPA exceeds the capacity of traditional evoked related potentials (ERP) univariate-level analysis to reveal fine-grained representations (Pantazis et al., 2017).

However, decoding results must be interpreted carefully, since the features used by the machine to learn about the task could be different than the ones used by the brain. Combining decoding with RSA, which explicit specify the relevant stimulus features, is therefore

recommended (Cichy et al., 2014), and robust cross-validation schemes must be used to ensure reproducibility and avoid overfitting (Varoquaux, 2017).

### 1.5.2 Overview of this dissertation

The dissertation is organized in three main chapters, corresponding to the three studies that I conducted in collaboration with Dror Dotan, Amy Daitch, Josef Parvizi, Manuela Piazza and Stanislas Dehaene.

In **Chapter 2**, I present a novel application of the trajectory tracking method to investigate simple arithmetic, with the goal of overcoming the limitations inherent to the *mental chronometry* approach, which has dominated the field during the past four decades. Subjects solved single-digit additions and subtractions on a tablet computer, and responded by pointing to the position of the result on a horizontal number line, while their finger trajectory was continuously monitored. By applying a series of successive multiple regression models, in which the dependent variable was the position of the finger at each time point and the predictors were several features of the calculation (e.g., first and second operands, the operation sign, etc.), I characterize the series of covert processing stages underlying mental calculation.

In **Chapter 3**, I investigate at a fine-grained level the neural correlates of some of the mechanisms identified in Chapter 2. I was specifically interested in re-evaluating the functional roles of the main hubs for arithmetic processing in the LPC and VTC, in light of the recent hypothesis that the VTC contains neuronal populations that are selectively engaged in mathematical reasoning, above and beyond simple digit recognition. For that, I analyzed ECoG signals from a task in which subjects were asked to judge the correctness of visually presented additions in a fixed form of ‘ $13+5=17$ ’, in which we systematically varied the magnitude of the operands. This allowed me to test if, how and when the activity in the IPS, SPL and pITG are modulated by the arithmetic problem-size.

In **Chapter 4**, I examine the neurocognitive mechanism of arithmetic calculations at the whole brain level, using time-resolved multivariate decoding and RSA applied to MEG signals. Subjects were asked to verify the correctness of additions and subtractions such as ‘ $3+2=5$ ’, in

which the successive symbols were presented sequentially. Results provided a comprehensive picture, at the single-trial level, about the temporal evolution of the representational codes underlying the operands and a cascade of partially overlapping successive processing stages underlying mental calculation and decision-making.

Finally, in **Chapter 5** I summarize, integrate and discuss the original contributions of the dissertation, acknowledge the main limitations and outline some of the future directions of my research program.

## Chapter 2. FINGER-TRACKING REVEALS THE COVERT STAGES OF MENTAL ARITHMETIC

---

### 2.1 Motivation

As discussed in the **Introduction**, the cognitive arithmetic literature has traditionally relied on the chronometric properties of the arithmetic problem-size effect to build models of mental calculation. But the *mental chronometry* approach is completely blind to the order and absolute timing in which each successive mental operation occurs.

In the first study of the dissertation, my goal was to overcome this limitation, by developing a continuous behavioral method, based on trajectory tracking, to directly observe the covert stages involved in combining two numbers into a third. The following main questions motivated this study. Are the two operands processed serially or in parallel? And does the processing of the operands differ between additions and subtractions? Is there a stage whose duration increases linearly with the size of the numerical quantities, as implied by models of counting or movement along the mental number line? Can we determine the moment when the visuospatial biases underlying addition and subtraction occur?

## 2.2 Abstract

We introduce a novel method capable of dissecting the succession of processing stages underlying mental arithmetic, thus revealing how two numbers are transformed into a third. We asked adults to point to the result of single-digit additions and subtractions on a number line, while their finger trajectory was constantly monitored. We found that the two operands are processed serially: the finger first points towards the larger operand, then slowly veers towards the correct result. This slow deviation unfolds proportionally to the size of the smaller operand, in both additions and subtractions. We also observed a transient operator effect: a plus sign attracted the finger to the right and a minus sign to the left and a transient activation of the absolute value of the subtrahend. These findings support a model whereby addition and subtraction are computed by a stepwise displacement on the mental number line, starting with the larger number and incrementally adding or subtracting the smaller number.

## 2.3 Introduction

Despite decades of research in cognitive arithmetic, how the brain performs elementary arithmetic calculations remains largely unknown. The widely replicable problem-size effect is the finding that reaction times (RTs) and error rates increase as a function of the size of the operands to be added or subtracted. By investigating the properties of the problem-size effect across operations and during development, researchers have proposed different cognitive models of arithmetic (Zbrodoff & Logan, 2005).

In their seminal study, Groen and Parkman (1972) found that the best predictor of single-digit addition RTs in first graders was the size of the smaller operand (*min*). They proposed that children use a counting strategy to solve additions by starting from the larger operand and then incrementing it with the *min*, with a slope of about 410 ms per unit. A much smaller slope, however, was found in adults (20 ms/unit). This seemed too fast for a counting strategy, and the authors proposed that adults directly retrieve the results from long-term memory.

Fact retrieval is thought to be a dominant strategy in adults, but some data show that it is also supplemented by other strategies (Lefevre & Kulak, 1994; Siegler, 1987; Zbrodoff & Logan, 2005). For instance, Butterworth, Zorzi, Girelli, & Jonckheere and (2001) proposed that, given the commutativity of addition, only half of the table may be stored in long-term memory (problems in which the first operand is larger than the second, which could be progressively committed to memory as a result using the *min* counting strategy at a younger age). To solve problems presented in the opposite order (e.g., 2+7), participants would reorder the operands prior to retrieval. Adults' RTs for additions were indeed found to be higher when the first operand was smaller, presumably due to this additional reordering stage.

Some models propose that arithmetic problems are solved by quantity manipulation, possibly relying on an “mental number line” (Dehaene, Spelke, Pinel, Stanescu, & Tsivkin, 1999). Considerable research indicates that children and adults possess such a space-like left-to-right numerical representation, and that arithmetic may involve internal movements on this representation (Barrouillet & Thevenot, 2013; Dehaene & Changeux, 1993; Fayol & Thevenot,

2012; Knops, Viarouge, Dehaene, et al., 2009; Knops, Thirion, et al., 2009; Mathieu et al., 2016; McCrink et al., 2007; Restle, 1970; Uittenhove et al., 2016). Accordingly, mental arithmetic causes spatial biases similar to the SNARC effect with single numbers (Dehaene, Bossini, & Giraux, 1993): addition draws attention and eye movements towards the right side of space, and subtraction towards the left (Knops, Viarouge, Dehaene, et al., 2009; Mathieu et al., 2016; Pinhas, Shaki, & Fischer, 2014). There is also a tendency to overestimate the results of addition and to underestimate the results of subtractions, which can be interpreted as an excessive motion on the number line and has therefore been termed the “operational momentum” (OM) effect (Knops, Viarouge, Dehaene, et al., 2009; McCrink et al., 2007). However, it is still unknown whether those effects betray a genuine use of the number line during calculation, or merely an automatic attraction to the result after it has been calculated.

Progress in understanding mental arithmetic is impeded by the fact that RTs and error rates provide only a single summary measure of the entire calculation process, blind to the succession of intermediate stages. Here, we introduce an on-line measurement method that addresses this temporal dissection problem: continuous finger tracking (Dotan & Dehaene, 2013, 2015; Song & Nakayama, 2009; see also Freeman & Ambady, 2010 for a similar approach with mouse tracking). Participants solved single-digit additions and subtractions on a tablet computer, and responded by pointing to the position of the result on a horizontal number line ranging from 0 - 10, while their finger trajectory was continuously monitored. By identifying which cognitive factors affect finger location at each time point, we aimed to answer several questions: Are the two operands processed serially or in parallel? Is there a stage whose duration increases linearly with the size of the numerical quantities, as implied by models of counting (*min*) or motion on the number line? Can we visualize a reordering of the two operands when solving additions, as predicted by the comparison model? And can we determine the moment when the visuo-spatial biases underlying addition and subtraction occur?

## 2.4 Methods

Thirty right-handed French adults, aged between 20 and 45 (mean = 24; sd = 5) participated in the study. The participants saw a series of single-digit addition and subtraction problems on a tablet computer and were instructed to point at the position of the result on a horizontal number line marked with 0 and 10 at its extremities (see Figure 2.1). On each trial, participants first touched an initiation rectangle, which made a fixation cross appear above the middle of the number line. When participants started moving their finger towards the number line, an arithmetic operation appeared at fixation for 250 ms. Participants then continued moving their finger to what they judged to be the position of the result. When the finger reached the number line, a feedback arrow indicated the location where the finger landed.

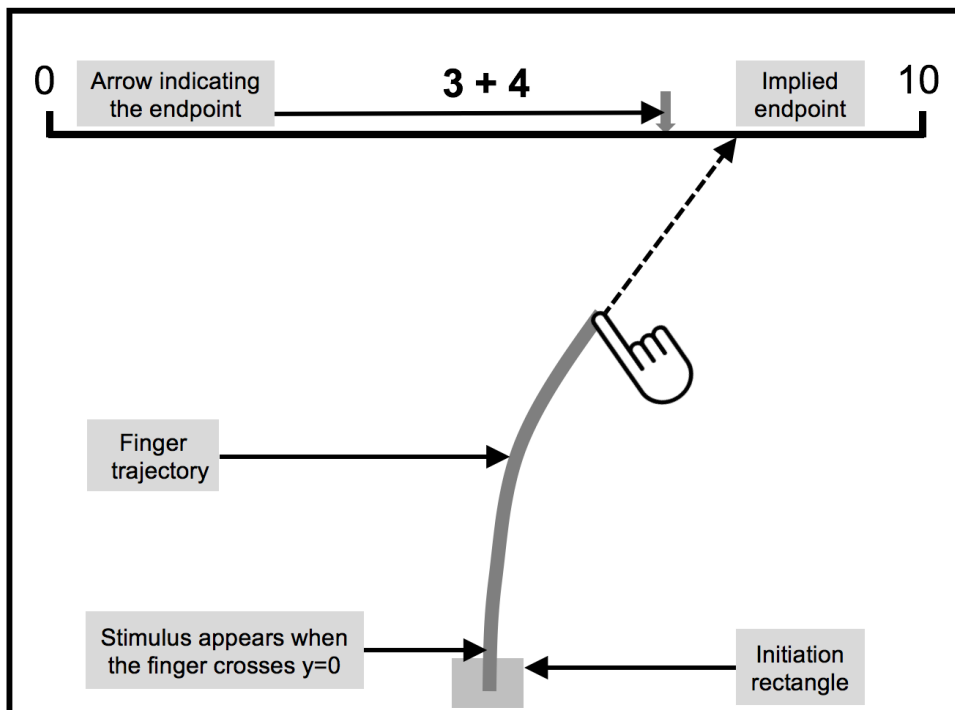


Figure 2.1 Finger-tracking task and screen layout

Using an Apple iPad-2 in landscape orientation, finger position was sampled at 60 Hz (1 ms accuracy), resampled at exactly 100 Hz using cubic spline interpolation, and smoothed (Gaussian,  $\sigma = 20$  ms). For each time point, we calculated the instantaneous direction as the

vector difference between the finger coordinates at times  $t-10$  ms and  $t$ , and the *implied endpoint* (*iEP*) as the position on the number line that the finger would reach if it kept moving straight in this direction.

The experiment included two blocks, presented in random order, both mixing single-digit additions and subtractions (individual digits were also presented, but are not reported here). The blocks were designed to control for possible confounds in the analyses of the OM effect. Block 1 included all single-digit addition and subtraction problems with matched operands between 1 and 9 (e.g., 4+3 and 4-3), resulting in 25 additions with larger-first operand (denoted L+S, where L is the larger and S the smaller number) and 25 subtractions (L-S). Each problem was repeated six times, for a total of 300 trials. In this block, addition results are generally larger than subtraction results, and thus the presence of an OM effect could be due to this bias. As a control, we therefore used matched results in block 2. We started from the 54 additions and 45 subtractions with operands ranging from 0 to 9 and results ranging from 1 to 9 (thus including L+S, S+L, and L-S problems). If each problem appeared exactly once, the distribution of addition and subtraction results would again be asymmetrical. Therefore, we over-repeated some problems to obtain exactly 20 addition and 20 subtraction trials for each of the results 1-9 (total of 360 trials). By construction, block 2 contained all the problems presented in block 1. Therefore, the OM effect could be investigated in a most unbiased manner by restricting the analysis to addition and subtraction problems from block 1 (with identical operands) that were presented in block 2 (with equalized distributions of response locations). The two blocks also allowed us to test the stability of our findings.

Trajectory analysis followed the method introduced in Dotan and Dehaene (2013). First, for each participant, one regression was run per time point in 30 ms intervals. The dependent variable was the *iEP*. Predictors were the two operands, the operator (- or +, coded as -1 and 1), the spatial-reference-points-based bias function (SRP, see Supplementary Materials) and the result of the previous trial. The latter two predictors were added in all regressions in order to capture maximal variance, as they were significant in previous studies (Dotan & Dehaene, 2013). As their effect was virtually identical in all conditions, they are only reported in Supplementary Materials.

At a second stage, we compared the b values of the different predictors (paired *t-test* or repeated-measures ANOVA). To examine whether a given predictor has a significant group-level effect in each time point, we compared the participant's b values to zero using one-sample *t-test*. Each b value (also called regression weight) provides a quantitative measure of the extent to which each element of the operation influences the finger trajectory at each time point. The reported *p* values are one-tailed, since we assumed that all effects of all predictors included would be positive.

## 2.5 Results

### 2.5.1 Movement time

We first analyzed the overall movement time (MT) from stimulus presentation to number-line touch (equivalent to RT in oral calculation tasks). In both blocks, MT was longer for subtractions compared to additions L+S (Block 1: additions L+S: mean = 966 ms, SD = 118 ms; subtractions: mean = 1040 ms, SD = 138 ms;  $t_{(29)} = -14.72$ ;  $p < .001$ ;  $d = -.58$ . Block 2: additions: mean = 982 ms, SD = 127 ms; subtractions: mean = 1,072 ms, SD = 156 ms;  $t_{(29)} = -12.55$ ;  $p < .001$ ;  $d = -.64$ ). In agreement with the COMP model of Butterworth et al. (2001), additions L+S were solved 14 ms faster than additions S+L (Block 2: additions L+S: mean = 976 ms, SD = 128 ms; additions S+L: mean = 990 ms, SD = 125 ms;  $t_{(29)} = -5.23$ ;  $p < .001$ ;  $d = -.11$ ). To investigate the problem-size effect, we performed a stepwise multiple regression with MT as the dependent variable and the *Min operand*, *Max operand* and *Result* as predictors, separately for additions and subtractions in each experimental block. The best predictor of MT was always the *Min operand* (insets in Figure 2.2). For additions, the *Min operand* had a b value of 26 ms per unit ( $p < .001$ ) in block 1 and of 21 ms per unit ( $p < .001$ ) in block 2. The *Max operand* had a small but significant negative effect in block 1 ( $b = 8$  ms per unit;  $p < .001$ ), but a null effect in block 2 ( $p = .895$ ). Finally, the *Result* had a null effect in both blocks ( $p = 0.8$ ). For subtractions, the *Min operand* had a b value of 62 ms per unit ( $p < .001$ ) in block 1 and of 44 ms per unit ( $p < .001$ ) in block 2. The *Max operand* had a null effect in both blocks ( $p > 1$ ). Finally, the *Result* had a small but significant effect in both blocks ( $b = -4.53$  ms;  $p = .002$  in block 1 and  $b = -7.07$

ms;  $p < .001$  in block 2). Overall, the dominant effect of the *Min operand* is therefore consistent across both blocks and operations.

### 2.5.2 Accuracy

Next we analyzed response accuracy, that is, the location where participants landed their finger (endpoint) in relation to the ideal location. The *endpoint error* is the absolute difference between the endpoint and the correct result (in numerical units). The *endpoint bias* is the mean difference between the endpoint and the correct result, with positive values indicating rightward bias. Subtractions produced larger endpoint errors, but this difference only reached statistical significance in block 1 (block 1: additions L+S: mean = .43, SD = .13; subtractions: mean = .47, SD = .180;  $t_{(29)} = -2.47$ ;  $p = .019$ ;  $d = -.26$ . Block 2: additions L+S: mean = .47, SD = .150; subtractions: mean = .48, SD = .180;  $t_{(29)} = -.20$ ;  $p = .841$ ,  $d = -.06$ ). Additions L+S produced a slight greater leftward endpoint bias compared to subtractions, but this difference was only significant in block 2 (block 1: additions L+S: mean = -.12, SD = .16; subtractions: mean = -.06, SD = .170;  $t_{(29)} = -1.24$ ;  $p = .226$ ;  $d = -.37$ . Block 2: additions L+S: mean = -.22, SD = .14; subtractions: mean = .02, SD = .160;  $t_{(29)} = -6.92$ ;  $p < .001$ ,  $d = -1.63$ ). Note that this effect is the opposite of the OM effect. A comprehensive analysis of the entire time course of the OM effect is presented further below (see Figure 2.5), but here we simply note that in block 2 subtractions had overall larger first operands as compared to additions (in order to yield matched results), which may have dragged responses further to the right for subtractions. No significant differences in endpoint error or endpoint bias were found between additions L+S and additions S+L (Block 2, endpoint error: additions L+S: mean = .45, SD = .15; additions S+L: mean = .47, SD = .160;  $t_{(29)} = -1.95$ ,  $p = .061$ ;  $d = -.13$ ; endpoint bias: additions L+S: mean = -.19, SD = .13; additions S+L: mean = -.20, SD = .16;  $t_{(29)} = .59$ ;  $p = .553$ ;  $d = .07$ ). Finally, with respect to the problem-size effect, the *Min operand*, which was the best predictor of movement times, was also a significant predictor of endpoint error in both additions and subtractions in both blocks (block 1 - additions:  $b = .41$ ,  $p < .001$ , subtractions:  $b = .43$ ,  $p < .001$ ; block 2 – additions:  $b = .44$ ,  $p < .001$ , subtractions:  $b = .42$ ,  $p < .001$ ).

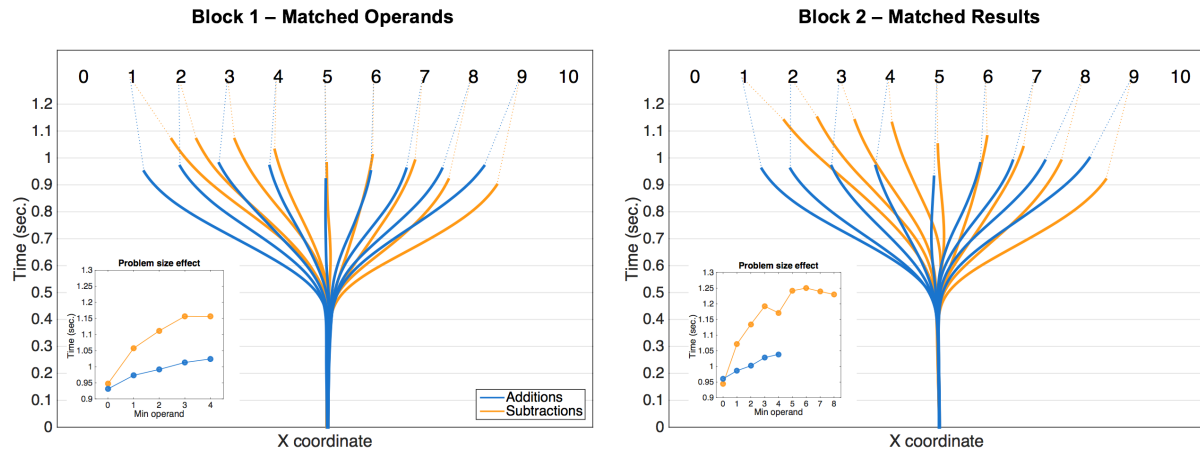


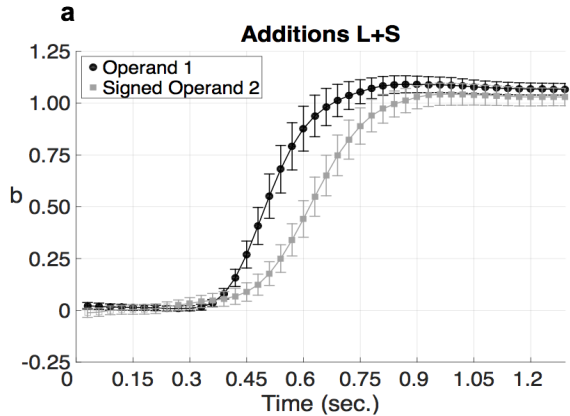
**Figure 2.2 Reconstructed trajectories averaged across subjects**

Insets show how movement time increases as a function of the *Min operand*.

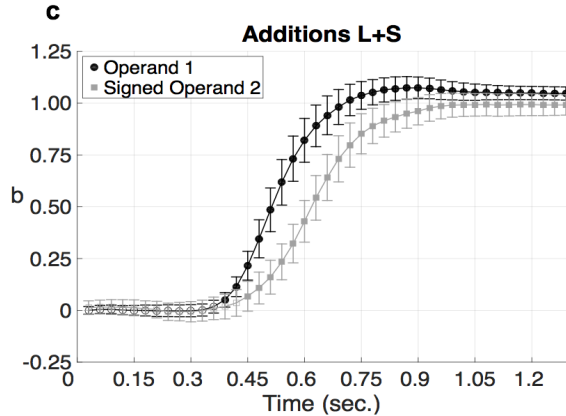
### 2.5.3 Trajectory dynamics

Next, we analyzed the full trajectories (Figure 3). The first question we considered was whether the operands are processed in parallel or serially. In additions with larger operand first ( $L+S$ ), regressions indicated that the finger first moved according to the first operand, and only then a significant effect of the second operand emerged. The first operand has a significantly higher effect compared to the second starting at 420 ms ( $p = .017$ ) in block 1 and at 450 ms in block 2 ( $p < .001$ ) and this difference remained significant until the end of the trajectory. Remarkably, for additions with smaller operand first ( $S+L$ ), the order was reversed: the second operand (larger number) had a higher weight compared to the first operand (smaller number) from 390 ms on ( $p = .047$ ), compatible with the assumption that the two operands are reordered prior to effecting the finger movement. This pattern remained stable until the end of the trajectory. In fact, the second operand (larger) deviated from zero at 390 ms ( $b[\text{signed\_op2}] = .057$ ,  $R^2 = 0.036$ ,  $t_{(29)} = 2.998$ ,  $p < .034$ ), 120 ms before the effect of the first operand at 510 ms ( $b[\text{op1}] = .064$ ,  $R^2 = .020$ ,  $t_{(29)} = 1.943$ ,  $p = .030$ ).

### Block 1 – Matched Operands



### Block 2 – Matched Results



**Comparison of b values to 0:**

- $p < .05$
- NS

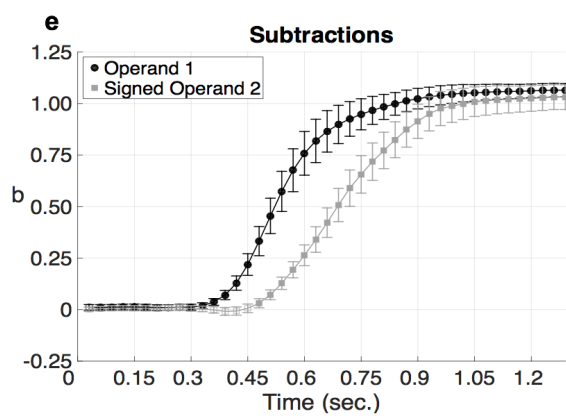
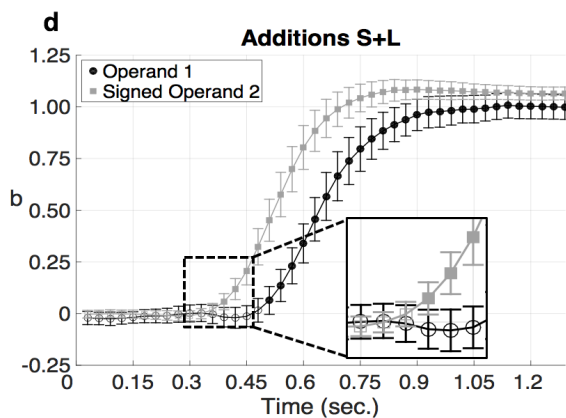
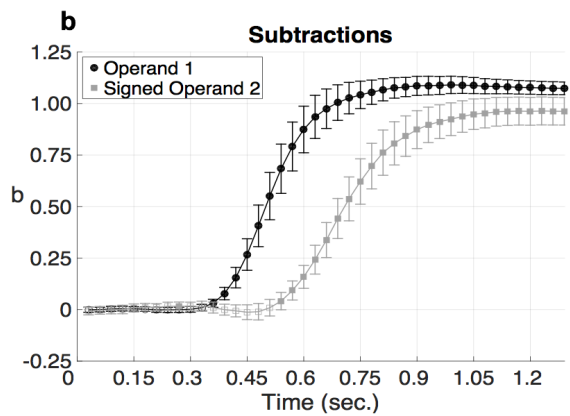


**Figure 2.3 Time course of the regression effects for additions per condition**

A,B) Block 1. C,D,E) Block 2. The b values were averaged over participants and plotted as a function of time. The b values were compared to zero (t-test), black dots denote  $p < .05$ . Error bars represent 95% confidence intervals.

In subtractions, a serial effect was again observed. The first operand had a higher effect than the second during almost the entire trajectory (from 390 ms on in block 1 and from 360 ms on in block 2). Both operations therefore indicate that the operands are processed serially: participants start processing the larger operand followed by the smaller, regardless of the order in which they appeared. Additional analyses (see Supplementary Materials) revealed that the finger first moved according to the larger operand L at the same time in all arithmetic operations, and then a correction was introduced for the smaller operand S at different delays ( $L+S < S+L < L-S$ ).

To directly visualize this serial processing pattern, we returned to the individual trajectories for specific problems. Figure 4a shows the example of subtraction problems “9-S” (where S ranges from 0 to 8), in which we could investigate the full spectrum of results 1-9. The plot shows that the finger first deviates towards the right (i.e., in the direction of the larger operand 9) and then to the correct result. Additionally, the latter correction seems to be progressive, as if the finger goes through intermediate stages. This is most clearly seen for the problem 9-8: the trajectory first coincides with that for 9-0, then 9-1, 9-2, etc. To characterize these effects, we subtracted consecutive trajectories (9-7)-(9-8), (9-6)-(9-7), etc., and plotted the resulting difference trajectories, thus revealing the time course of their divergence (Figure 4b). We then examined whether the divergence times increased with the *Min Operand*. Divergence time was measured as the moment when the difference in finger location ( $\Delta x$ ) achieved a threshold value. Regardless of the particular choice of threshold, regressions indicated that the divergence time increased with the number being subtracted ( $p < .001$ ) with a stable slope of about 60 ms per additional unit. Similar results were found for subtractions 8-S, 7-S, 6-S, etc. (slopes = 75, 66, 68 ms, respectively). In order to test whether the same pattern was also present in additions, we selected the problems 5+S and 5-S, since they have the larger range of S that can be matched between operations. Both subtractions 5-S (mean slope = 55 ms) and additions 5+S (mean slopes = 52 ms) showed a progressive deviation from the larger operand, proportional to the size of the *Min Operand*.

To investigate the OM effect, we pooled additions and subtractions (Figure 5). In block 1, the operator had a significant transient effect from 480 ms to 810 ms ( $b[\text{operator}] > .048$ ,  $R^2 > .005$ ,

$t_{(29)} > 2.335$ ,  $p < .013$ ), reaching its peak value at 630 ms ( $b[\text{operator}] = .170$ ,  $R^2 = .014$ ,  $t_{(29)} = 8.673$ ,  $p < .001$ ).

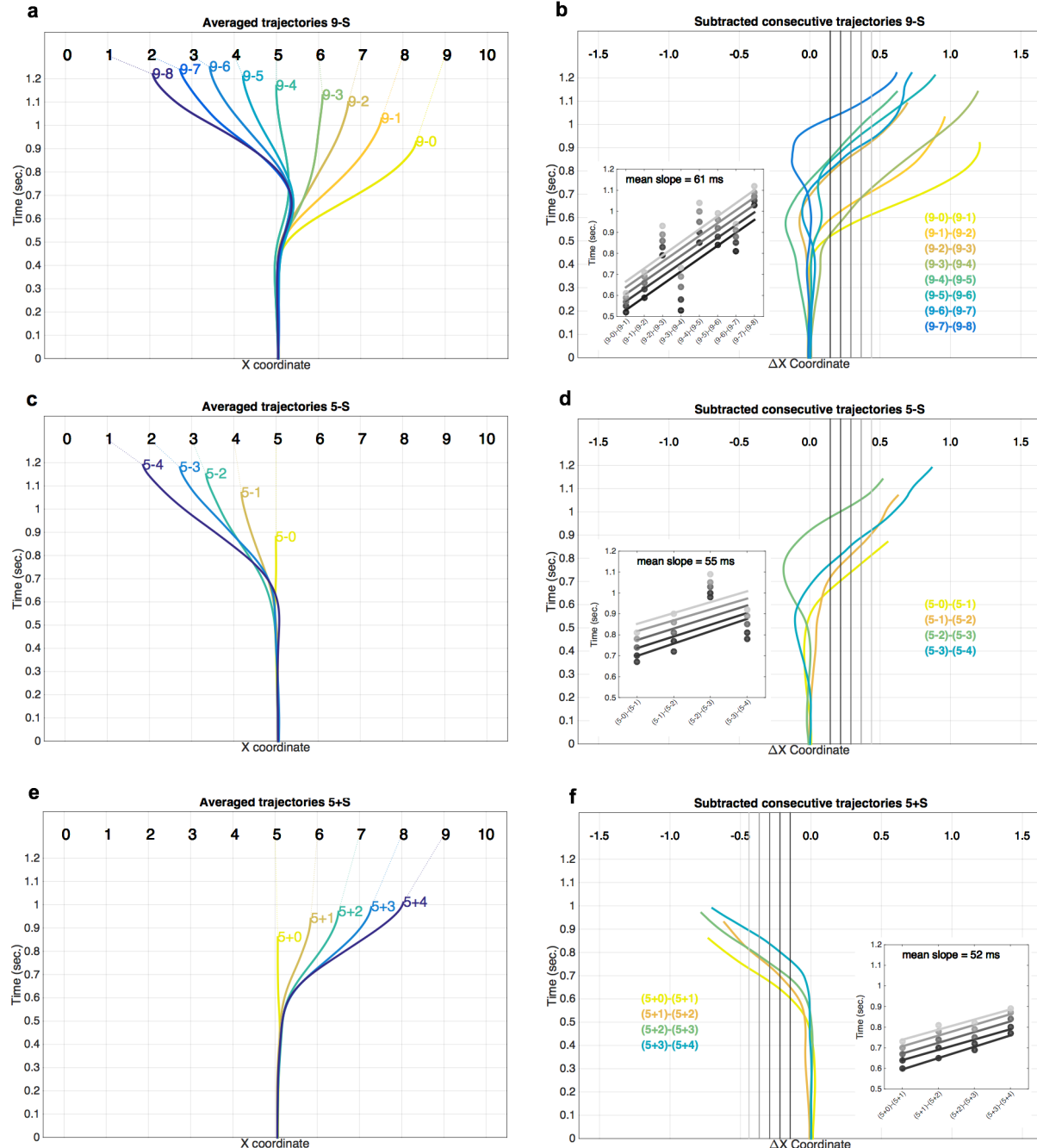


**Figure 2.4 Stepwise-displacement during additions and subtractions**

A,C,E) Reconstructed trajectories per operation, averaged across subjects. B,D,F). Subtracted consecutive trajectories. Insets show the divergence time as a function of the number being subtracted, for different  $\Delta X$  coordinate threshold.

The effect was positive, indicating that an addition sign transiently distorts the trajectory towards the right side of the number line, and a subtraction sign towards the left side, as expected from the OM effect. The results remained essentially unchanged when we analyzed the same arithmetic problems as in block 1, but now using the data from block 2, i.e., with an unbiased distribution of result size for addition and subtraction. There was a significant positive transient effect of the operator (210 ms) from 510 ms to 720 ms. ( $b[\text{operator}] > .069$ ,  $R^2 > .009$ ,  $t_{(29)} > 1.913$ ,  $p = .033$ ), reaching its peak  $b$  value at 600 ms ( $b[\text{operator}] = .096$ ,  $R^2 = .008$ ,  $t_{(29)} = 3.973$ ,  $p < .001$ ) and then progressively dropping until loosing statistical significance at 750 ms.

An interesting visualization of the OM effect is provided by addition and subtraction problems involving zero ( $x+0$  and  $x-0$  problems), which can be directly compared with single-digit controls where  $X$  alone is presented. As shown in Figure S3, when plotting the implied endpoints per time, subtractions show a systematic transient leftward bias, additions a rightward bias, and single-digits tend to fall in between. This variant of the OM effect was statistically confirmed in a regression analysis comparing additions  $x+0$  and subtractions  $x-0$  (insets in Figure S3).

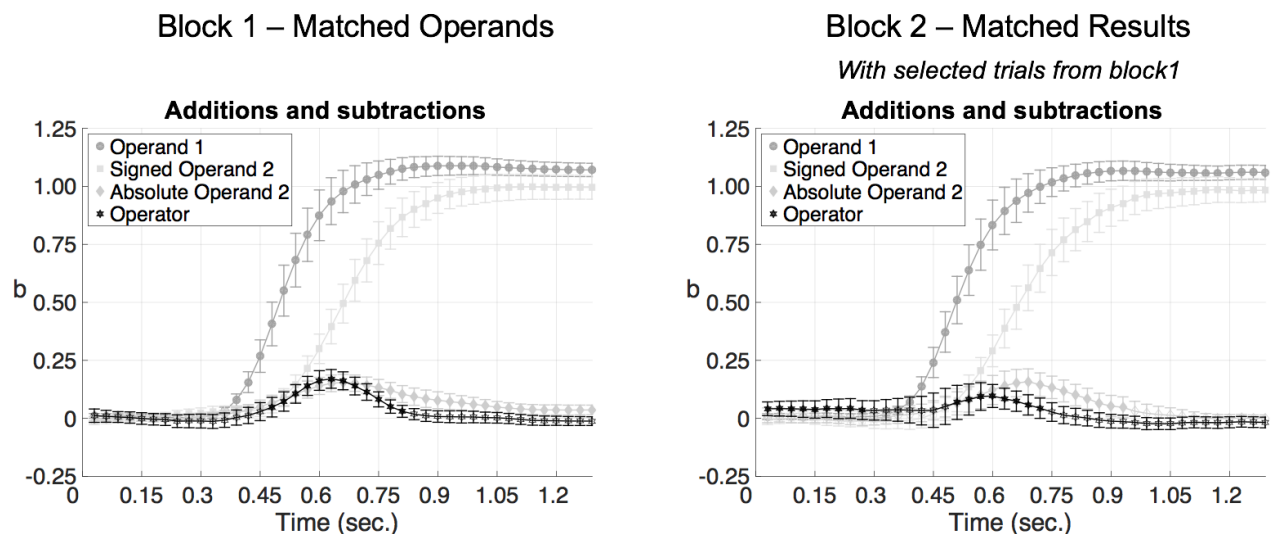


**Figure 2.5 Time course of the Operational Momentum effect**

A) Block 1. B) Block 2 with the selected trials of block 1.

Interestingly, at about the same time as the effect of the operator, we observed a significant transient effect of the absolute value of the second operand in both blocks (block 1: from 330 ms on  $b[abs\_2op] = .017$ ,  $R^2 = .003$ ,  $t_{(29)} = 1.994$ ,  $p < .028$ , peak b at 510 ms; block 2 from 510 ms to 960 ms,  $b[abs\_2op] > .078$ ,  $R^2 > .012$ ,  $t_{(29)} > 3.233$ ,  $p < .001$ ; peak b at 690 ms). The effects of  $b[op1]$  and  $b[signed\_op2]$  were highly similar to the ones found in previous regression analyses, with the effect of  $b[signed\_op2]$  delayed as compared to  $b[op1]$ .

In brief, the temporal dynamics of the OM effect revealed a spatial bias induced by the operator coinciding with the time that participants are processing the second operand. Furthermore, participants also seemed to transiently represent the absolute value of the subtrahend.

## 2.6 Discussion

By continuously measuring finger position in an original calculate-and-point task, we obtained a detailed picture of the processing stages underlying addition and subtraction. Importantly, overall movement time and accuracy replicated previous findings in cognitive arithmetic, indicating that our task did not depart radically from previous oral calculation tasks. Subtractions were solved slower and less accurately than additions, and within additions, those with smaller first operand were solved 14 ms slower than those with larger first operand (Butterworth et al. (2001) reported a 13 ms difference). This effect is not trivial, since it runs opposite to what could have been predicted in the light of spatial-numerical congruency effects, such as the SNARC (Dehaene, Bossini, & Giraux, 1993) - i.e., that additions S+L, where digits are in the proper left-to-right order, would be solved faster than L+S.

In line with Barrouillet and Thevenot (2013) and Uittenhove et al. (2016), we also detected a robust problem-size effect in single-digit additions, even with operands in the range 0-4. The best predictor of movement time was the smaller operand (*Min*) in both additions and subtractions. The slopes that we found for additions (21 ms per unit in block 1 and 26 ms in block 2) match the slope of 26 ms reported by Barrouillet and Thevenot (2013). Finally, subtractions showed a

higher problem size effect than additions, also consistent with previous studies (Seyler, Kirk, & Ashcraft, 2003).

The main contribution of our study is to investigate the covert processing stages underlying arithmetic calculations. Regression analyses on instantaneous finger direction allowed us to uncover two new effects. First, in both additions and subtractions, the operands were processed in a serial way: participants started processing the larger operand, then the smaller operand, irrespectively of the order in which they appeared. In particular, we could directly observe a reordering in S+L additions, as predicted by the COMP model (Butterworth et al., 2001). The presence of an additional reordering stage may also explain why S+L additions were slower than L+S additions.

Comparing each predictor across additions and subtractions further revealed that the larger operand is processed at about the same time in all conditions, and then a correction is introduced for the smaller operand, at a variable delay (additions L+S < additions S+L < subtractions). A possible explanation for the higher delay in subtraction, revealed by regression, is that participants transiently represent the absolute value of the subtrahend. One additional processing stage may therefore be involved in subtractions: the conversion of the absolute value of the subtrahend into a negative number. Additionally, within addition problems, a possible explanation for the difference between L+S and S+L additions is that the selection of the smaller operand is faster when the numbers are in the appropriate left-to-right order.

Most importantly, we discovered a possible origin of the *Min* effect, reflected by a serial influence of the size of the second operand on finger trajectories. During an operation such as 9-8, the finger did not instantaneously point to the result 1, but slowly veered towards it, successively pointing to each intermediate location 9-0, 9-1, 9-2, etc. Analysis confirmed that, when the second operand increased, the trajectories diverged at increasingly later times: 9-8 diverged from 9-7 at a later time than 9-7 diverged from 9-6, and so on. Thus, calculation always starts with the larger operand and then the correct result is attained in a slow and incremental manner, proportional to the *Min* operand, with a slope of about 50-60 ms per unit.

The two serial stages that we identified - first point to the larger operand, then serially deviate towards the target number - strongly constrain the models of mental arithmetic that we outlined in the introduction. Our results are most compatible with models where arithmetic operations are solved by serial quantity manipulation, possibly relying on a mental number line (Dehaene et al., 1999). They fit precisely with the original Groen & Parkman (1972)'s *Min* Model of addition, in which subjects start with the larger number and count up the smaller quantity. The slope of that serial process was thought to be too fast for counting, but the present results do suggest a slow and serial incremental process. Its fast speed suggests a series of "jumps" on the mental number line, where quantities are chained by successor and predecessor operations, rather than an explicit verbal counting process.

Our finger-tracking task could have biased subjects to use approximation or other quantity-based manipulations. This possibility is unlikely, however, given that our movement-time results converge with classical studies of the problem-size effect (Groen & Parkman, 1972) and two of its most recent reexaminations. Using a classical calculation task with oral responses, Barrouillet and Thevenot (2013) and Uittenhove et al. (2016) presented robust evidence that additions are solved using "fast procedures that scroll an ordered representation such as a number line". The convergence of results suggest that the proposed model may not be restricted to the current experimental design, but may be generalized to other methods of measuring mental calculation. While previous studies could infer this underlying mechanism only indirectly, from the patterns of RT, our method provides a more direct look at the underlying processing stages.

The hypothesis of a mental displacement in quantity space also accounts for another aspect of the results, namely the operational momentum (OM). As previously reported (McCrink et al., 2007), additions produced a transient bias towards larger numbers and subtractions towards smaller numbers. Our results reject the hypothesis that OM originates solely from post-calculation processes, when the retrieved result attracts attention left or right. Rather, the present work shows that the OM effect coincides with the processing of the second operand, suggesting that movement on the number line occurs during the single-digit calculation process. This result concurs with the only study that actually investigated the timing of the OM effect during calculation, using mouse

tracking rather than finger tracking (Marghetis et al., 2014). It also fits with other studies suggesting that the visual-spatial attention system is actively involved in arithmetic calculations (Knops, Viarouge, Dehaene, et al., 2009; Knops, Thirion, et al., 2009; Mathieu et al., 2016; McCrink et al., 2007; Pinhas & Fischer, 2008).

Our results impose strong restrictions on retrieval-based models of single-digit additions (Ashcraft, 1992; Campbell, 1987; Siegler, 1987; Zbrodoff & Logan, 2005). These models postulate a direct access to a memory for arithmetic facts and therefore have no reason to postulate either a faster influence of the larger number, a linear effect of the smaller number, or an OM effect. Indeed, existing models of arithmetical retrieval typically assume that (1) the ease of retrieval depends on the frequency with which a problem has been encountered (Hamann & Ashcraft, 1986); (2) after a competition process, only a single result is ultimately selected (Ashcraft, 1992; Campbell, 1987; Siegler, 1987). Both properties fail to explain why the finger first points to the larger number and then slowly veers towards the correct result, in proportion to the *min*.

In order to preserve the memory retrieval model, one would have to propose a table-search model (Ashcraft & Battaglia, 1978) according to which calculation time reflects a search for the proper entry in a stored table of arithmetic facts. For instance, for a problem like 6+3, subjects would first identify the larger number (6), then list all 6+x problems, and finally search serially among them (6+1=7, 6+2=8, 6+3=9). Such a model is functionally equivalent to the above proposal, the only difference being that the movement occurs on a memorized table rather than a number line.

Overall, our findings highlight how a precisely timed series of operations underlies simple arithmetic. They also demonstrate that even complex mental operations can be continuously reflected in finger-pointing movements, as previously demonstrated in simpler cases (Song & Nakayama, 2009). Within the existing methods for investigating covert serial processes (King & Dehaene, 2014; Resulaj et al., 2009; Sternberg, 1969; Tanenhaus, Spivey-Knowlton, Eberhard, & Sedivy, 1995), finger tracking may play a special role as a simple and powerful behavioral method.

## **2.7 Acknowledgments**

This research was sponsored by INSERM, CEA, and the Bettencourt-Schueller Foundation. Dror Dotan is grateful to the Azrieli Foundation for the award of an Azrieli Fellowship. Pedro Pinheiro-Chagas gratefully acknowledges a Science Without Borders Fellowship from the Brazilian National Council for Scientific and Technological Development (CNPq) (nr. 246750/2012-0).

## 2.8 Supplementary Materials

### 2.8.1 Regression Analyses

The spatial-reference-points-based bias function (SRP, defined in equation [1]) and the result of the previous trial were added as predictors in all regressions in order to capture maximal variance, as they were significant in previous studies using the same method (Dotan & Dehaene, 2013). The SRP (or similar functions) was found important in several number-to-position studies and may reflect an anchoring on the middle and ends of the number line (Barth & Paladino, 2011; Dotan & Dehaene, 2013; Rouder & Geary, 2014; Slusser, Santiago, & Barth, 2013).

$$SRP(N) = 10 * \frac{\log(N + 1)}{\log(N + 1) + \log(11 - N)} \quad [1]$$

Overall, the results of these two predictors were very stable across all conditions. Figure 2.6 shows the example of the conditions in block 1. While the b[SRP] started around the beginning of the trajectory at 400 ms and remained stable with a moderate size ( $b = .5$ ) until the end of the movement, b[R-1] had a small initial effect ( $b = .2$ ), which vanished around 500 ms. This result was virtually the same for the conditions present in block 2.

Block 1 – Matched Operands

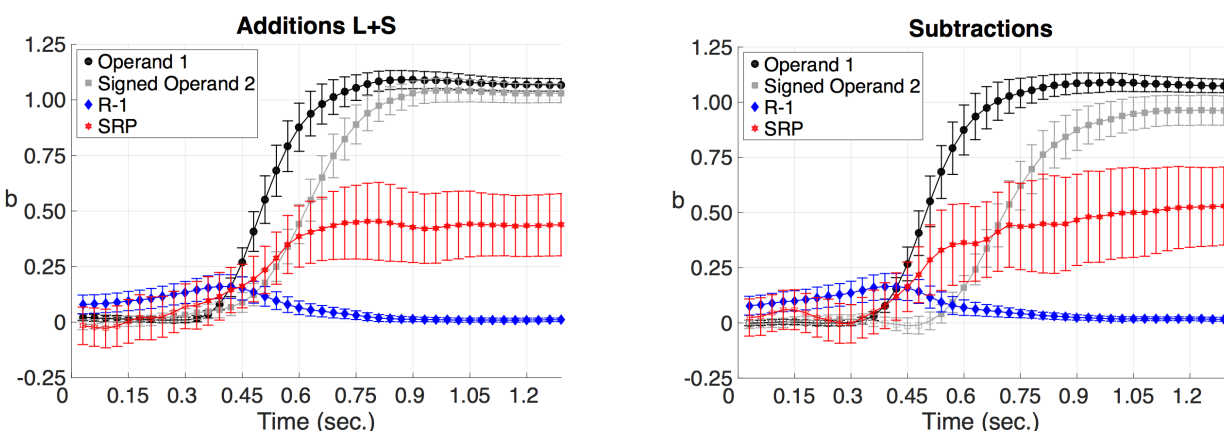
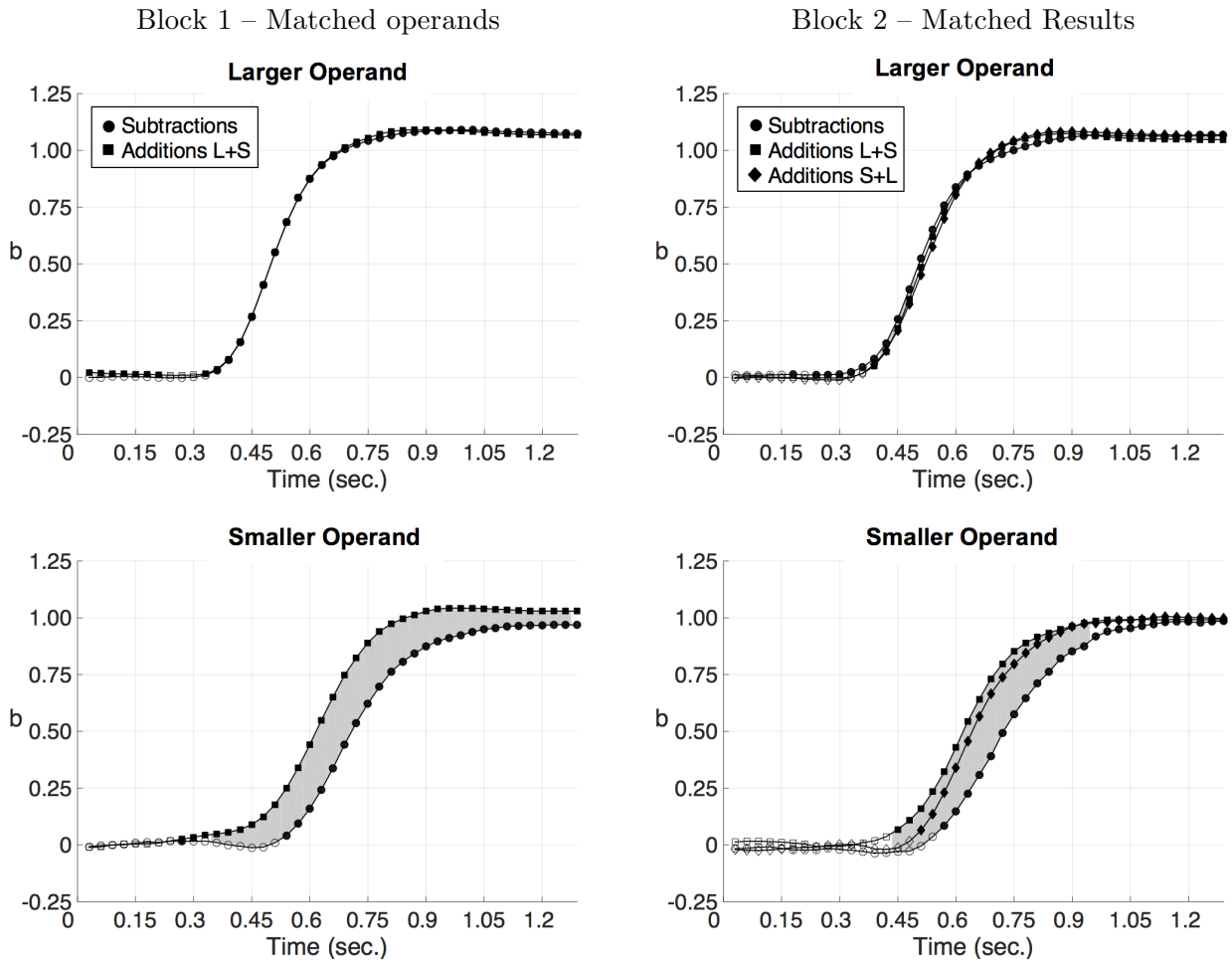


Figure 2.6 Time course for the regression effects of the predictors R-1 and SRP

## 2.8.2 Regression effects of smaller and larger operands.

To better understand the similarities and differences between additions and subtractions, we directly compared the b values between conditions, separately for larger and smaller operands (Figure 2.7). To ensure comparability of the results, in block 2 we selected only the subtractions that had the same range of operands as in block 1 (larger operand from 2 to 5 and smaller operand from 1 to 4). Interestingly, the effect of the larger operand was overall indistinguishable between all conditions in both blocks during the entire trajectory (block 1:  $t_{(2g)} > 1.634$ ,  $p > .066$  and block 2:  $F_{(2,2g)} > 1.292$ ,  $p > .059$ ), except for small time windows between 420 – 480 ms and 1230-1290 ms:  $F_{(2,2g)} < 2.172$ ,  $p < .038$ ). In contrast, the smaller operand showed significant differences between the conditions starting around 400-450 ms. In block 1, b[smaller] was larger in additions L+S compared to subtractions (from 450 ms until the end of the trajectory,  $F_{(2,2g)} > 2.29$ ,  $p < .03$ ). In block 2, the ANOVA showed a significant effect from 450 ms to 930 ms ( $F_{(2,2g)} > 2.484$ ,  $p < .0190$ ), with higher values in the additions L+S, followed by additions S+L and then by subtractions. In summary, those results indicate that (1) the finger first moves according to the larger operand L independently of the arithmetic operation; (2) a correction is then introduced for the smaller operand, at a variable delay (L+S < S+L < L-S). To precisely quantify this delay calculated the difference in time  $\Delta(t)$  between b[op1] and b[signed\_op2] when they reached a value of 0.5, i.e., the middle of the regression curves (a b value of 1 on both operands indicates perfect pointing to the result). Subtractions show a larger delay between the first and the second operand, compared to both types of additions in block 1 (additions L+S: mean = 107 ms, SD = 53 ms; additions S+L: mean = 124 ms, SD = .59 ms; subtractions: mean = 221 ms, SD = 103 ms;  $F_{(2,2g)} = 19.520$ ;  $p < .001$ ) and in block 2 (additions L+S: mean = 109 ms, SD = 37 ms; subtractions: mean = 207 ms, SD = 60 ms;  $t_{(2g)} = -8.352$ ;  $p < .001$ ;  $d = 2.001$ ).



**Figure 2.7 Comparison of the time course of the regression effects**

The shaded area indicates a significant difference ( $p < 0.05$ )

### 2.8.3 Operational momentum effect in zero-problems

When selecting only the zero-problems (problems such as  $x +/- 0$ ), which sometimes are referred as a more “pure” measure of the OM effect (Pinhas & Fischer, 2008), we observe a perfect organization of the spatial bias (Figure 2.8). In all operations and of both blocks, there is a transient stronger leftward bias for the implied endpoints in subtractions as compared to additions in the middle parts of the trajectories, which coincides with the transient operator effect that we found in the regression analysis (~450 to ~800 ms). Furthermore, for most the results (specially in Block 1), single digits fall in between additions and subtractions during this transient period. To confirm the OM effect in zero-problems, we pulled together the zero-problems of additions and

subtractions and ran a regression model with the operand 1 and the operator as predictors. As expected, the operator had a significant transient effect in both blocks (block 1: from 510 ms on  $b[\text{operator}] > .038$ ,  $R^2 > .010$ ,  $t_{(29)} > 1.773$ ,  $p < .043$ , peak b at 630 ms; block 2 from 510 ms to 750 ms,  $b[\text{operator}] > .083$ ,  $R^2 > .016$ ,  $t_{(29)} > 2.127$ ,  $p < .021$ ; peak b at 600 ms).

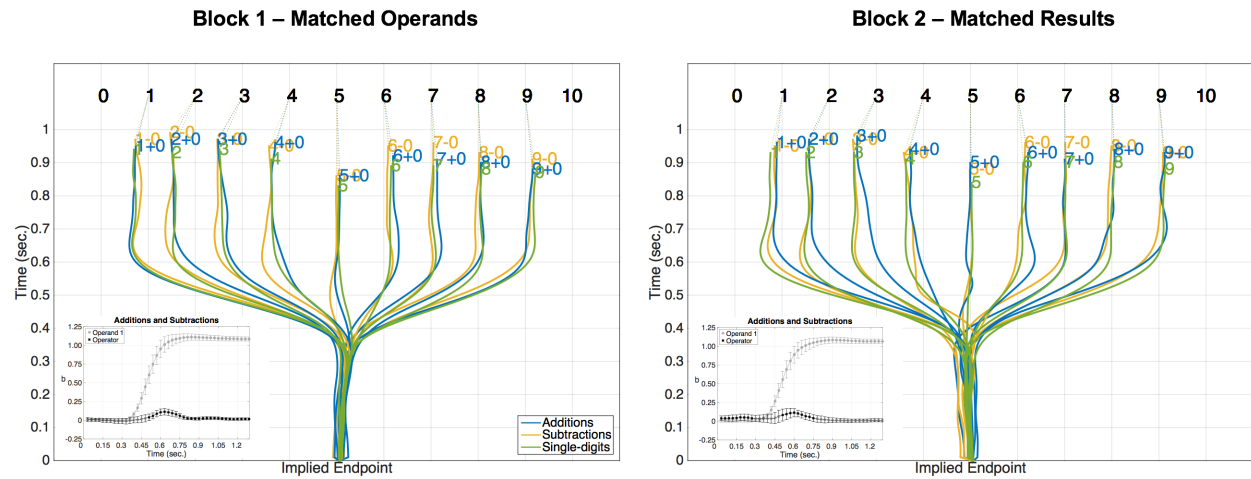


**Figure 2.8 Operational Momentum effect in zero-problems relative to single-digits**

Subtractions and additions produced a transient leftwards and rightwards bias respectively as compared to single digits. Insets show the significant transient effect of the operator in the additions and subtractions.

## Chapter 3. BRAIN MECHANISMS OF ARITHMETIC: A CRUCIAL ROLE FOR VENTRAL TEMPORAL CORTEX

---

### 3.1 Motivation

Mental calculations engage a complex interplay between several brain regions (Arsalidou & Taylor, 2011). As revised in the **Introduction**, the traditional view considers that the LPC contains the main hubs engaged in the calculation mechanism *per se*, and that the VTC plays a central role in recognizing Arabic numerals. However, recent findings are converging to the idea that VTC might contain neuronal populations involved in other aspects of arithmetic reasoning beyond symbol recognition.

In **Chapter 3**, my goal was to re-evaluate the roles of the LPC and VTC in arithmetic processing, by recording electrophysiological activity directly from the human brain. Subjects implanted with grids of electrodes were asked to verify addition problems in the form of  $15+3=18$ , in which we systematically varied the size of the problems (i.e., magnitude of the operands), while preserving the same structure and number of characters, thus separating numerical from low-level visual features of the stimuli.

This allowed me to investigate several questions. First, can we replicate the findings of **Chapter 2**, showing that the unfolding procedure and, therefore, the time to solve arithmetic calculations, is proportional to the size of the *min operand*? If so, we can use the *min operand* as an index of problem-size/difficulty and probe if, how and when it modulates the activity in calculation-selective neuronal populations in the LPC and VTC, thus clarifying their precise roles in mental arithmetic.

### 3.2 Abstract

Elementary arithmetic requires a complex interplay between several brain regions. The classical view, arising from functional magnetic resonance imaging (fMRI), is that the intraparietal sulcus (IPS) and the superior parietal lobe (SPL) are the main hubs for arithmetic calculations. However, recent studies using electrocorticography (ECoG) have discovered a specific site, within the posterior inferior temporal cortex (pITG), that activates during visual perception of numerals, with widespread adjacent responses when numerals are used in calculation. Here, we re-examined the contribution of the IPS, SPL and pITG to arithmetic by recording ECoG signals while subjects solved addition problems. Behavioral results showed a classical problem-size effect: RTs increased with the size of the operands. We then examined how high-frequency broadband (HFB) activity is modulated by problem size. As expected from previous fMRI findings, we showed that the total high-frequency broadband (HFB) activity in IPS and SPL site increased with problem size. More surprisingly, pITG sites showed an initial burst of HFB activity that decreased as the operands got larger, yet with a constant integral over the whole trial, thus making these signals invisible to slow fMRI. While parietal sites appear to have a more sustained function in arithmetic computations, the pITG may have a role of early identification of the problem difficulty, beyond merely digit recognition. Our results ask for a re-evaluation of the current models of numerical cognition and reveal that the ventral temporal cortex contains regions specifically engaged in mathematical processing.

### 3.3 Introduction

Elementary arithmetic requires a complex interplay between several brain regions. The classical Triple-Code model for numerical cognition proposed that the lateral parietal cortex (LPC) hosts the main hubs for numerosity representation and manipulation (Dehaene, Piazza, Pinel, & Cohen, 2003). More specifically, studies have found that the intraparietal sulcus (IPS) is selectively activated by number comparison (Piazza et al., 2004, 2007; Pinel, Dehaene, Rivie, & Lebihan, 2001) and calculation (Menon et al., 2000; Stanescu-Cosson et al., 2000). Furthermore, reflecting the classical behavioral problem-size effect - increase in reaction time (RTs) as a function of the magnitude of the operands (Ashcraft, 1992), IPS activity has also been shown to increase as problems become bigger/harder (De Smedt et al., 2011; Dehaene et al., 1999; Kanjlia et al., 2016; Molko et al., 2003; Visscher et al., 2015). Moreover, the superior parietal lobe (SPL) is also activated during calculation (Knops, Thirion, et al., 2009), and recent studies have reported that it hosts a topographic map of numerosity (Harvey, Klein, Petridou, & Dumoulin, 2013; Harvey, Ferri, & Orban, 2017).

In addition to the LPC, the Triple-Code model predicted that the ventral temporal cortex (VTC) would have a key role in number recognition. Indeed, recent studies using electrocorticography (ECoG) have confirmed the existence of a region in the posterior inferior temporal gyrus (pITG) that selectively activates during visual identification of Arabic numerals (the ‘number form area’, NFA), as compared to other similar morphometric symbols, such as letters (Shum et al., 2013). Subsequent ECoG studies have demonstrated that distinct neuronal populations adjacent to the NFA, also within the pITG, respond higher (Hermes et al., 2015) or exclusively (Daitch et al., 2016) to numerals when they are in the context of a calculation and that these pITG sites have high functional connectivity with the IPS (Daitch et al., 2016). These results raised the possibility that pITG might be involved in arithmetic processing beyond visual recognition of mathematical symbols, which is unexpected from previous fMRI and neuropsychological findings, unpredicted by neurocognitive models of arithmetic, and surprising given the traditional view of the VTC as the last stage of the ventral “what” visual pathway,

associated with object categorization (Grill-Spector & Weiner, 2014). However, these prior studies that investigated the role of pITG in arithmetic processing were restricted to either contrasts between numerals and similar morphometric symbols or between calculation and other tasks (e.g., memory/sentence comprehension), thus never testing if, how and when the activity in pITG is modulated by numerical features of calculations. Consequently, the precise role of pITG in mathematical cognition remains largely elusive.

In the present study, we aimed at re-evaluating the roles of IPS, SPL and pITG in mental calculation with an unprecedented level of precision, by recording electrophysiological signals directly from the human cortex (ECoG). We asked subjects to verify the correctness of visually presented additions, in the form of “ $13+5=17$ ”, in which we systematically varied the size of the problems (i.e., magnitude of the operands), while preserving the same structure and number of characters, thus separating numerical from low-level visual features of the stimuli. Based on previous fMRI findings, we predicted that the overall activity in the IPS and SPL would be sustained and increase as a function of problem size. Furthermore, this parametric modulation should be correlated with RT. However, we were less certain about the pITG. If it is only involved in the visual recognition of numerals, we should expect a brief transient burst of activity with no parametric modulation by problem size. But, since multi-digit calculations might require subjects to mentally re-evaluate the problem a few times before they reach a final decision, pITG activity may be sustained across the trial and increase as a function of problem size, possibly reflecting the top-down attentional modulation from LPC. Finally, the pITG could be parametrically modulated by problem size, but in a different way and with a different latency as compared to IPS and SPL, thus revealing an unpredicted role in calculation.

## 3.4 Methods

### 3.4.1 Subjects

We recorded electrocorticography data from 10 patients with epilepsy who were implanted with intracranial electrodes over the VTC and/or LPC as part of their pre-surgical evaluation at

Stanford University Medical Center. Demographic information for each subject is included in Table 3.1. Each subject was monitored in the hospital for approximately 6-10 days following surgery, during which they participated in our study. Before participating, all subjects provided verbal and written consent, which was approved by the Stanford Institutional Review Board. Part of the data of the present cohort was already published elsewhere (Daitch et al., 2016; Hermes et al., 2015; Shum et al., 2013). The inclusion criterion in this study was the completion of at least 80 trials (corresponding to two blocks) of the Math condition, to have enough power to investigate parametric modulations within condition (see below).

### **3.4.2 Behavioral tasks**

#### **3.4.2.1 Math & Memory Verification**

Subjects were asked to verify the correctness of either addition calculations (e.g., “ $13+5=17$ ”, Math condition) or autobiographical memory statements (e.g., “I ate fruit yesterday”, Memory condition), visually presented and randomly intermixed within the same block. For the proposes of the present study, the “Memory condition” served as a sentence/language comprehension control condition for Math. Additions were always composed of a 2-digit operand (ranging from 10 to 87), a 1-digit operand (ranging from 1 to 9, excluding 3) in either order and a 2-digit proposed result. In half of the trials, the proposed result was correct. The absolute deviant for the incorrect proposed results ranged from 1-16 (Table 3.7). Subjects responded in the self-paced manner, by pressing one of two keypad buttons. The trials were interspersed with fixation periods (5s or 10s), during which subjects were simply asked to fixate at a crosshair in the center of the screen. A 200 ms ITI separated trials. All subjects but one verified 80 additions and 50 memory statements (S1 evaluated 120 additions and 100 memory statements), divided in 2 blocks of 40 additions and 25 memory statements each.

#### **3.4.2.2 Symbol Identification**

Subjects were visually presented with a series of symbols falling under one of three categories: (1) Arabic numerals (ranging from 1-9), (2) letters in the Latin alphabet (A, C, D, E,

H, N, R, S, or T), or (3) letters in foreign alphabets. Each category had 36 trials, which were randomly shuffled. For each symbol, subjects had to press a given button if they could read the symbol (i.e., numbers or letters in the Latin alphabet) and another button if they could not read it (i.e., symbols in foreign alphabets). Subjects had up to 15 s to respond to each stimulus and trials were separated by a 500-ms ITI. The tasks were presented on a laptop computer (Apple MacBook or MacBook Pro), using MATLAB's Psychtoolbox (Brainard, 1997).

### 3.4.3 Electrodes

Each subject was implanted with grids and/or strips of subdural platinum electrodes (AdTech Medical Instruments Corporation), whose locations were determined purely for clinical reasons. Each electrode had an exposed diameter of 2.3 mm, with inter-electrode spacing of 10mm, 7mm, or 5mm for higher density arrays. **Electrode localization.** Electrode locations were mapped on each subject's own cortical surface with the following steps: 1) A post-surgical CT (with electrodes) was aligned to a pre-surgical T1-weighted MRI using SPM8 (<http://www.fil.ion.ucl.ac.uk/spm/>). 2) Electrode coordinates were manually localized within the aligned CT as the center of high image intensity spheres. 3) The identified electrode coordinates were adjusted for minor cortical shifts following surgery, with a local projection defined separately for each grid or strip (Hermes, Miller, Noordmans, Vansteensel, & Ramsey, 2010). 4) Cortical surface reconstructions of each subject's brain were obtained by manually segmenting the white matter from the subject's T1-weighted MRI using ITKGray (<http://vistalab.stanford.edu/newlm/index.php/ItkGray>), and growing out 2 layers of grey matter from the white matter surface. Finally, electrodes were labeled by an expedient neuroanatomist, based on the subdivision of LPC and VTC showed in Figure 3.1. For group plots, each subject's electrode coordinates, defined in native brain space, were realigned to a normalized brain (MNI Colin 27 (<http://www.bic.mni.mcgill.ca/ServicesAtlases/Colin27>)), and coordinates across subjects were plotted in this common space. Note that the location of each electrode site projected in MNI space may look slightly different (relative to gyral landmarks, etc) than in native

space, and was done purely for visualization purposes. Anatomical parcellations within the VTC and LPC were determined based on each subject's own gyral landmarks in native brain space.

### **3.4.4 Data acquisition and analysis**

ECoG data were recorded from subdural electrodes via a multichannel recording system (Tucker David Technologies). Data were acquired with a band pass filter of 0.5-300 Hz and sampling rate of 1525.88 Hz. An electrode outside the seizure zone with the most silent electrocorticographic activity was selected as an online reference during acquisition.

#### **3.4.4.1 Preprocessing**

First, electrodes with epileptiform activity, or those corrupted by electrical noise, were eliminated from subsequent analyses. Electrodes were also excluded whose overall power was five or more standard deviations above or below the mean power across channels, and those whose power spectrum strayed from the normal 1/f power spectrum, based on visual inspection. All non-excluded channels were then notch filtered at 60 Hz and harmonics to remove electric interference, then re-referenced to the mean of the filtered signals of the non-excluded channels. The re-referenced signal at each electrode was then band-pass filtered between 70 and 180 Hz (high frequency broadband, HFB) using sequential 10 Hz width band-pass windows (70-80 Hz, 80-90 Hz, etc.), using two-way, zero-lag, FIR filters. The instantaneous amplitude of each band-limited signal was computed by taking the modulus of the Hilbert Transformed signal. The amplitude of each 10 Hz band signal was normalized by its own mean, then these normalized amplitude time series were averaged together, yielding a single amplitude time-course for the HFB band.

### **3.4.5 Task-related HFB changes**

Our analyses were focused on task-induced changes in HFB activity (70-180 Hz), due to its high correlation with local spiking activity and the fMRI BOLD signal (Foster, Rangarajan, Shirer, & Parvizi, 2015; Logothetis, Pauls, Augath, Trinath, & Oeltermann, 2001; Manning, Jacobs, Fried, & Kahana, 2009; Parvizi et al., 2012; Ray & Maunsell, 2011). For the **Math &**

**Memory verification task**, we first identified electrodes within the VTC and LPC that responded selectively during mathematical calculations relative to reading sentences comprehension/memory retrieval. We classified all sites into six groups based on their relative responses during math vs. memory trials. 1) ***Math active*** channels were defined as those with significantly greater HFB activity during math trials (0 - 1,000 ms following stimulus onset) than during baseline (200 ms inter-trial interval); 2) ***Math selective*** channels satisfied 1, and also exhibited significantly greater HFB activity during math than memory trials (0 - 1,000 ms following stimulus onset for each condition); 3) ***Math-only*** channels satisfied 1 and 2, and additionally exhibited no significant increase in activity during memory trials (0 - 1,000 ms following stimulus onset). 4-6) ***Memory-active, memory-selective, and memory-only*** channels were classified using equivalent criteria as 1-3, but comparing activity during memory trials to that during baseline or math trials. For the **Symbol identification task**, a similar procedure was used to determine channel selectivity, but using a time-window of (0 – 400 ms after stimuli onset) and a baseline of (-200 ms before stimuli onset). Channels were classified as 1) ***Numerical active*** if they showed significantly greater HFB activity during numerals identification as compared to baseline; 2) ***Numerical selective*** channels satisfied 1 and also exhibited significantly greater HFB activity during numerals identification as compared to Latin and foreign letters. Unpaired permutation tests were run to test for differences in HFB power between different task conditions, while paired permutation tests were run to test for a difference in HFB power between a task condition and baseline. All p-values in all analyses were FDR corrected by the total number of VTC and LPC channels within each subject.

### 3.5 Results

We recorded brain activity of 10 subjects implanted with intracranial electrodes (ECoG) in VTC and LPC for epilepsy monitoring purposes while they performed a mental calculation task, in which they had to verify the correctness of addition problems (e.g.,  $13+5=17$ ). In a control language/sentence comprehension condition, they evaluated autobiographical memory statements

(e.g., ‘I ate fruit yesterday’) (Figure 3.1C). Accuracy for the Math condition was high (80% or higher) in 9/10 subjects (Table 3.1). To model RTs in each subject, we calculated stepwise regression models with the smaller operand (*min*), the larger operand (*max*), the sum and the absolute deviant as predictors. Results revealed that the *min* operand was a significant and the best predictor of RT in 9/10 subjects (betas > 0.32, p < 0.003), while the sum and the absolute deviant were significant predictors only in 2 subjects (betas > 0.28, p < 0.01). The *max* operand was not a significant predictor of RT in any model (Table 3.3, supporting Figure 3.1). These results corroborates previous findings using different tasks, in which the *min* operand was also found to be the best predictor of RT (Barrouillet & Thevenot, 2013; Groen & Parkman, 1972; Pinheiro-Chagas, Dotan, Piazza, & Dehaene, 2017; Uittenhove et al., 2016), thus providing incremental evidence that the *min* operand is a robust and reproducible index of problem-size/difficulty across a variety of mental calculation experiments.

**Table 3.1 Subject demographics and behavioral performance.**

Subject	Gender	Age	IQ	Handedness	Hemi	Behavior Performance		
						Math Acc (%)	Avg Math RT (s)	Avg Memory RT (s)
S1	M	41	129	R	R	96	3.18	2.15
S2	F	36	N/A	R	L	95	3.69	2.1
S3	F	22	N/A	R	L	89	5.78	3.12
S4	M	46	N/A	A	R	93	5.24	3.38
S5	F	31	71	R	L	63	3.61	3.11
S6	M	29	77	R	L	88	2.85	3.13
S7	M	47	74	L	L	96	3.3	3.23
S8	M	67	N/A	R	R	94	2.02	2.84
S9	F	65	113	R	R	80	3.28	2.35

This table shows the gender, age at time of surgery, IQ (N/A indicates that the IQ test was not performed before surgery), handedness (R, right-handed; L, left-handed; A, ambidextrous) and Hemi (hemisphere of coverage) of all subjects participating in study. It also shows the accuracy and average response times (RT) for each condition (Math and Memory).

### 3.5.1 Selectivity for Math in pITG, aIPS and SPL sites

Next, we investigated the Math vs. Memory selectivity in several recording sites across all subjects. We found that our Math-ROIs - pITG, aIPS, and SPL - were highly selective to mathematical processing, as previously reported (Daitch et al., 2016; Hermes et al., 2015) and in

line with a recent fMRI study that used an analogous task (Amalric & Dehaene, 2016). 40% of sites within the pITG (11/28), 21% of sites around the aIPS (7/33) and 25% of sites within the SPL (13/53) responded exclusively during the math condition (Figure 3.1C). Moreover, most of the math-selective sites in these regions exhibited sustained activity during the computation. In sharp contrast, the Memory condition produced activity in the language network including LPC regions such as the angular gyrus and superior temporal sulcus (Pallier, Devauchelle, & Dehaene, 2010) and in more medial portions of the inferior temporal cortex, close to the visual word form area (VWFA, Hannagan, Amedi, Cohen, Dehaene-Lambertz, & Dehaene, 2015). Non-selective sites, showed either transient activity following stimulus onset in both conditions, likely involved in the visual processing of the stimulus, or later activity just prior to subjects' motor response, probably engaged in motor planning.

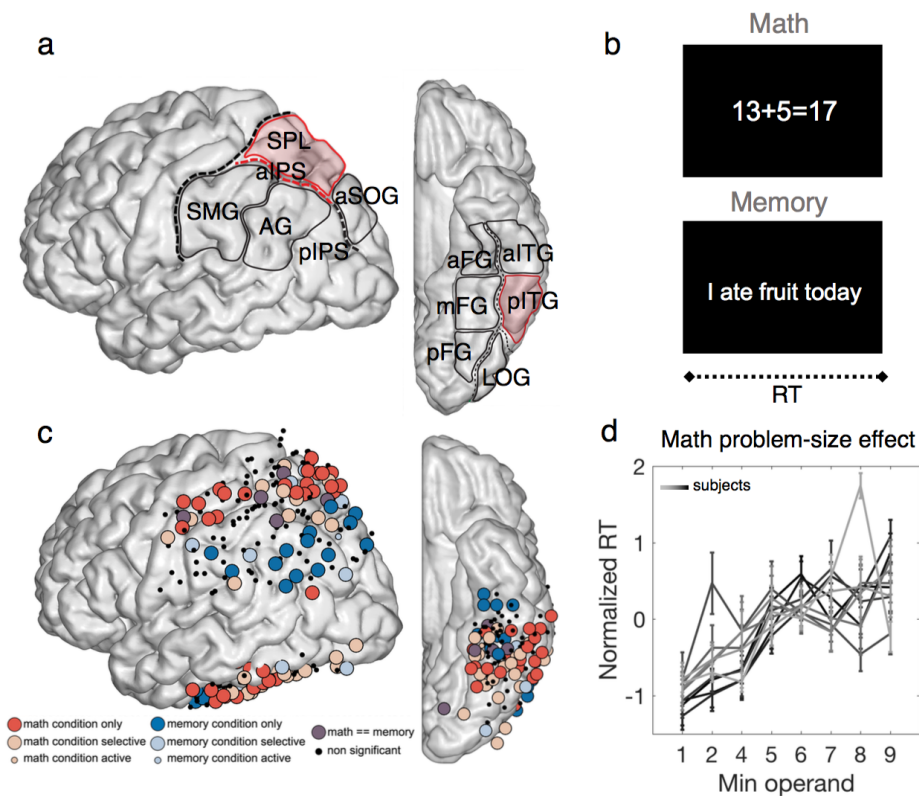


**Figure 3.1 Anatomical subdivisions, task, recording sites, and behavioral problem-size effect**

A) The anatomical subdivisions within the lateral parietal cortex (LPC) and ventral temporal cortex (VTC) considered in this study, as seen in the left hemisphere from a slightly posterior viewpoint. LPC: AG, angular gyrus; aIPS, anterior intraparietal sulcus; aSOG, anterior superior

occipital gyrus; pIPS posterior intraparietal sulcus; SMG, supramarginal gyrus; SPL, superior parietal lobule. VTC: aFG, anterior fusiform gyrus; aITG, anterior inferior temporal gyrus; pFG, posterior fusiform gyrus; mFG, mid fusiform gyrus; pITG, posterior inferior temporal gyrus. Math-ROIs marked in red. B) Exemplar stimuli of the Memory & Math verification task (See Table 3.7). In each trial, subjects were asked to verify the correctness of visually presented additions or a memory statements, by pressing one of two buttons. C) LPC and VTC sites from all 10 subjects are projected onto a single left hemisphere using the MNI space (see *Electrodes Localization* in the Methods), with the color of each site indicating its selectivity for math versus memory. Bright blue and bright red mark the most selective sites, passing three criteria for significance (e.g. math > baseline; math > memory; and memory indistinguishable from baseline). Faded red and blue indicate the selective sites that met only the first two criteria. Small faded red and blue indicate sites that met only the first criteria. Sites colored in purple were activated similarly during the two conditions, and sites marked by small black dots were not significantly active during either condition. Significance was defined as  $P < 0.05$ , FDR corrected within subject. D) Behavioral problem-size effect (*min* operand) in each subject (different shades of gray): average RT plotted as a function of *min* operand (normalized within each subject by subtracting the mean and dividing by the standard deviation). Complete statistics of the stepwise regression can be found in Table 3.3.

### 3.5.2 Parametric modulation of the HFB power by *min* operand in pITG, aIPS and SPL

Given the behavioral evidence that the *min* operand was the best index of problem size/difficulty, we next investigated if, how and when the *min* operand modulated the activity in our Math-ROIs. To do so, we performed linear regression analysis on the HFB activity at each recording site on two time windows: *initial activity* (averaged power over 0 - 1,000 s following stimulus onset, where greater activity was observed) and *total activity* (the integral - area under the curve - from stimulus onset to subject's RT).

As expected from previous fMRI findings, the *total activity* increased as a function of *min* operand in several aIPS (5/12 sites, 42% in 3/7 subjects with aIPS coverage) and SPL (7/17 sites, 41% in 3/7 subjects with SPL coverage) sites ( $p < 0.05$ , FDR corrected; Figure 3.2B and Figure 3.4a, Table 3.4). Importantly, no site in pITG showed this effect. Surprisingly, however, we found that the *initial activity* significantly decreased as a function of *min* operand ( $p < 0.05$ , FDR corrected) in several math-selective pITG sites (10/17, 59% in 6/7 subjects with pITG coverage)

and in 1 anterior ITG site, just adjacent to the pITG. Examples of activation profiles at the single trial level are shown in Figure 3.2a (see also Figure 3.3 and Figure 3.4a, Table 3.4). This proportion increased when considering only the math-selective channels that did not show any significant response during the memory condition (math-only channels: 8/11, 72%). The same effect was also observed in a small proportion of the math-selective channels in the aIPS and SPL (aIPS: 2/12, 17% in 2/7 subjects with aIPS coverage; SPL: 2/17 sites, 12% in 2/7 subjects with SPL coverage). No significant increases were found.

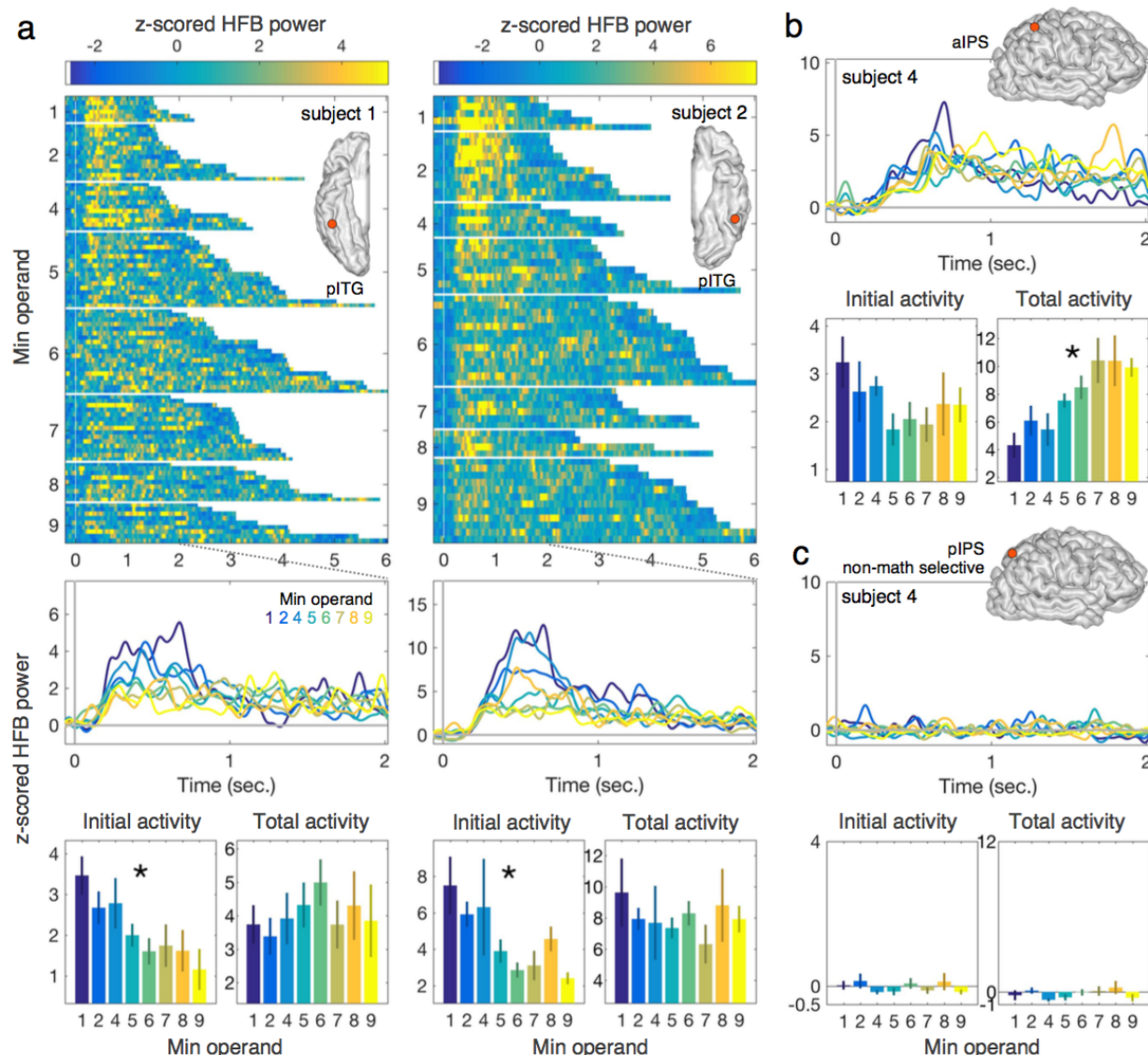


Figure 3.2 Exemplar sites whose activity was modulated by the min operand

A) Two exemplar channels showing decreased HFB initial activity in the pITG as a function of *min* operand (both math selective, one in each hemisphere in two different subjects). The location of each electrode is shown as the inset of the first plot. The first plot in each column shows the time course of activity for each trial, sorted by *min* operand and then by RT. The second plot in each column shows the time course of activity averaged across trials with a given *min* operand (zoomed in the first two seconds of the trial). Bar plots underneath in each column show average initial activity (within the first second of a trial), and average total activity (integrated over the whole trial) as a function of *min* operand. B) Exemplar math selective channel in the aIPS showing increased HFB total activity as a function of *min* operand. C) Exemplar channel of a non-math selective channel in the posterior IPS of the same subject as in B showing no HFB modulation by *min* operand. An asterisk indicates that a regression analysis found a significant effect of *min* operand on either initial or total HFB activity ( $P < 0.05$ , FDR corrected).

To evaluate the specificity of these results, we next analyzed functional control sites, where activity was memory-selective or equally responsive to math and memory (Table 3.5), as well as anatomical control sites (math-selective channels that were outside of our Math-ROIs, Table 3.6). None of the memory selective channels, nor channels that equally responded to math and memory, across any brain region, showed a significant decrease in the initial HFB activity as a function of *min* operand. Very few non-math-selective channels in the ROIs showed an increase of total HFB activity as a function of *min* operand. Likewise, very few math selective channels located outside the ROIs showed either a decrease in the initial HFB activity or an increase in the total HFB activity as a function of *min* operand.

Finally, we measured the selectivity for symbols of the VTC math-selective sites which showed a decreased initial activity as a function of *min* operand, using the symbol verification task (Table 3.2), to investigate whether these sites were selective for or modulated by numerical information in any context, or only during mathematical calculations. We found that 7/11 sites were active for Arabic numerals, but they equally responded to Latin and foreign letters. And the remaining 4/11 were not even active for any symbol. Only one pITG site showed selectivity for numerals (NFA). In fact, that was the only NFA site observed in this study. Next we performed a linear regression analysis on the averaged HFB power between 0 – 500 ms, where higher activity was observed, with the Arabic numerals (ranging from 1-9) as predictors. In none of the 11 channels we found a significant effect of the number magnitude ( $p>0.1$ , FDR corrected for only the 11

channels, to be more liberal). Therefore, the engagement and selectivity to mathematical objects/processing in the VTC was much higher during calculation as compared to digit recognition and, crucially, the parametric modulation by number magnitude (*min operand*) was exclusively present during calculation.

In summary, parametric modulations were almost entirely dissociated into two categories, found in both left and right hemispheres (Figure 3.4a): (1) decreases in *initial activity* with increasing *min operand*, showing a high specificity to math-selective sites mostly in pITG (Figure 3.3), and (2) increases in *total activity* with increasing *min operand* in aIPS and SPL math selective sites (Figure 3.5).

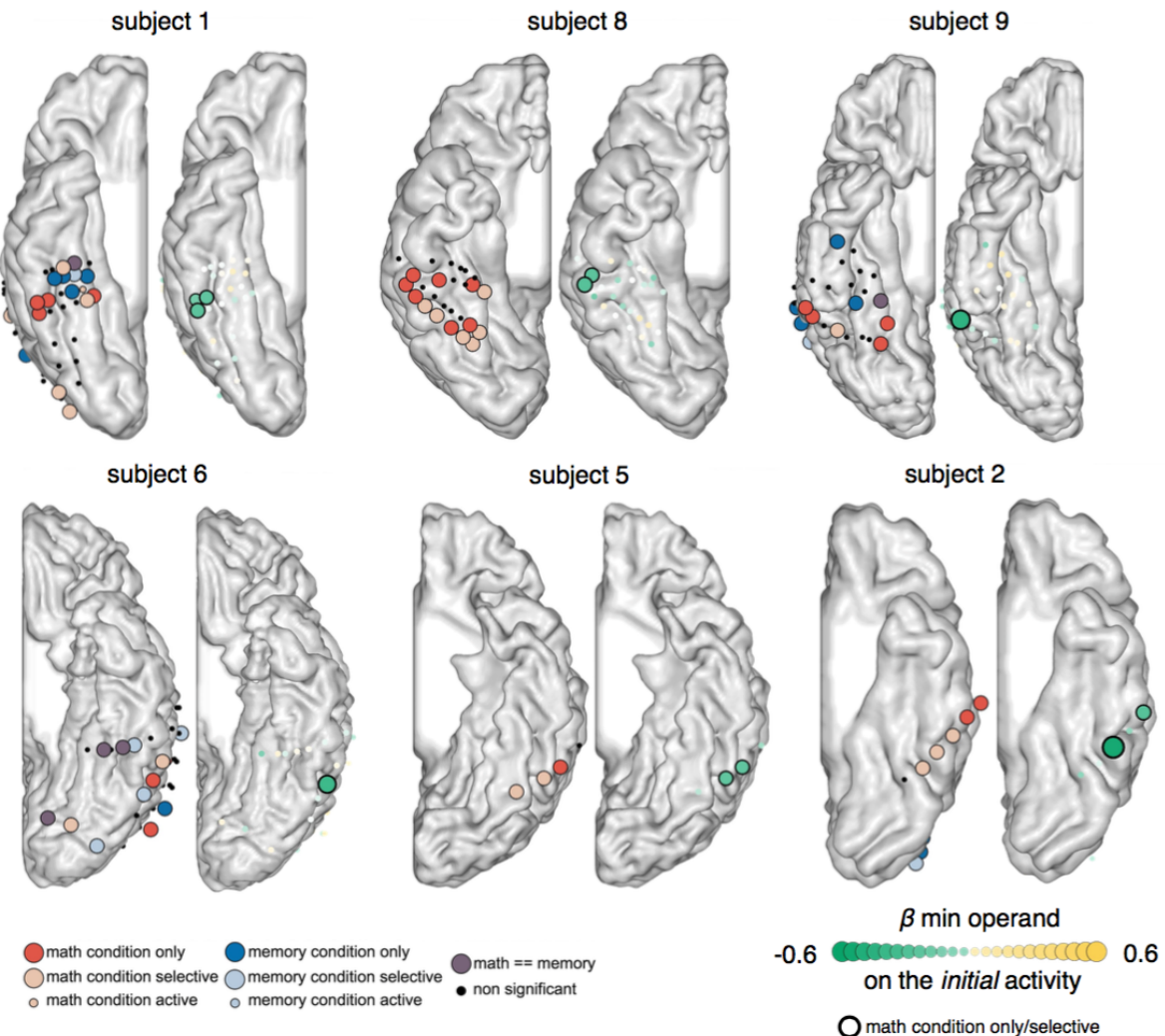


Figure 3.3 Anatomical and functional specificity of the HFB activity modulation in the VTC

The figure illustrates the relationship, in VTC, between (1) selectivity for math vs. memory (left brain, same color code as Figure 3.1b) and (2) the effect of the *min* operand on initial activity (right brain). The figure shows all 6 (out of 7) subjects with pITG coverage who showed the effect. All channels whose initial activity decreased with problem size were located within the pITG (except for the most posterior channel of subject 2 and were math selective (thick black ring). For the *min* effect, dot color indicates the size and sign of the regression coefficient and dot size indicates the size of the regression coefficient (standardized) ( $P < 0.05$ , FDR corrected). Small dots indicate non-significant channels. Complementary data for LPC channels can be found in Figure 3.5.

**Table 3.2 Selectivity and modulation related to the recognition of Arabic numerals in the VTC channels that showed decreased initial activity as a function of min operand.**

Subject	Hemi	Region	Numerical active	Numerical selective	Modulation by numeral
S1	R	pITG	✓	-	-
S1	R	pITG	✓	-	-
S1	R	pITG	-	-	-
S2	L	pITG	✓	-	-
S2	L	aITG	-	-	-
S5	L	pITG	✓	-	-
S5	L	pITG	✓	-	-
S6	L	pITG	-	-	-
S8	R	pITG	✓	✓	-
S8	R	pITG	✓	-	-
S9	R	pITG	-	-	-

Hemi, hemisphere; Numerical active (relative to baseline); Numerical selective (relative to baseline, Latin letters, and foreign letters). (✓) Statistically significant at  $P < 0.05$ , FDR corrected.

### 3.5.3 Dissociation from reaction time

Finally, to verify if the parametric modulation by *min* operand directly translated to behavior, thus being independent of other factors that influence RT, such as attention, decision making and motor preparation, we used multiple linear regression to model HFB activity as a function of both *min* operand and RT (Figure 3.4b and c). When regressing out the effect of RT, the *initial activity* at most pITG sites remained significantly modulated by *min* operand at 9 of the 10 observed sites. Conversely, once we regressed out the effect of RT from the *total activity* in aIPS and aSPL, the effect of *min* operand completely vanished in all sites (Figure 3.4b). Finally, as shown in Figure 3.4c, the *total activity* in almost all VTC and LPC sites significantly correlated

with RT, independently of *min* operand. Therefore, in contrast with the increase in *total activity* as a function of *min* operand observed in aIPS and SPL sites which proved to be directly related to final decision making, the parametric decrease of the *initial activity* as a function of *min* operand observed in pITG was partially dissociated from RT, possibly indicating a role in the earlier stages of the calculation that do not seem to be linearly additive to the subsequent stages.

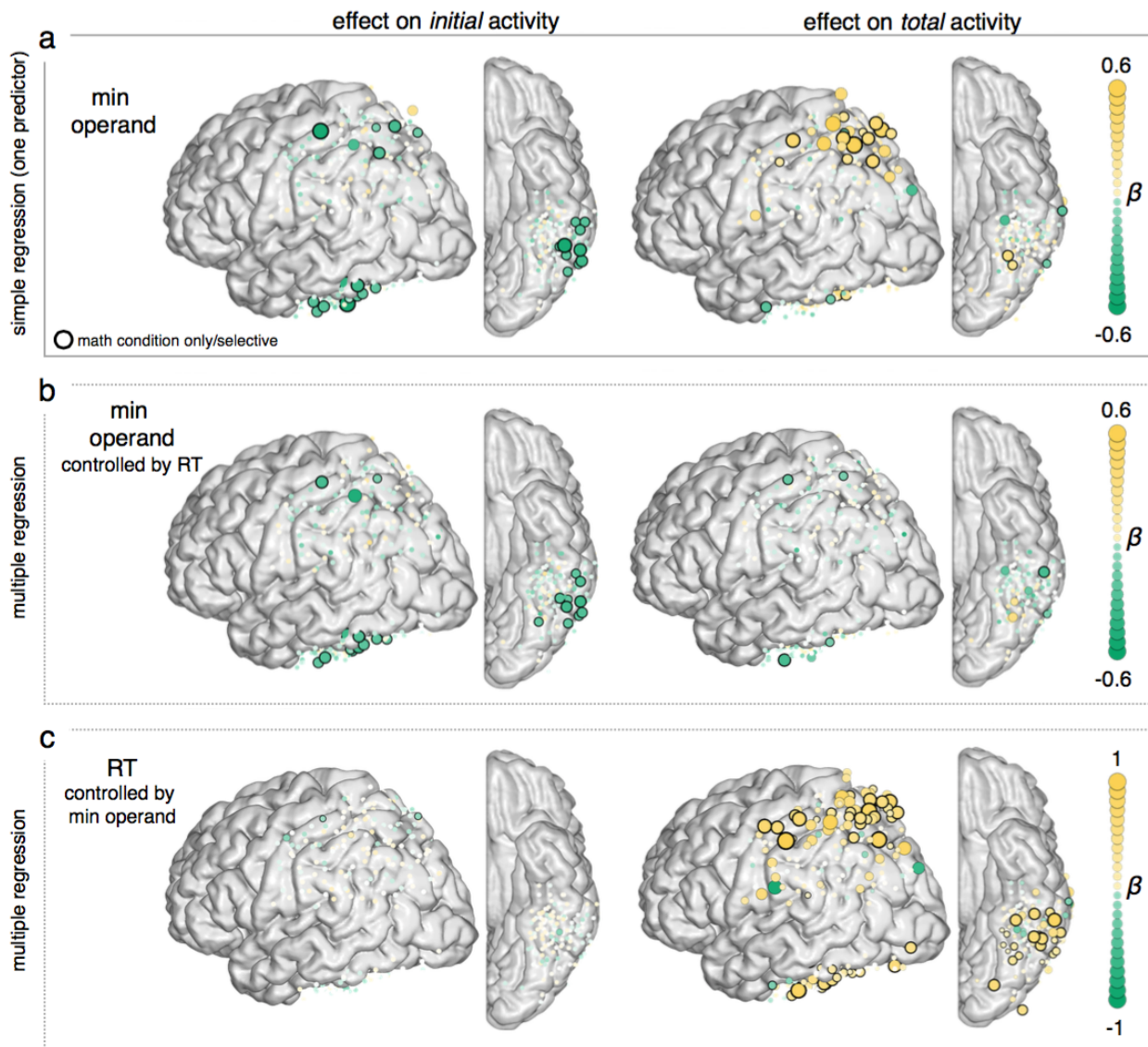


**Figure 3.4 Separating the effects of number and reaction time**

Regression analysis, where activity is modeled as a function of *min operand* in the initial activity (within the first second of a trial, left column) and total activity (integrated over the whole trial, right column). **A.** The effect of the *min* operand in a simple regression (one predictor). **B.** The effect of the *min* operand in a multiple regression that included both the *min* operand and the RT controlled by the *min* operand. **C.** The effect of the *min* operand in a multiple regression that included both the *min* operand and the RT controlled by the *min* operand.

as predictors. **C.** The effect of the RT in a multiple regression that included both the *min* operand and the RT as predictors. For all plots, dot color indicates the size and sign of the regression coefficient and dot size indicates the size of the regression coefficient significant (standardized). A thick black ring indicate that the channel is also math selective. Small dots indicate non-significant channels. Significance:  $P < 0.05$ , FDR corrected. Complementary data can be found in Table 3.4, 3.5 and 3.6.

### 3.6 Discussion

By recording electrophysiological signals directly from the human cortex (ECoG) with remarkable temporal and spatial resolution, we characterized the response selectivity and parametric modulation patterns in neuronal populations of the lateral parietal and ventral temporal cortices during mental arithmetic. Our results demonstrated a high degree of selectivity for calculations in a network comprised of the aIPS and SPL in the LPC and the pITG in the VTC, almost completely dissociated from the selectivity observed during sentence comprehension (Memory condition), observed in the angular gyrus and STS and the medial inferior temporal cortex, known to be involved in language comprehension (Pallier et al., 2010) and reading (Hannagan, Amedi, Cohen, Dehaene-Lambertz, & Dehaene, 2015), respectively. These results are in line with previous reported ECoG results (Daitch et al., 2016; Hermes et al., 2015), with a recent fMRI study that used an analogous task (Amalric & Dehaene, 2016) and with a series of prior fMRI findings (Arsalidou & Taylor, 2011).

Virtually all subjects performed the addition task with high accuracy, and their RT patterns reflected the most widely replicated behavioral effect in cognitive arithmetic: the problem-size effect (Ashcraft, 1992; Zbrodoff & Logan, 2005). More specifically, we found that the best predictor of RT, and therefore problem size/difficulty, was the smallest of the two operands (called *min*), corroborating several studies which used a variety of calculation tasks (Barrouillet & Thevenot, 2013; Groen & Parkman, 1972; Pinheiro-Chagas, Dotan, et al., 2017; Uittenhove et al., 2016). Next, we investigated if, how and when the *min* operand modulated the activity in the LPC and VTC math-selective regions.

As predicted, we found that the total HFB activity (integral of HFB power across the

whole trial from stimuli onset to subject's RT) increased as a function of the problem-size in aIPS and SPL math-selective sites. These results replicate previous fMRI findings (De Smedt et al., 2011; Dehaene et al., 1999; Kanjlia et al., 2016; Molko et al., 2003; Visscher et al., 2015), but with a much greater level of anatomical precision within the single subject level. Most surprisingly, however, we found almost the inverse pattern in pITG, that is, the initial HFB activity (averaged within the time window of 0-1,000 ms following stimuli onset) decreased with problem-size.

Recent ECoG findings revealed the existence of neuronal populations in the pITG that selectively respond to Arabic numerals (NFA) as compared to other similar stimuli, such as letters (Shum et al., 2013). However, subsequent ECoG studies showed that responses to numerals in the VTC are more complex than what it was previously predicted by the Triple-Code model (Dehaene & Cohen, 1995), by revealing that, adjacent to the NFA, there are neuronal populations that respond to numerals more strongly (Hermes et al., 2015) or even exclusively (Daitch et al., 2016) when they are in the context of calculation, possibly reflecting top-down modulation coming from the LPC. Furthermore, recent fMRI studies showed that voxels around the pITG are also active for number processing in blind subjects who learned to associate number shapes with sounds (Abboud, Maidenbaum, Dehaene, & Amedi, 2015) and when professional mathematicians evaluate high-level mathematical statements auditory presented (Amalric & Dehaene, 2016). These results suggest that pITG might be involved in calculation beyond visual recognition of mathematical objects.

However, the precise role of pITG was not carefully examined, since none of the prior studies investigated if, how and then activity in pITG is modulated by numerical features of the calculations. Our results, showing a parametrical decrease in the initial activity as a function of problem-size independent of RT in several pITG sites (replicated across several subjects), suggest that the pITG activation during multi-digit calculation are directly linked to quantity-related features of calculations and do not simply reflect top-down attentional modulation or sustained working memory subserving regions that execute the actual computation. If that was the case, the total activity in pITG, as in the aIPS and sPL, should have increased as a function of *min* operand. Crucially, since fMRI is only sensitive to the activity integrated over a temporal window

of several seconds, the initial modulation observed in pITG would be undetectable with fMRI. This may explain why previous fMRI studies did not observe modulation in the pITG by arithmetic problem size, but exclusively in a parietal-frontal network, including mainly the bilateral aIPS and SPL and the left inferior frontal gyrus (Kanjlia et al., 2016; Molko et al., 2003; Stanescu-Cosson et al., 2000). Note that in the present study, LPC contained sites whose total HFB activity in a trial was positively correlated with *min* operand, yet which were not selective for math processing (e.g., were active during both math and memory trials). Those sites might therefore have been engaged in sustained attention, decision making, or some other non-math-selective process.

The behavioral paradigm used here, which involves judging the correctness of an equation, requires at least two decision processes: first, computing the sum of the two operands, and second comparing the sum with the proposed result. Although our study cannot explicitly separate the neural processes corresponding to those two stages, it seems likely that the *min*-related activity observed mainly in pITG sites and in a few aIPS and SPL sites is primarily related to the computation stage since, 1) the most salient effects are observed during the beginning of a trial, and 2) the *min* effect remains at most sites even after regressing out the effect of RT, while we would expect decision-related processes to be more correlated with RT.

Why would pITG activity related to calculation decrease for more difficult problems? Simple arithmetic problems appear to induce a temporal concentration of activity into a fast and strong initial peak. Conversely, for more complex problems, the same total amount of activity appeared to be diluted in time. These findings suggest that pITG may index the difficulty or amount of evidence available for a calculation problem. In this respect, our findings, in a high-level semantic task, parallel the observations made during perceptual decision-making tasks, for instance the fact that activity in area MT indexes the amount of perceptual evidence for a motion-based decision and therefore varies inversely with task difficulty (Britten, Shadlen, Newsome, & Movshon, 1993). A possible alternative interpretation could be that the higher initial activity observed in the pITG for smaller *min* operands reflects tuning to more familiar symbols, since it is known that the frequency of number words and digits decrease as a function of numerosity

(Dehaene & Mehler, 1992). However, an important argument against this interpretation is the fact that the pITG sites that showed a decreased initial activity as a function of *min* operand falls adjacent to, but not directly in the ‘number form area’ and do not show selective responses to isolated numerals as compared to other similar visual objects. Crucially, even the pITG sites that were active during Arabic digit recognition, did not show any modulation by the magnitude of the numbers, that is, they equally responded to digits ranging from 1-9. Furthermore, as all elements of the addition were presented simultaneously in the screen, is very unlikely that the pITG would be tuned to the frequency of only one of the elements. Another possibility is that pITG stores visual representations the whole addition problem, as suggested by an early fMRI study (Rickard et al., 2000). In this case, the pITG modulation could potentially reflect the frequency of individual problem. Further studies, using a larger stimuli list and more adapted experimental design should try to arbitrate between these hypotheses.

Several sites in the aIPS and SPL showed an increasing effect of *min* operand on total power, which was in fact driven by RT. This suggests that the aIPS and SPL may be involved in the slow accumulation of evidence needed to achieve a decision (Gonzalez et al., 2015; Tosoni, Galati, Romani, & Corbetta, 2008) during mental arithmetic. To better dissociate distinct processes within numerical cognition, future work could use simpler tasks such as number comparison or single-digit arithmetic, which would be more conducive to testing accumulation-of-evidence models (Dehaene, 2007; Gold & Shadlen, 2007).

In sum, our results confirmed the selective engagement of aIPS and SPL in mental calculation and reveal an unexpected pattern of parametric modulation in pITG, that is, higher initial activity for simple as compared to more complex problems, possibly reflecting a role in the early identification of the difficulty/amount of evidence associated with a given computation. In the absence of reported bilateral focal lesions in the pITG region, its role in calculations remained unsuspected by previous neuropsychological studies (Cappelletti, 2015, for a recent review) and asks for a re-evaluation of the neurocognitive models of arithmetic and acquired and developmental dyscalculia. Updated models should incorporate the pITG as an important hub for mental calculation and any future study on numerical cognition should include it as a ROI. More broadly,

our results challenge the classical view of ventral temporal cortex as the last stage of the visual object categorization network, and shows that it contains regions crucially involved in mathematical processing.

### **3.7 Acknowledgments**

We thank all the patients for volunteering their time to participate in this study; members of the Laboratory of Behavioral and Cognitive Neuroscience at Stanford University for their help in the initial and early stages of this study. This work was supported by research Grant R01NS078396 from the National Institute of Neurological Disorders, Stroke; Grant 1R01MH109954-01 from the National Institute of Mental Health (NIMH), Grant BCS1358907 from the National Science Foundation (NSF) (all to J.P.) and by the INSERM, CEA, and the Bettencourt-Schueller Foundation (France). Postdoctoral Fellowship 1F32HD087028-01 from the National Institute of Child Health and Human Development (to A.L.D.); Science Without Borders Fellowship from CNPq – Brazil (nr. 246750/2012-0). The views presented in this work do not necessarily reflect those of the National Institutes of Health. The authors declare no conflicts of interest.

### 3.8 Supplementary Materials

**Table 3.3 Arithmetic problem-size effect by subject**

Subject	Min operand				Max operand				Sum				Absolute deviant			
	Beta	In	t	p	Beta	In	t	p	Beta	In	t	p	Beta	In	t	p
S1	0.45	✓	5.55	1.7E-07	0.08	-	0.99	0.32	-0.02	-	-0.29	0.78	0.08	-	0.99	0.32
S2	0.58	✓	6.30	1.6E-08	0.08	-	0.82	0.41	0.05	-	0.52	0.60	0.08	-	0.82	0.41
S3	0.71	✓	8.76	3.5E-13	0.13	-	1.68	0.10	0.03	-	0.34	0.74	0.14	-	1.68	0.10
S4	0.40	✓	4.11	1.0E-04	0.00	-	0.00	1.00	0.16	-	1.61	0.11	0.31	✓	3.15	2.4E-03
S5	0.05	-	0.41	0.68	-0.01	-	-0.07	0.94	0.29	✓	2.63	1.0E-02	0.00	-	-0.02	0.98
S6	0.32	✓	3.01	3.5E-03	0.07	-	0.69	0.49	0.02	-	0.16	0.87	0.08	-	0.69	0.49
S7	0.47	✓	4.43	3.1E-05	0.12	-	1.16	0.25	0.15	-	1.36	0.18	0.12	-	1.16	0.25
S8	0.37	✓	3.58	6.1E-04	0.00	-	0.00	1.00	0.31	✓	3.05	3.2E-03	0.29	✓	2.92	4.7E-03
S9	0.44	✓	4.01	1.4E-04	-0.10	-	-0.96	0.34	0.04	-	0.31	0.88	-0.01	-	-0.96	0.34
S10	0.53	✓	5.38	8.1E-07	0.00	-	0.00	1.00	-0.15	-	-1.44	0.15	0.15	-	1.67	0.09

This table shows the statistics of the stepwise regression analysis, which included the RT as the dependent variable and the min operand, max operand, sum and absolute deviant as predictors. ‘In’ indicates if the predictor was included (✓, p < 0.05) or not (-) in the final model.

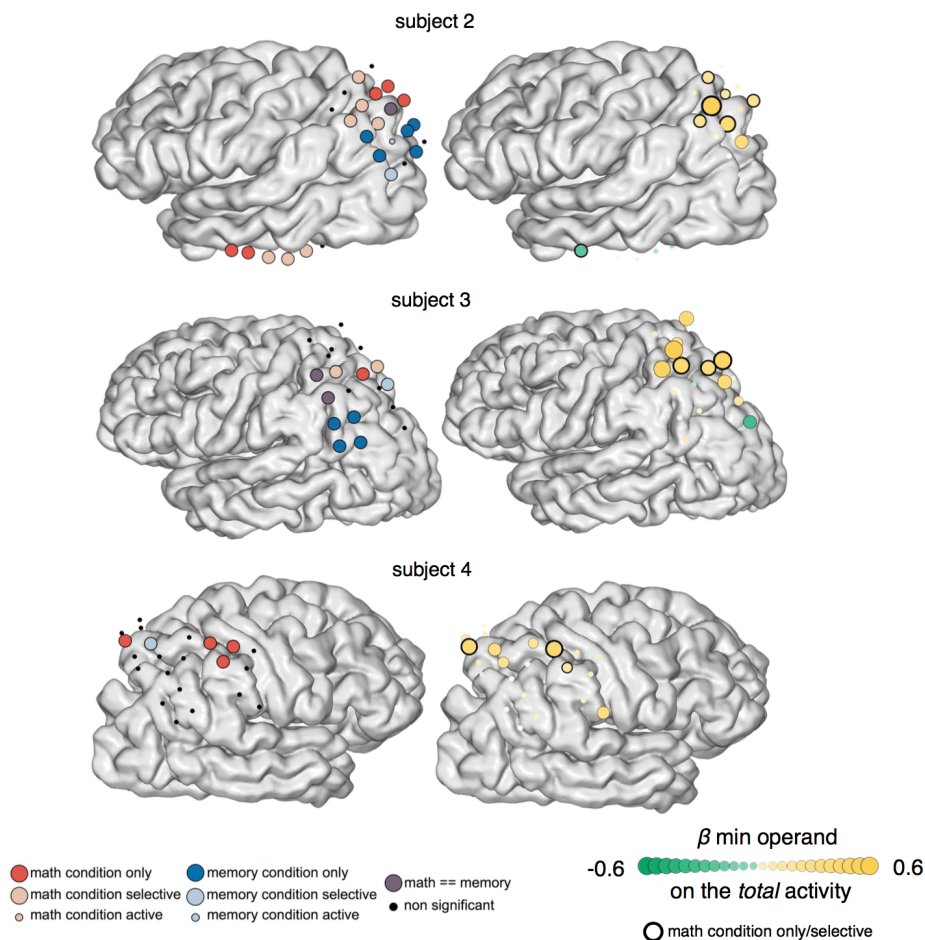


**Figure 3.5 Anatomical and functional specificity of the HFB activity modulation in the LPC**

The figure illustrates the relationship, in LPC, between (1) selectivity for math vs. memory (left brain, same color code as Figure 1B) and (2) the effect of the min operand on total activity (right brain). The figure shows all 3 (out of 7) subjects with LPC coverage who showed the effect. Most channels whose total activity increased with problem size were located within the aIPS and SPL and were math selective, but some channels that showed this effect felt outside aIPS and SPL and/or were not math selective. For the min effect, dot color indicates the size and sign of the regression coefficient and dot size indicates the size of the regression coefficient. A thick black ring indicate that the channel is also math selective. Small dots indicate non-significant channels. P-values were FDR-corrected within subject.

**Table 3.4 Number of electrodes showing *math* selectivity and modulation by the min operand, by subject/anatomical region.**

Subject	Hemi	pITG					aIPS					aSPL							
		TOT	MA	MS	MO	DecIN	IncTO	TOT	MA	MS	MO	DecIN	IncTO	TOT	MA	MS	MO	DecIN	IncTO
S1	R	5	3	3	3	3,3,3	-,-,-	6	2	2	2	-,-,-	-,-,-	8	3	2	1	-,-,-	-,-,-
S2	L	2	2	2	-	1,1,-	-,-,-	4	2	2	-	1,1,-	2,2,-	8	6	5	3	1,1,1	4,4,2
S3	L	-	-	-	-	-,-,-	-,-,-	3	2	1	-	-,-,-	2,1,-	7	2	2	1	-,-,-	2,2,1
S4	R	-	-	-	-	-,-,-	-,-,-	4	2	2	2	-,-,-	1,1,1	7	1	1	1	-,-,-	1,1,1
S5	L	3	2	2	1	2,2,1	-,-,-	-	-	-	-	-,-,-	-,-,-	5	2	2	2	1,1,1	-,-,-
S6	L	5	4	2	1	1,1,1	-,-,-	5	3	3	2	1,1,1	-,-,-	12	5	5	5	-,-,-	-,-,-
S7	L	4	1	1	1	-,-,-	-,-,-	4	-	-	-	-,-,-	-,-,-	5	-	-	-	-,-,-	-,-,-
S8	R	6	5	5	3	2,2,2	-,-,-	-	-	-	-	-,-,-	-,-,-	-	-	-	-	-,-,-	-,-,-
S9	R	3	2	2	2	1,1,1	-,-,-	4	2	1	-	-,-,-	-,-,-	1	-	-	-	-,-,-	-,-,-
S10	L	-	-	-	-	-,-,-	-,-,-	3	1	1	1	-,-,-	-,-,-	-	-	-	-	-,-,-	-,-,-
TOTAL		28	19	17	11	10,10,8	-,-,-	33	14	12	7	2,2,1	5,4,1	53	19	17	13	2,2,2	7,7,4

Hemi, hemisphere; TOT, total number of electrodes; MA, math condition active (relative to baseline); MS, math condition selective (relative to baseline and memory); MO, math condition only (math selective and memory not active relative to baseline); DecIN, decreased initial activity as a function of min operand; IncTO, increased total activity as a function of min operand. The numbers separated by commas correspond to MA, MS, MO respectively. Electrodes included are statistically significant at  $p < 0.05$  FDR-corrected within subject.

**Table 3.5 Number of electrodes showing *memory* selectivity and modulation by the min operand, by subject/anatomical region.**

Subject	Hemi	pITG						aIPS						aSPL					
		TOT	mA	mS	mO	DecIN	IncTO	TOT	mA	mS	mO	DecIN	IncTO	TOT	mA	mS	mO	DecIN	IncTO
S1	R	5	-	-	-	-,-,-	-,-,-	6	-	-	-	-,-,-	-,-,-	8	3	1	-	-,-,-	-,-,-
S2	L	2	2	-	-	1,-,-	-,-,-	4	3	1	1	1,-,-	2,-,-	8	3	-	-	-,-,-	2,-,-
S3	L	-	-	-	-	-,-,-	-,-,-	3	1	-	-	-,-,-	1,-,-	7	1	-	-	-,-,-	1,-,-
S4	R	-	-	-	-	-,-,-	-,-,-	4	-	-	-	-,-,-	-,-,-	7	1	1	-	-,-,-	1,1,-
S5	L	3	1	-	-	1,-,-	-,-,-	-	-	-	-	-,-,-	-,-,-	5	-	-	-	-,-,-	-,-,-
S6	L	5	2	2	-	-,-,-	-,-,-	5	-	-	-	-,-,-	-,-,-	12	-	-	-	-,-,-	-,-,-
S7	L	4	-	-	-	-,-,-	-,-,-	4	-	-	-	-,-,-	-,-,-	5	-	-	-	-,-,-	-,-,-
S8	R	6	2	-	-	-,-,-	-,-,-	-	-	-	-	-,-,-	-,-,-	-	-	-	-	-,-,-	-,-,-
S9	R	3	-	-	-	-,-,-	-,-,-	4	1	-	-	-,-,-	-,-,-	1	-	-	-	-,-,-	-,-,-
S10	L	-	-	-	-	-,-,-	-,-,-	3	-	-	-	-,-,-	-,-,-	-	-	-	-	-,-,-	-,-,-
TOTAL		28	7	2	-	2,-,-	-,-,-	33	5	1	1	1,-,-	3,-,-	53	8	2	-	-,-,-	4,1,-

Hemi, hemisphere; TOT, total number of electrodes; mA, memory condition active (relative to baseline); mS, memory condition selective (relative to baseline and math); mO, memory condition only (memory selective and math not active relative to baseline); DecIN, decreased initial activity as a function of min operand; IncTO, increased total activity as a function of min operand. The numbers separated by commas correspond to mA, mS, mO respectively. Electrodes included are statistically significant at  $p < 0.05$  FDR-corrected within subject

**Table 3.6 Number of electrodes showing modulation by the min operand by subject in other anatomical regions**

Subject	Hemi	Other anatomical regions (outside pITG, aIPS and SPL)										
		TOT	MA	MS	MO	DecIN	IncTO	mA	mS	mO	DecIN	IncTO
S1	R	45	10	7	2	1,1,1	-,-,-	10	7	6	-,-,-	-,-,-
S2	L	12	3	3	2	1,1,1	-,-,-	7	5	4	-,-,-	1,-,-
S3	L	9	1	-	-	-,-,-	-,-,-	6	5	4	-,-,-	-,-,-
S4	R	11	1	1	1	-,-,-	1,1,1	-	-	-	-,-,-	-,-,-
S5	L	1	1	1	-	-,-,-	-,-,-	1	-	-	-,-,-	-,-,-
S6	L	26	8	3	1	-,-,-	-,-,-	7	3	1	-,-,-	-,-,-
S7	L	9	2	2	1	-,-,-	-,-,-	-	-	-	-,-,-	-,-,-
S8	R	20	8	8	4	-,-,-	2,2,1	4	-	-	-,-,-	1,-,-
S9	R	23	4	3	2	-,-,-	-,-,-	6	5	4	-,-,-	-,-,-
S10	L	12	1	1	-	-,-,-	-,-,-	4	3	3	-,-,-	-,-,-
TOTAL		168	39	29	13	2,2,2	3,3,2	45	28	22	-,-,-	2,-,-

Hemi, hemisphere; TOT, total number of electrodes; MA, math condition active (relative to baseline); MS, math condition selective (relative to baseline and memory); MO, math condition only (math selective and memory not active relative to baseline); mA, memory condition active (relative to baseline); mS, memory condition selective (relative to baseline and math); mO, memory condition only (memory selective and math not active relative to baseline); DecIN, decreased initial activity as a function of min operand; IncTO, increased total activity as a function of min operand. The numbers separated by commas correspond to MA, MS, MO or mA, mS, mO respectively. Electrodes included are statistically significant at  $p < 0.05$  FDR-corrected within subject.

**Table 3.7 Stimuli list for the Math task**

10+1=11	78+2=80	4+25=29	5+87=92	56+6=62	24+7=31	16+8=24	45+9=54
1+18=19	78+2=65	4+25=32	5+87=93	56+6=64	26+7=33	16+8=22	45+9=55
1+18=25	2+52=54	24+5=29	28+6=34	67+6=73	26+7=34	47+8=55	47+9=56
1+41=42	2+52=56	24+5=39	28+6=36	6+22=28	59+7=66	47+8=54	47+9=56
1+41=50	2+60=62	33+5=38	38+6=44	6+22=33	59+7=65	8+30=38	53+9=62
11+2=16	2+60=72	33+5=32	38+6=42	6+36=42	7+34=41	8+30=45	53+9=63
24+2=26	20+4=24	81+5=86	42+6=48	6+36=43	7+34=42	8+65=73	9+23=32
24+2=19	20+4=17	81+5=92	42+6=59	6+39=45	7+43=50	8+65=74	9+23=34
61+2=63	54+4=58	5+63=68	51+6=57	6+39=47	7+43=63	44+9=53	9+86=95
61+2=75	54+4=65	5+63=56	51+6=71	24+7=31	7+67=73	44+9=51	9+86=96

## Chapter 4. DECODING THE PROCESSING STAGES OF MENTAL ARITHMETIC WITH MAGNETOENCEPHALOGRAPHY

---

### 4.1 Motivation

The results presented in **Chapter 2** and **3** offer several new insights on the neurocognitive mechanisms of mental calculations. However, they did not provide any indication of the nature of the underlying neural codes of the operands, neither a comprehensive picture of the series of unfolding computations in the brain. In **Chapter 4**, I apply time-resolved multivariate pattern analysis to magnetoencephalography (MEG) signals with the goal of characterizing the series of processing stages and mental transformations involved in an arithmetic verification task.

Specifically, I aimed at answering the following questions. Can we decode the identity of operands? If so, can we distinguish neural codes for digit symbols and for the corresponding quantities? Can we track in time the emergence of the internally computed result? Can we dissect the comparison and decision processes by which subjects classify the proposed result as correct or incorrect? Are these processes completely serial or do they partially overlap in a form of a cascade of computations that can be simultaneously decoded?

## 4.2 Abstract

Elementary arithmetic is one of the most prevalent cultural inventions in our daily lives. However, despite decades of research, we still lack a comprehensive understanding of how the brain computes simple additions and subtractions. We applied machine learning techniques to magnetoencephalography (MEG) signals in order to characterize the processing stages and mental transformations underlying elementary arithmetic. Adults subjects verified single-digit addition and subtraction problems such as  $3+2=9$  in which each successive symbol was presented sequentially. MEG signals revealed a cascade of partially overlapping brain states. While the first operand could be transiently decoded above chance level, primarily based on its visual properties, the decoding of the second operand was more accurate and lasted longer. Representational similarity analyses suggested that this decoding rested on both visual and magnitude codes. We were also able to decode the operation type (additions vs. subtraction) during practically the entire trial after the presentation of the operation sign. At the decision stage, MEG indicated a fast and highly overlapping dynamics for (1) identifying the proposed result, (2) judging whether it was correct or incorrect, and (3) pressing the response button. Surprisingly, however, the internally computed result could not be decoded. Our results provide a first comprehensive picture of the unfolding processing stages underlying arithmetic calculations at a single-trial level, and suggest that externally and internally generated neural codes may have different neural substrates.

### 4.3 Introduction

Cultural inventions such as mathematics are unique to humans and can radically enhance our native cognitive competence. Therefore, understanding how mathematics is implemented in the brain is fundamental to our comprehension of the mechanisms of high-level symbolic cognition. Arithmetic is the most elementary branch of mathematics and yet, despite decades of research, how the brain solves simple calculations is still largely unknown.

Traditionally, research in cognitive arithmetic has relied on behavioral methods and used mental chronometry to infer the covert processing stages of mental calculations. Behavioral research discovered that response time (RT) during calculation increases with the size of the operands, a finding which has been called the “problem-size” effect and which led to the proposal of several models of mental arithmetic (Ashcraft & Battaglia, 1978; Butterworth, Zorzi, Girelli, & Jonckheere, 2001; Campbell, 1994; Groen & Parkman, 1972; Uttenhove, Thevenot, & Barrouillet, 2016; Zbrodoff & Logan, 2005).

However, since RT is only a summary measure of the entire processing chain, it can only provide indirect information on the nature and relative timing of the various stages. Recently, more direct behavioral methods, such as continuous measures of finger pointing, have helped characterized the covert processing stages of arithmetic processing (Dotan & Dehaene, 2013, 2015; Pinheiro-Chagas, Dotan, et al., 2017). Pinheiro-Chagas et al. (2017) monitored the finger trajectory of adult subjects, while they were asked to point to the result of single-digit calculations on a number line. Results revealed that additions and subtractions are computed by a stepwise displacement on the mental number line, starting with the larger operand (*max*), irrespectively of its position in the problem, and incrementally adding or subtracting the smaller operand (*min*). They also found a transient effect of the operator sign (a plus sign attracted the finger to the right [larger results] and a minus sign to the left [smaller results]) around the time that subjects were processing the second operand. However, while such behavioral methods can be considerably informative about the duration and serial organization of cognitive computations, they remain limited in capturing processes that may happen simultaneously.

To supplement behavioral research, several studies have tried to decipher the neural code for numbers. Initial electrophysiology findings revealed the existence of single neurons tuned to specific numerosities in the monkey ventral intraparietal (VIP) and lateral prefrontal cortices (lPFC) (Nieder, 2016). These results were corroborated by human fMRI studies that demonstrated tuning curves for numbers in the intraparietal sulcus (IPS) (Piazza et al., 2004, 2007) and a topographical organization of numerosites in the lateral parietal cortex (Harvey et al., 2013). Machine learning was also used to successfully decode the identity of numbers from fMRI activity in parietal cortex (Eger, Pinel, Dehaene, & Kleinschmidt, 2015; Eger et al., 2009). However, these studies only investigated simple magnitude perception and comparison tasks. At present, due to the difficulty of training monkeys in arithmetic tasks, electrophysiological studies have not yet obtained direct information about the neural transformations underlying mental calculation, and fMRI measurements in humans are probably too slow to characterize them.

Only a few studies have tried to decompose the brain states during arithmetic processing, using a combination of mental chronometry and time-resolved brain imaging. Dehaene (1996) combined event relate potentials (ERPs) and the additive-factors method (Sternberg, 1969) to parse the processing stages involved in a number comparison (between two visually presented stimuli). By manipulating orthogonal features of the stimuli and the task, the author showed that the ERPs were first modulated by notation (Arabic numerals vs. number words, at ~110 - 170 ms), followed by the numerical distance (close vs. far, at ~190-300 ms) and finally by the lateralization of motor response (left vs. right, at ~250 – 400 ms). More recently, using a modified version of the arithmetic verification with ERPs, Avancini, Soltész, & Szucs (2015) identified a series of overlapping cognitive processes during calculation, such as the identification of the stimuli properties, magnitude comparison and judgment of correctness.

Progress in understanding the spatial-temporal dynamics of mental calculations have recently increased with a series of novel electrocorticography (ECoG) findings. Using a sequentially presented addition task, a recent study revealed a series of successive brain activations: starting around ~90 ms, the number form area (NFA, lateral ventral temporal cortex) responds to digits, irrespective of whether or not they are presented in a calculation context (Shum et al., 2013);

slightly later at ~100 ms, adjacent sites in the posterior inferior temporal gyrus (pITG) respond to numbers only when they are manipulated in the context of a calculation. Furthermore, activity at those ventral calculation-selective populations showed high correlations with activity in the vicinity of the intraparietal sulcus (IPS), which is traditionally considered the main number processing hub in the brain (Dehaene et al., 2003). Pinheiro-Chagas, Daitch, Parvizi, and Dehaene, (2017) further determined that both of these regions were affected by problem-size, though in different ways: pITG shows a fast peak which was inversely proportional to problem size, while IPS shows a more progressive activity whose integral is proportional to problem size. Thus, both of these regions seem to be involved in magnitude processing, but these findings do not resolve the nature of the underlying neural codes for the operands, nor do they provide a comprehensive picture of the series of unfolding computations.

In the present study, we aimed to evaluate whether magnetoencephalography (MEG) could resolve this issue. We combined MEG recordings with time-resolved multivariate pattern analysis (MVPA), specifically decoding (King & Dehaene, 2014) and representational similarity analysis (Kriegeskorte & Kievit, 2013), in order to characterize the series of processing stages and mental transformations underlying elementary arithmetic. Time-resolved decoding has been shown to be a powerful tool to investigate the temporal dynamics of cognitive tasks, because it can determine the precise time at which a given mental content becomes decodable from brain activity (King & Dehaene, 2014). Furthermore, MVPA can then shed light on the nature of underlying codes (Diedrichsen & Kriegeskorte, 2017), exceeding the capacity of traditional ERP univariate-level analysis to capture fine-grained representations (Pantazis et al., 2017). Decoding and MVPA have been successfully applied to characterize several cognitive functions such as working memory (King et al., 2016; Trübutschek et al., 2017; Wolff, Jochim, Akyürek, & Stokes, 2017) and object recognition and categorization (Carlson et al., 2011, 2013; Cichy et al., 2014; Isik et al., 2014). MVPA has been shown to exceed the capacity of traditional ERP univariate-level analysis to reveal fine-grained representations (Pantazis et al., 2017).

In the present task, subjects were asked to verify single-digit addition and subtraction problems, such as  $3+2=5$ . Each of the symbols was presented sequentially for 400 ms, separated

by 385 ms, so that we could analyze brain activity at each step. Specifically, we aimed at answering the following questions. First, can we decode the identity of operands? If so, can we distinguish neural codes for digit symbols and for the corresponding quantities? What is their temporal dynamics? Is this information sustained or transient? When and for how long can we decode the operation type? Can we then track the emergence of the internally computed result? Can we dissect the comparison and decision processes by which subjects classify the proposed result as correct or incorrect? Are these processes completely serial or do they partially overlap in a form of a cascade of computations that can be simultaneously decoded? Finally, are the neural codes independent of each other, or do they overlap? We were particularly interested in the possibility that the neural codes for addition versus subtraction (active just after the presentation of the operation sign) would overlap with those for large versus small numbers, as such an overlap would readily explain the psychological observation that additions induce a bias towards larger numbers and subtraction towards smaller numbers (Knops, Viarouge, Dehaene, et al., 2009; Knops, Thirion, et al., 2009; McCrink et al., 2007; Pinhas & Fischer, 2008; Pinheiro-Chagas, Dotan, et al., 2017).

## 4.4 Methods

### 4.4.1 Protocol and experimental design

Twenty healthy adults were scanned with MEG ( $23 \pm 2$  years old, 10 females, all right handed). Subjects had normal vision. The experiment lasted  $\sim 45$  minutes, for which subjects were financially compensated. The study was approved by the local Ethics Committee and all subjects provided written informed consent before participation.

Subjects were asked to verify the accuracy of sequentially presented single-digit additions and subtractions problems in the form of  $A \pm B = C$  (see Figure 4.1A). Each stimulus appeared for 400 ms, with an inter-stimuli interval of 385 ms. Subjects were instructed to generate an internal estimate of the result in advance of its appearance, and to further incite them, on half of the trials the appearance of  $C$  was delayed for an additional 385 ms. Inter-trial interval was 2,000 ms. Stimuli were white with a  $1.5^\circ$  visual angle, presented on a black background and projected

on a screen with a refreshing rate of 60 Hz, placed 100 cm away from subject's head. The experiment was programmed in Python, mostly using the PsychoPy package (Peirce, 2007).

Subjects were asked to respond as fast and as accurate as possible if C was correct or incorrect, by pressing a button with their left or right thumb. In half of the blocks, left/right were associated with correct/incorrect and then switched. The association order was randomized across subjects. Stimuli were composed of the 16 addition and 16 subtraction problems consisting of all combinations of the operands: A = [3, 4, 5, 6] and B = [0, 1, 2, 3]. The correct results C ranged from 0 to 9, in the following proportions: 0 : 3.12 %, 1 : 6.25 %, 2 : 9.38 %, 3 : 15.62 %, 4 : 15.62 %, 5 : 15.62 %, 6 : 15.62 %, 7 : 9.38 %, 8 : 6.25 %, 9 : 3.12 %. On half the trials, C was correct. On the other half, C was  $\pm$  [1, 2, 3, 4] distant from the correct result. A list of incorrect C's was generated for each subject with the single goal of maximizing the homogeneity of their distribution across trials.

Each experimental block took  $\sim$ 4.5 min and consisted of 32 calculation trials and 8 non-calculation trials, of the form "A = = = C", which are not analyzed in the current publication. Subjects completed 10 experimental blocks, comprising a total of 320 calculation trials.

#### 4.4.2 Preprocessing

MEG signals were recorded with an ElektaNeuromag® MEG system (Helsinki, Finland), comprising 306 sensors (102 triples of 2 orthogonal planar gradiometers and 1 magnetometer) in a helmet-shaped array. Subjects' head position relative to the MEG sensors was estimated with four head position coils (HPI) placed on the frontal and pre-auricular areas, digitized with a 3-dimensional Fastrak system (Polhemus, USA), and triangulated before each block of trials. Three pair of electrodes recorded electrocardiograms (EMG) as well as the horizontal and vertical electro-oculograms (EOG). All signals were sampled at 1 kHz. MEG signals were hardware band-pass filtered between 0.1 Hz and 330 Hz, and active compensated for external noise with Maxshield (ElektaNeuromag). After visual inspection of bad channels, raw MEG signals were cleaned with the signal space separation method (Taulu & Simola, 2006) provided by MaxFilter (ElektaNeuromag) to 1. suppress magnetic interferences and 2. interpolate bad sensors. All further

preprocessing steps were done with the Matlab Fieldtrip Toolbox (Oostenveld, Fries, Maris, & Schoffelen, 2011).

The MEG raw signals were epoched between -500 ms and +4,500 ms with respect to the onset of the first operand (A, see Figure 1A) and downsampled to 250 Hz. Trials contaminated by muscular or other artifact, were identified and rejected in a semi-automated procedure that used the variance across the MEG sensors. Next, we applied independent component analysis (ICA) to identify and remove artifacts caused by eye blinks and heartbeats. We then visually inspected the topographies of the first 30 components and subtracted the contaminated components from the data.

Further preprocessing was dependent on the nature of the analysis. For decoding and representational similarity analysis (RSA), epochs were low-pass filtered at 30 Hz and downsampled to 125 Hz. For time-frequency analysis, the spectral power of the non-low-pass-filtered epochs were estimated with parameters adapted to low and high frequency ranges. For the low-frequency range (2 – 34 Hz, steps: 1 Hz), data segments extracted from a sliding time window (length: 500 ms, steps: 40 ms) between 2 and 10 Hz and with a length of 5 oscillation cycles per frequency between 10 and 34 Hz was tapered with a single Hanning window. For the high-frequency range (34 – 100 Hz, steps: 2 Hz), data segments extracted from a sliding time window (length: 200 ms, steps: 40 ms) were multitapered and the frequency smoothing was set to 20% of each frequency value. Finally, epochs were cropped in three time windows: time-locked to A (-200 ms to 3,200 ms), time-locked to C (-200 ms to +800 ms) and time-locked to the response (-800 ms to +200 ms).

#### 4.4.3 Decoding

The multivariate estimators aimed at predicting a vector of labels ( $y$ ) from a matrix of features composed by single-trial MEG amplitude signals ( $X$ , shape =  $n_{trials} \times (n_{sensors} \times 1_{time\ sample})$ ). Decoding analyses systematically consisted of the following steps: (1) fitting a linear estimator to a training subset of  $X$  ( $X_{train}$ ); (2) predicting an estimate of  $y$  on a separate test set ( $\hat{y}_{test}$ ); (3) assessing the decoding score of these predictions as compared to the true value of  $y$ . This procedure

was repeated for each time sample separately. First, we used a standard transformation to z-scores in each channel at each time point across trials, in order to concomitantly include all 306 MEG sensors, pooling over magnetometers and gradiometers. Next, we fitted the data with a linear model to find the hyperplane that maximally predicts  $y$  from  $X$  while minimizing the loss function. Two main estimators were used: linear support vector machine (SVM) and Ridge Regression, both with a class-weight parameter to compensate for any potential class imbalance in the dataset. For multiclass problems using SVM, a ‘one-versus-one’ decision function was used. All decoding analyses were performed within subject and across trials, with an 8-fold stratified folding cross-validation scheme to maximize the homogeneity of distribution across training and testing sets. Decoding scores ( $y, \hat{y}$ ) were quantified using the average classification accuracy for SVM and the Kendall’s  $\tau$  for ridge regression. Statistical analyses were based on second-level tests across subjects. More specifically, we tested whether the classification scores were higher than chance value or 0, for classification accuracy and Kendall’s  $\tau$ , respectively, using one-sample t-test with random-effect Monte-Carlo cluster statistics for multiple comparison correction (Maris and Oostenveld, 2007), using the default parameters of the MNE `spatio_temporal_cluster_1samp_test` function.

#### 4.4.3.1 Temporal generalization

We also tested if each estimator fitted across trials at time  $t$  could accurately predict the  $\hat{y}$  value at time  $t'$ , therefore probing whether the coding pattern is similar between  $t$  and  $t'$ . We applied this systematically across all pairs of time samples, resulting in a temporal generalization matrix (King & Dehaene, 2014).

#### 4.4.3.2 Riemannian geometry

We also applied an estimator based on Riemannian geometry, using a covariance matrix estimation that integrates the temporal information. More specifically, the model relies on the tangent space mapping of the covariance matrix described in (Barachant, Bonnet, Congedo, & Jutten, 2013). We started by decomposing the low-pass filtered data with a Principal Component

Analysis (PCA) and taking the first 70 components for dimensionality reduction. Next, we used the ERPCov model (Barachant & Congedo, 2014), which is useful to capture both evoked and task induced responses, since it embeds the temporal information of the signal by concatenating, along the sensor axis, the averaged ERF (across trial) of each class before estimating the spatial covariance matrix. Finally, we mapped the covariance matrix to the tangent space and fitted a SVM or logistic regression with our standard cross-validation scheme. The use of Riemannian geometry has been shown to increase performances in sensorimotor rhythm (SMR)-based brain-computer interface (BCI) and more recently in MEG decoding of cognitive features (Biomag 2016 Decoding Competition). All decoding analysis were performed using the Python Scikit-Learn (Pedregosa et al., 2011) and MNE (Gramfort et al., 2013) packages, with some open source tools developed by Jean-Rémi King and Alexandre Barachant (<https://github.com/kingjr/jr-tools>, <https://github.com/Team-BK/Biomag2016>).

#### 4.4.4 Representational Similarity Analysis (RSA)

Several RSA models were constructed to test specific relationships between different dimensions of the stimuli and the MEG signals (Cichy et al., 2014; Diedrichsen & Kriegeskorte, 2017; Kriegeskorte & Kievit, 2013). RSA analyses systematically consisted of (1) averaging conditions across trials; (2) pair-wise correlating the conditions across the MEG sensors at each time point; (3) creating a symmetric dissimilarity matrix, equal to 1 - Spearman's rank correlation coefficient; (4) correlating the observed matrix with the theoretical similarity matrices predicted by different types of neural codes for the stimuli (see below). This procedure was repeated for each time sample separately. From the z-scored data, 32x32 representational dissimilarity matrices (RDM) were constructed using the 32 additions and subtraction problems, sorted by first operand, then by operation (additions first) and finally by second operand (3+0, 3+1, 3+2, 3+3, 3-0, 3-1, 3-2, 3-3, etc.). Seven theoretical RDM were constructed with the same structure and based on the magnitude dissimilarity (numerical distance) or visual dissimilarity (see method below) of operand 1, operand 2 and correct result and based on category for addition vs. subtractions (see Figure 4.4). Visual dissimilarity matrices were calculated using the Gabor Filterbank method, as 104

implemented in the Matlab Image Similarity Toolbox. ([https://github.com/daseibert/image\\_similarity\\_toolbox](https://github.com/daseibert/image_similarity_toolbox)).

This method projects the image onto a Gabor wavelet pyramid as a model for primary visual cortex, simplified from (Kay, Naselaris, Prenger, & Gallant, 2008). The filters span eight orientations (multiples of  $.125\pi$ ), four sizes (with the central edge covering 100%, 33%, 11%, and 3.7% of the image), and  $X$ ,  $Y$  positions across the image (such that filters tile the space for each filter size). The resulting vector of filter responses are then compared between images, using the Euclidean distance. The method replicates the dissimilarity matrix of neural responses of the inferior temporal cortex (IT) in both humans and monkeys (Kriegeskorte et al., 2008) (Readme File of the toolbox).

We then used Spearman's rank correlation test to evaluate the relationship between the observed and theoretical matrices. All RSA analyses were first computed within each subject, then statistical analyses were based on second-level tests across subjects, using the same method as in the decoding analysis, to test if the correlation coefficient was higher than 0.

## 4.5 Results

Twenty healthy adults were asked to verify the accuracy of successively presented single-digit additions and subtractions problems with matched operands in the form of  $A \pm B = C$ , where in half of the trials  $C$  was incorrect (see Figure 4.1A and Methods). Accuracy was very high (average = 98.8%). Reaction time was faster for correct as compared to incorrect proposed results ( $\text{mean}_{\text{correct}} = 519$  ms,  $\text{SD}_{\text{correct}} = 117$  ms,  $\text{mean}_{\text{incorrect}} = 622$  ms,  $\text{SD}_{\text{incorrect}} = 134$  ms,  $F(1, 19) = 68.796$ ,  $p = 0.013$ ;  $\eta^2 = 0.149$ ). Within the trials with an incorrect result, no distance effect was found across the four absolute distances between the proposed and the correct results ( $\text{mean}_1 = 630$  ms,  $\text{SD}_1 = 145$  ms,  $\text{mean}_2 = 616$  ms,  $\text{SD}_2 = 130$  ms,  $\text{mean}_3 = 628$  ms,  $\text{SD}_3 = 136$  ms,  $\text{mean}_4 = 615$  ms,  $\text{SD}_4 = 141$  ms,  $F(3, 57) = 0.781$ ,  $p = 0.508$ ;  $\eta^2 = 0.002$ ). And no significant difference was observed when combining the trials in which parity was violated (distance 1 or 3) and those in which it was preserved (distance 2 or 4) ( $t(19) = 0.437$ ,  $p = 0.662$ , Cohen's  $d = 0.097$ ). Finally, we also did not observe a

problem-size effect, considering both operand 1 (*max*) ( $b = 4.919$  ms;  $p = 0.69$ ) and operand 2 (*min*) ( $b = -3.249$  ms;  $p = 0.797$ ). This is expected, since calculation was probably performed between the onset of operand 2 and the equal sign, therefore subjects most likely already had the correct result in mind when the proposed result was presented.

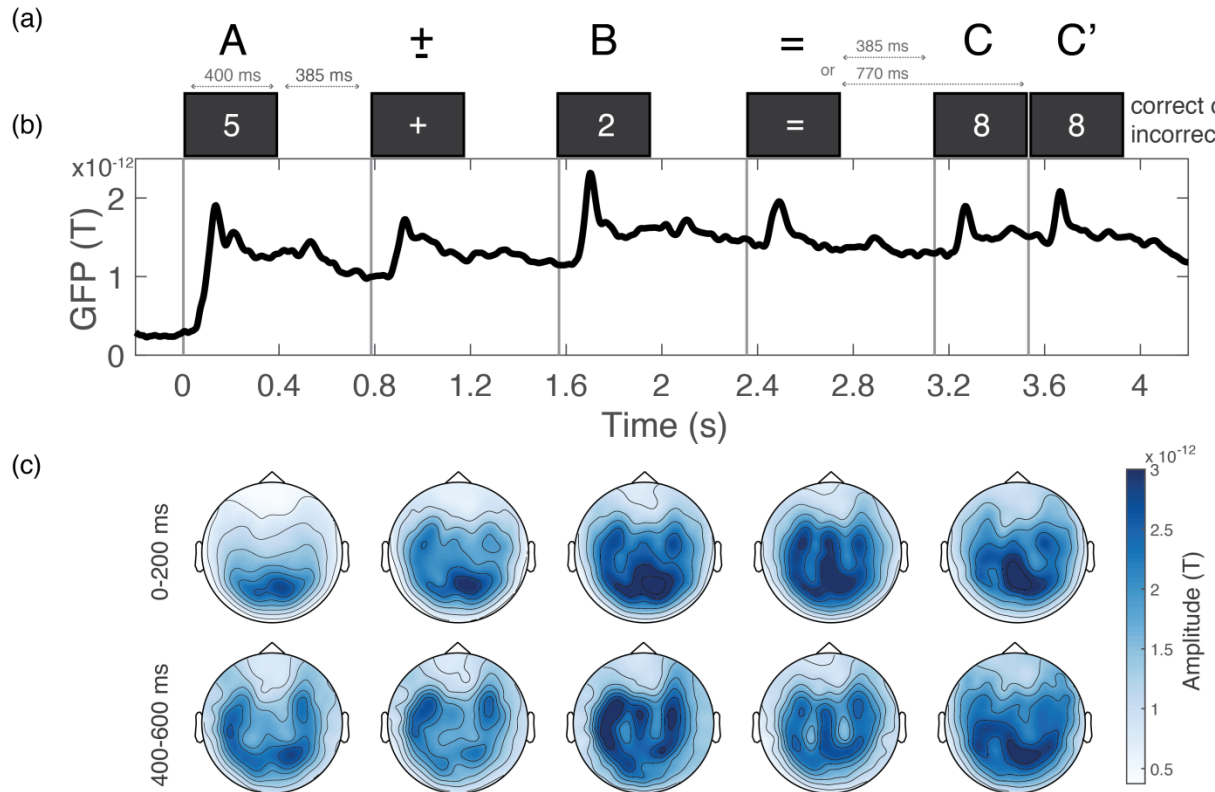


**Figure 4.1 Sustained activity and signal propagation from posterior to anterior sensors**

(A) Experimental design. Subjects were asked to verify the accuracy of sequentially presented single-digit additions and subtractions problems in the form of  $A \pm B = C$ , with an 785 ms asynchrony. On half the trials, the presentation of  $C$  was delayed by an additional 385 ms. (B) Global Field Power (GFP), estimated using the MEG gradiometers and baseline corrected. After the onset of each stimulus event, GFP sharply peaked and remained above baseline for the entire trial. (C) Averaged MEG gradiometers topographies calculated between 0 – 200 ms and 400 – 600 ms after each stimulus. The signal propagates from posterior to anterior sensors after the onset of each stimulus and overall across the entire trial.

#### **4.5.1 Sustained activity across the entire trial**

In order to investigate whether overall activity was transient or sustained across the entire trial, we calculated the Global Field Power (GFP) (Lehmann & Skrandies, 1980), for the MEG gradiometers sensors and then normalized with the reference of a baseline period of -200 ms from the onset of operand 1.. As can be seen from Figure 4.1B, GFP increases right after ( $\sim$ 100 ms) the presentation of each event and then slowly decreased until the presentation of the next event, but without returning to baseline, thus confirming that the overall activity was sustained across the entire trial. The evoked brain activity evolved across time from more anterior sensors in the first 200 ms after the stimuli onset to more posterior sensors in the following period of 400 – 600 ms. Qualitative exploration showed that the second operand produced a higher and wider occipital-parietal-frontal activation as compared to the first operand, in both early and later time windows (Figure 4.1C). Therefore, this sustained activity allows us to investigate in more detail the mental transformations occurring during the entire trial.

#### **4.5.1 Decoding the processing stages of mental arithmetic**

We next investigated whether we could decode the series of processing stages underlying mental calculation, from the perception and representation of the operands to the operation type and response selection. For this purpose, we cropped the epochs in three different time windows: time-locked to operand 1 (-200 ms to 3,200 ms), time-locked to C (-200 ms to +800 ms) and time-locked to the RT (-800 ms to +200 ms). For each time window, we used seven different classifiers (SVM, see Methods) to decode operand 1 [values: 3, 4, 5, 6], operation [additions, subtractions], operand 2 [0, 1, 2, 3], correct result [3, 4, 5, 6; chance = 0.25], proposed result [3, 4, 5, 6], correctness of the operation as judged by the subject [correct or incorrect, including only the accurate responses], and response side [left vs. right button press, including only the accurate responses]. Note that for the correct and proposed result we only included the trials in which their values were [3, 4, 5, 6], since those were homogeneously distributed (15.62 % of trials each, see Methods).

#### 4.5.1.1 Operand 1

The classification accuracy for operand 1 became significantly above chance starting at 112 ms after its onset, with a peak at 152 ms, and lasted until 640 ms ( $p < 0.05$ , corrected for multiple comparisons).

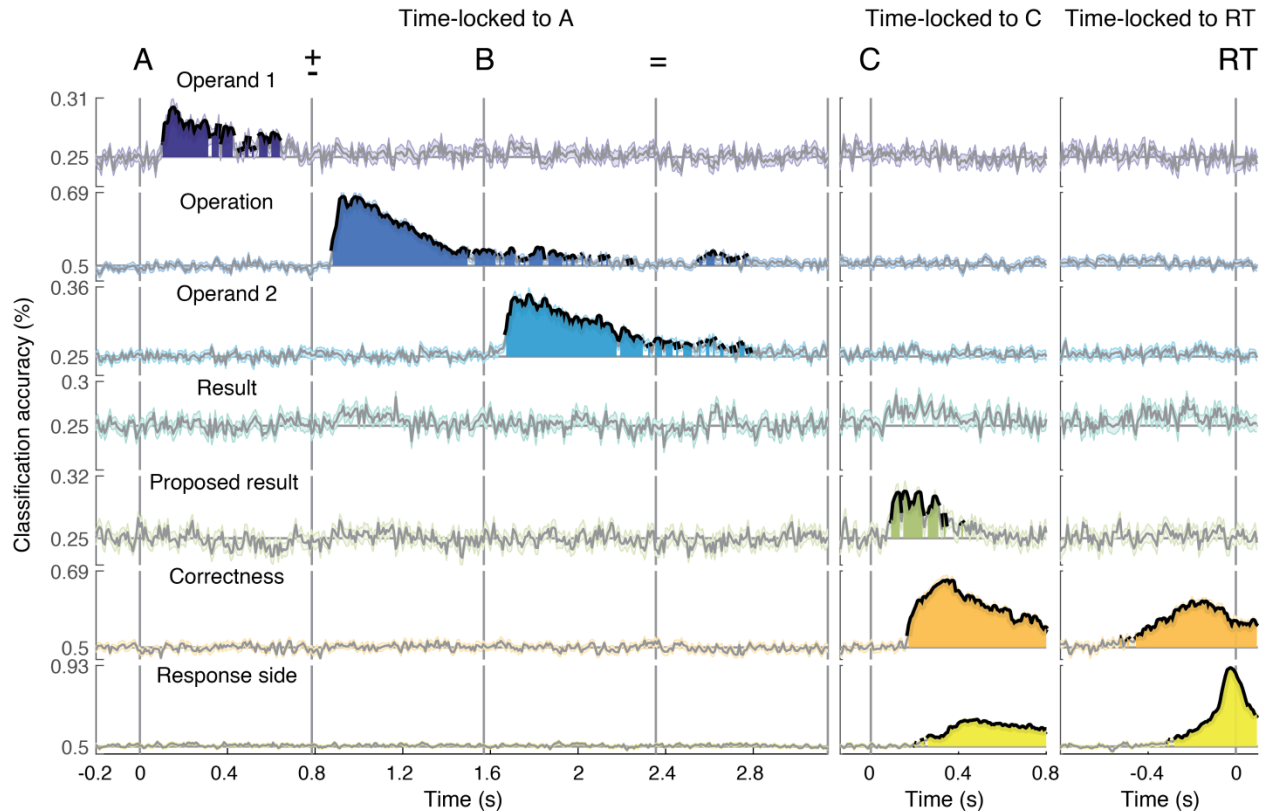


**Figure 4.2 Decoding the time course of the processing stages underlying calculation**

A series of SVM estimators were applied to classify the different features at each time sample, using the signal amplitude of all MEG sensors. Trials were time-locked to three windows of interest: after the onset of the operand 1 (A), proposed result (C) and RT. Gray horizontal lines indicate theoretical chance level. Operand 1, operand 2, result and proposed result involved 4 classes each (theoretical chance level = 25 %) and operation, correctness and response side involved binary classifiers (theoretical chance level = 50 %.). Thick lines and filled areas represent time periods in which the second-level statistical tests across subjects revealed a classification accuracy significantly above chance (cluster corrected for multiple comparisons,  $p < 0.05$ ).

#### 4.5.1.2 Operation type

The decoding scores for the operation became significantly higher than chance at 880 ms (i.e. 95 ms after the onset of the operation sign at 785 ms) with the peak at 928 ms, then dropping

after the offset of sign, but remaining above chance almost all the way through the onset of the equal sign, and then transiently recovering above-chance performance level after the onset of the equal sign ( $p < 0.05$ , corrected).

#### 4.5.1.3 Cross generalization from operation type to operand 2

The high initial classification score of the operation is most likely due to the visual difference between the plus and minus signs, but could also reflect task-specific preparation, such as operator priming (Fayol & Thevenot, 2012) as well as visual-spatial mechanisms or spatial-numerical associations (Hartmann, Mast, & Fischer, 2015; Masson & Pesenti, 2014; Mathieu, Epinat-duclos, Léone, Fayol, & Thevenot, 2017; Mathieu et al., 2016). Indeed, behavioral studies have shown that addition leads to a bias towards large numbers, and subtraction a bias towards small numbers (Knops, Viarouge, Dehaene, et al., 2009; Knops, Thirion, et al., 2009; McCrink et al., 2007; Pinhas & Fischer, 2008), which could suggest that the neural codes for add/subtract and for larger/smaller numbers overlap. To test this hypothesis, we trained a logistic regression estimator to decode subtractions vs. additions and tested if it could cross-generalize to small vs. larger numbers for both operand 1 (in which 3 & 4 received the same label as subtraction and 5 & 6 as addition) and operand 2 (in which 0 & 1 received the small label as subtraction and 2 & 3 as addition). As can be seen in Figure 4.3, cross-generalization from operation was only significant at the time of operand 2, but not for operand 1 (even when using a more robust Riemannian geometry based model which integrates the temporal information). Those results therefore suggest the existence of a transient (~128 – 288 ms) common code between subtractions and additions and smaller and larger operands 2, respectively.

#### 4.5.1.4 Operand 2

The decoding scores for operand 2 started to be significantly above chance at 1,672 ms (i.e. 102 ms after its onset at 1,570 ms) with a peak at 1,776 ms, then dropping after its offset, but remaining above chance until 2,770 ms ( $p < 0.05$ , corrected). Therefore, between the onset of

operand2 and the offset of the equal sign, both the operation (addition vs. subtractions) and the operand 2 could be decoded simultaneously from the same MEG data.

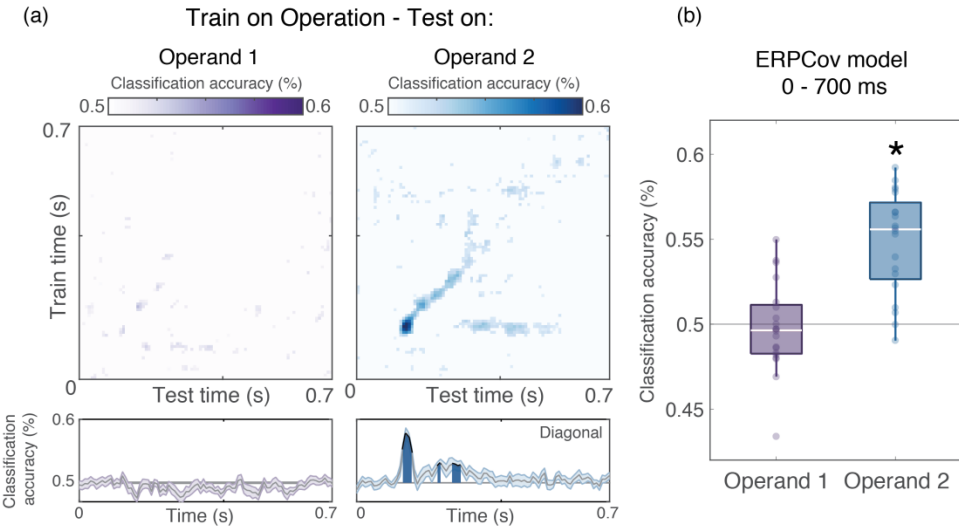


**Figure 4.3 Cross-decoding from operation to operands**

A logistic regression estimator was used to decode subtractions vs. additions and then tested if it could generalize to respectively smaller vs. larger numbers for both operand 1 (in which 3 & 4 received the same label as subtraction and 5 & 6 as addition) and operand 2 (in which 0 & 1 – subtraction and 2 & 3 addition). The time window used was between 0 – 700 ms, locked to each stimulus. (A) Top squared plots show the generalization across time matrices, with only classification accuracies significantly above chance ( $p < 0.05$ , uncorrected). Bottom plots show the diagonal of the upper matrices, where train and test times were the same. Gray horizontal lines indicate theoretical chance level (0.5). Thick lines and filled areas represent time periods with classification accuracy significantly above chance (cluster corrected for multiple comparisons,  $p < 0.05$ ). (B) Boxplots represent classification scores across subjects (individual dots) for the ERPCov model, which integrates the information over 0 – 700 ms (\* =  $p < 0.01$ , second-level 1-sampled t-test).

Importantly, comparisons showed that operand 2 was decoded with higher classification accuracy than operand 1 (between 0 – 400 ms: mean operand 2 = 0.31, SD = 0.029; mean operand 1 = 0.27, SD = 0.016,  $F(1, 19) = 67.706$ ,  $p < 0.001$ ;  $\eta^2 = 0.414$  and between 400 - 800 ms: mean operand 2 = 0.284, SD = 0.018; mean operand 1 = 0.26, SD = 0.012,  $F(1, 19) = 41.776$ ,  $p < 0.001$ ;  $\eta^2 = 0.382$ ), and for a longer time period (see also Figure 4.11). This observation suggests that more intense brain activity occurred after operand 2 than after operand 1, in

agreement with the fact that, at this time, subjects were able to start their calculation, a process whose length depends on the size of the *min* operand (or the smallest operand) (Groen & Parkman, 1972; Pinheiro-Chagas, Dotan, et al., 2017; Uittenhove et al., 2016), which in the present experiment is always operand 2. A potential confound that could explain the higher decoding accuracy observed in operand 2 is the presence of 0, since it has been proposed that problems with 0 might engage a non-calculation rule-based strategy (Ashcraft & Battaglia, 1978), therefore facilitating their classification. We tested and refuted this possibility, by excluding the 0s. Even with a smaller data set, the classifier for operand 2 significantly outperformed the one for operand 1 (0 – 400 ms:  $p = 0.015$ ,  $\eta^2 = 0.146$  and 400 – 800 ms:  $p = 0.005$ ,  $\eta^2 = 0.188$ ).

#### **4.5.1.5 Proposed result**

As expected, the proposed result was not decodable before its appearance on screen. Similarly to operand 1, it was transiently decoded starting from 92 ms, with a peak at 166 ms and remained above chance only until around its offset ( $p < 0.05$ , corrected).

#### **4.5.1.6 Correctness**

The correctness of the trial judged by the subject was significantly classified above chance from 172 ms after the onset of the proposed result with a peak at 248 ms and remained significant all the way until the end of the epoch ( $p < 0.05$ , corrected). We did not observe any significant decoding score for the absolute distance between proposed and correct result (1 - 4), in line with the absence of a distance effect in RT. Relative to the onset of the proposed result, the response side started to be significantly classified above chance at 196 ms, with a peak at 484 ms, and this effect also lasted until the end of the epoch ( $p < 0.05$ , corrected). Note that the classifiers for response side and response correctness were orthogonal, since the response buttons were switched in the middle of the experiment (see Methods). A better way to look at the relationship between the judgment of the correctness and the response side, is to time-lock the epochs to the key press. This analysis clearly showed a slow ramping of the classification score for the correctness starting at -428 ms with a peak at -100 ms followed by a drop just before the response ( $p < 0.05$ , corrected).

On the other hand, the fast ramping of the classification score for the response side started at -212 ms and sharply increased to almost perfect classification at around 24 ms before the button press.

#### 4.5.1.7 Generalization across time

To investigate the dynamics of calculation, we conducted a generalization across time decoding analyses (King & Dehaene, 2014), which revealed that the features of operand 1, operation sign, and operand 2 were decodable when train and test times were approximately the same ('*diagonal decoding*' Figure 4.7). This analysis therefore suggests that each of these items launched a series of internal processes whose underlying codes dynamically changed along the trial. Nevertheless, the generalization-across-time matrix was broader for operation sign and for operand 2, transiently turning into a square pattern characteristic of sustained activity (Figure 4.7). Furthermore, while the operand 1 and the proposed result were only transiently decoded during the time window that the stimuli was visually present, the operation, operand 2, correctness and response side had classification scores above chance that lasted for a longer time window.

#### 4.5.2 Representational similarity

The decoding analysis does not directly reveal the precise stimulus dimensions that allowed the classifier to perform above chance level. In particular, we wanted to further investigate the representational geometries underlying the responses evoked by the operands and the result. For that, we turned to representational similarity analyses (RSA).

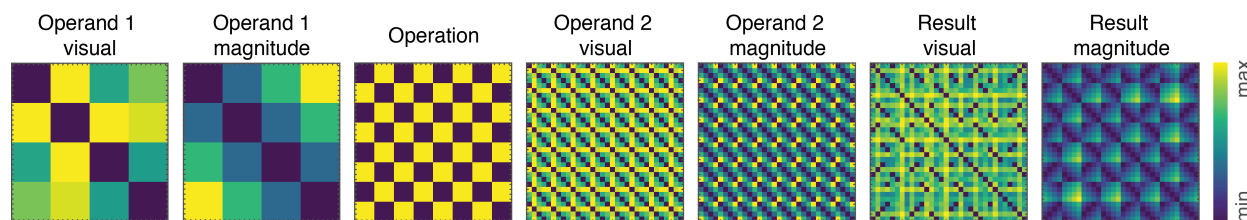


**Figure 4.4 Theoretical predictors of dissimilarity matrices**

Dissimilarity matrices were calculated using all 32 additions and subtraction problems, sorted by operand 1, then by operation (additions first) and finally by operand 2: (3+0, 3+1, 3+2, 3+3, 3-

0, 3-1, 3-2, 3-3, etc., see Figure 4.8). Visual models were calculated using a method that rates the similarity of the digits based on their putative responses in inferior temporal cortex. Magnitude models used the numerical distance between numbers. For the operation, the matrix was composed by 0s (same operation) and 1s (different operations).

Several RSA models were constructed to test specific relationships between different dimensions of the stimuli and the MEG signals. The theoretical representational dissimilarity matrices (RDM) were constructed using the 32 additions and subtraction problems, which were sorted by operand 1, then by operation (additions first) and finally by operand 2: (3+0, 3+1, 3+2, 3+3, 3-0, 3-1, 3-2, 3-3, etc., see Figure 4.8). Seven theoretical RDM matrices were constructed, either based on the magnitude dissimilarity (numerical distance) or visual dissimilarity (using a method that captures the hypothetical responses of inferior temporal cortex), separately for operand 1, operand 2, and the correct result, plus a matrix for category-based similarity for addition vs. subtractions (see Figure 4.4). Those theoretical matrices were used as regressors on the observed matrices derived from the MEG data, i.e., the dissimilarities between the 32 averaged event-related MEG topographies. Such regressions were conducted at each time step, thus allowing us to visualize the time course of the corresponding neural codes.

We first tested whether and when the visual and magnitude dimensions of the operands could be recovered from MEG signals. As can be seen from Figure 4.5, both the visual and magnitude models of the operands had significant correlations with the observed RDM following operand onset. Specifically, the visual model of operand 1 showed a significant effect at 128 ms after visual appearance of operand 1, with a peak at 168 ms and lasting up to 544 ms ( $p < 0.05$ , corrected for multiple comparisons). Around the same time, the magnitude model for operand 1 had a smaller, but significant effect, starting at 112 ms with a peak at 328 ms and lasting until 328 ms ( $p < 0.05$ , corrected). For operand 2 the pattern was somehow inverted. The magnitude model had a stronger effect which started at 1,664 ms (94 ms after the onset of operand 2, which occurred at 1,570 ms). This effect peaked at 1,704 ms and lasted until 2,608 ms ( $p < 0.05$ , corrected), i.e. longer than the visual model (start = 1,672 ms, peak = 1,808, lasting until 2,392 ms,  $p < 0.05$ , corrected).

Since the visual and magnitude models partially correlated with each other, we next investigated the unique variance explained by each model, while regressing out the effect of the other model.

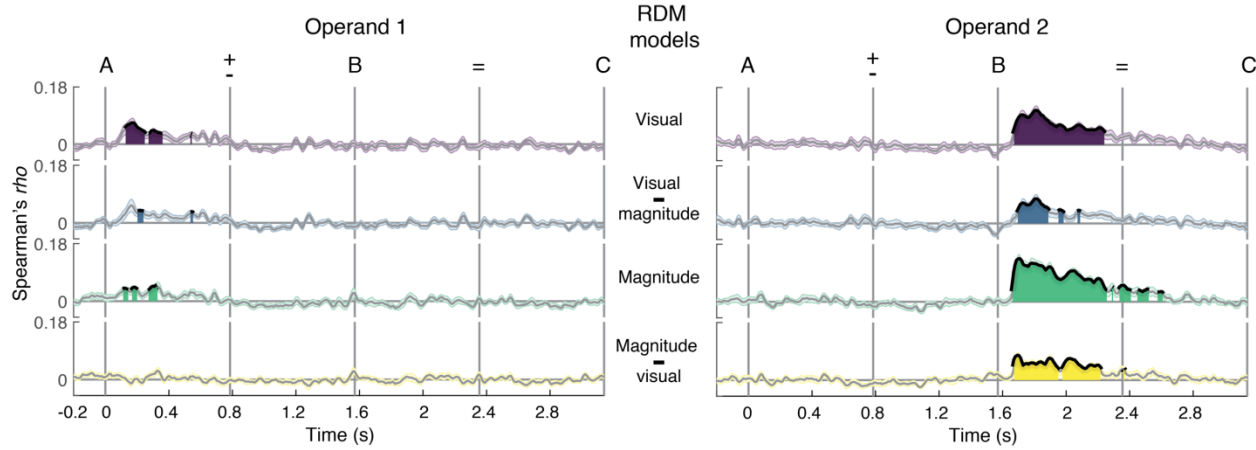


**Figure 4.5 Representational geometries of the operands**

A series of RSA models (see Figure 4.4) were used to investigate the temporal dynamics of the representation of operand 1 and operand 2. Correlations between the theoretical and observed dissimilarity matrix were performed at each time sample. We first correlated the RSA for single predictors (visual and magnitude, lines 1 and 3). Next, to test the unique variance explained by each model, we partialled out the effect of the other model (visual – magnitude and magnitude – visual; lines 2 and 4). Gray horizontal lines indicate theoretical chance level. Thick lines and filled areas represent time periods in which the second-level statistical tests across subjects revealed a correlation coefficient significantly above 0 (cluster corrected for multiple comparison,  $p < 0.05$ ).

For operand 1, the magnitude model did not reach statistical significance at any time point after regressing out the visual model. Conversely, the visual model had two small significant values at  $\sim 224$  ms and  $\sim 544$  ms after controlling for the magnitude model ( $p < 0.05$ , corrected). In contrast, the magnitude model remained significant for operand 2 after regressing out the effect of the visual model from 1,672 to 2,360 ms ( $p < 0.05$ , corrected). Conversely the visual model also remained significant after controlling for the magnitude model, but for a shorted period, from 1,696 to 2,103 ms ( $p < 0.05$ , corrected).

Overall, the RSA corroborates the decoding results, by showing that the representational geometry can be better retrieved from MEG signals for operand 2 compared to operand 1. Crucially, the RSA revealed that both visual and magnitude dimensions of the operands are coded

at about the same time. While the dominant dimension for operand 1 was visual, both visual and magnitude dimensions could be independently retrieved from operand 2, but with a predominance of the magnitude dimension.

#### 4.5.3 Inability to decode the internally computed result

We next searched the data for a representation of the internally computed correct result (i.e. A+B or A-B, depending on the operation) (Figure 4.6). The visual model had no significant effect across the entire trial. The magnitude model was transiently significant, but only right after the presentation of the operation sign, that is, before the actual calculation could have started. Therefore, this result was probably driven by the correlation between the magnitude and the operation sign, since our experimental design had additions and subtractions matched by operands, thus additions produced overall higher results and subtractions smaller results (see Methods). Confirming this intuition, after regressing out the effect of the operation model, the magnitude model did not explain any unique variance, whereas conversely the effect of operator was virtually unchanged when regressing out the magnitude model of the result and it even showed a transiently reactivation after the presentation of the equal sign, similarly to the decoding analysis (see Figure 4.2). Additional classifiers using Ridge Regression corroborated this finding: the correct result could only be transiently decoded right after the presentation of the operation sign, probably because the classifier learned to discriminate additions vs. subtractions (see Figure 4.9), which sufficed to classify the correct result slightly above chance level.

Because we were surprised at our inability to decode the internal computed result, we performed several additional analyses, but none were successful. Here we briefly describe the rationale behind each strategy. First, we explored event related fields (ERF) at the univariate level, using Fieldtrip cluster-based method. Within the time window between operand 2 and the equal sign, or between operand 2 and proposed result (when subjects are supposedly performing the exact calculation), the cluster-based permutation test did not reveal any cluster with a significant correlation with the correct result. We first did this analysis while grouping together

additions and subtractions, then replicated it while analyzing them separately, and also within each group of MEG sensors, to no avail.

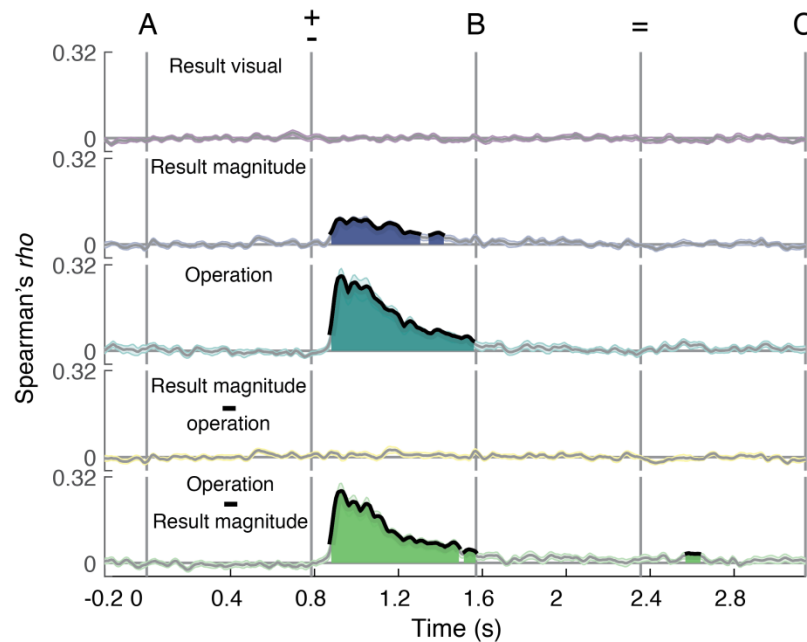


**Figure 4.6 Attempting to decode the internally computed result**

We first correlated the RSA for single predictors of the result (visual and magnitude, lines 1 and 2). Next, to test the unique variance explained by each model, we partialled out the effect of the operation (line 3) from the magnitude model (line 4) and vice versa (line 5). Gray horizontal lines indicate theoretical chance level. Thick lines and filled areas represent time periods in which the second-level statistical tests across subjects revealed a correlation coefficient significantly above 0 (cluster corrected for multiple comparison,  $p < 0.05$ ).

As regards multivariate analyses, we first attempted to predict whether the internally computed result was 3, 4, 5 or 6. The rationale, as explained in the Methods section, was that experimental design used additions and subtractions matched by operands, thus imposing an inhomogeneity on the distribution of results. Therefore, for the main decoding analysis, we only used the most homogeneously distributed results (numbers 3-6), which overall represented 62.48 % of the trials. As described earlier, this analysis did not result in any significant decoding score. We reasoned that if the brain signals associated with the computed results are weak, it might be better to first train the decoder on an explicitly presented number using a large training set, and only test its generalization to the internally computed result. This was done by training the model

to decode the operand 1 during the first 800 ms, and then testing its generalization to the internally computed result. At no time point prior to the presentation of the correct result did we find any significant cross-generalization classification score.

We also trained a classifier to decode the proposed result (when it was correct) time-locked to the proposed result (for 800 ms) and tested if it could generalize backwards to the correct result at the time window between the operand 2 and the proposed result. This model only included 30% of the trials and learning was not above chance for decoding the proposed result, therefore no generalization could be tested on the internally computed result.

Another possibility is that the result is coded in the spectral domain, perhaps within a specific frequency band. To explore that, we used a searchlight approach in time, sensor space and frequency (using the Matlab Cosmo MVPA Toolbox (Oosterhof, Connolly, & Haxby, 2016)). We fitted a series of linear discriminant analysis (LDA) estimators (instead of SVM, for computational simplicity) with our standard cross-validation scheme to classify the main variables of interest (operand 1, operation, operand 2 and result), with the following procedure. First, we selected two frequency bands (low: 1 – 34 Hz and high: 34 - 100 Hz). Next, we selected one sensor (only gradiometers) to be the center of the “sphere” and included its 10 closest neighbor sensors. The matrix of features was therefore composed of single-trial MEG frequency power signals ( $X$ , shape =  $n_{trials} \times (10_{sensors} \times 1_{time\ sample} \times 1_{frequencies})$ ). No significant classifications scores were found in the high frequencies. As can be seen in Figure 4.10, the operand 1, operation and operand 2 could be decoded generally from occipital-parietal sensors, at a short time window following their respective onsets and mostly between 3 to 20 Hz, a frequency band which corresponds to event-related signals and is a classical finding for visually presented stimuli (King, Pescetelli, & Dehaene, 2016). However, no sign of above-chance classification was found for the result in any group of sensors at the time point between the operand 2 and the proposed result and in any frequency. Finally, we reasoned that, if the computation time varied on a trial-by-trial basis, the brain response induced by the internally computed result could be brief and diluted in time, thus obscuring its decodability when the trials were time-locked to operand onset. We tried to overcome this timing issue by computing the Fourier spectrum of the low-pass signal in the low frequency

range (2 – 34 Hz) using the entire time window from B to C, then feeding the classifier with a feature matrix of single-trial MEG frequency power ( $X$ , shape =  $n_{trials} \times n_{frequencies}$ ). The logic is that once phase information is removed, the Fourier spectrum is invariant for temporal delays. No significant classification was found. Additionally, we tested a classifier based on Riemannian geometry using a covariance matrix estimation that integrates the temporal information (ERPCov, see Methods). This pipeline was applied to classify the operand 1, operation, operand 2 and result, in two time windows (0 – 800 ms and 800 – 1,600). Results are summarized in Figure 4.11. As can be seen, the ERPCov classifier boosted the classification accuracies for operand 1, operation and operand 2 (especially in the 0 – 800 ms window), but yielded no significant classification accuracy for the result. Therefore, we conclude that in the current dataset, the internally computed result could not be decoded from MEG signals.

## 4.6 Discussion

By combining time-resolved multivariate pattern analysis (MVPA) to MEG signals, we obtained a comprehensive picture of the unfolding processing stages underlying arithmetic calculations. Our verification task, using sequentially presented addition and subtraction problems, allowed us to investigate the main components of mental arithmetic: encoding of the operands, processing of the operation sign, calculation, decision of correctness, and finally response preparation and execution. Overall Global Field Power (GFP) revealed that the activity was sustained during the entire trial, with additional transient peaks at ~150 ms after each stimulus. MEG topographies showed that the evoked responses evolved across time from posterior to anterior sensors, both after each stimuli onset and also across the entire trial, which fits nicely with previous electrophysiological findings on arithmetic processing (Dehaene, 1996) and visual object processing in general (Cichy, Pantazis, & Oliva, 2014; King et al., 2016; Sergent, Baillet, & Dehaene, 2005).

#### **4.6.1 A cascade of partially overlapping processing stages in mental arithmetic**

Crucially, we could decode a series of calculation features, revealing a cascade of partially overlapping brain states during the solution of a problem as simple as  $3+2=5$ . First, we could transiently decode the identity of the operand 1 between 112 - 640 ms after stimuli onset. Next, the operation (addition vs. subtraction) could be decoded from 95 ms after the onset of the operation sign, dropping somewhat 700 ms after the sign, but remaining above chance until the offset of operand 2, with a subsequent transient recovery after the onset of the equal sign (significant decoding for  $\sim 2,000$  ms). The high initial classification score is most likely due to the visual difference between the operation signs, but could also reflect task-specific preparation, such as operator priming (Fayol & Thevenot, 2012) as well as visual-spatial mechanisms or spatial-numerical associations (Hartmann et al., 2015; Masson & Pesenti, 2014; Mathieu, Epinat-duclos, Léone, et al., 2017; Mathieu et al., 2016), as would follow from the idea that calculation is essentially a movement along the mental number line (Knops, Thirion, et al., 2009; Knops, Viarouge, & Dehaene, 2009; Pinheiro-Chagas, Dotan, et al., 2017). In line with this hypothesis, we found that a classifier trained on discriminating subtractions vs. additions cross-generalized and accurately discriminated smaller vs. larger numbers, respectively, but only at the time of presentation of operand 2, which is probably the stage in which subjects are calculating or manipulating quantities. In fact, the identity of the operand 2 could be decoded for an extended time window, ranging from 102 ms after stimulus onset till the offset of the equal sign, thus partially overlapping with the decoding of operation for about 1,000 ms. This results fits with our recent behavioral findings that the operator sign transiently affected the decision about the location of the result of arithmetic calculations on a number line (a plus sign attracted the finger to the right [larger results] and a minus sign to the left [smaller results]) around the time that subjects were processing operand 2 (Pinheiro-Chagas, Dotan, et al., 2017). The existence of a code that is partially common across the elaboration of an arithmetical sign and a number also

comes from behavioral data showing that both stimuli (an arithmetical sign and a number) trigger shifts in spatial attention that are consistent with a left-to-right oriented representation, thus facilitating target detection (Fischer et al., 2003; Mathieu et al., 2016).

Importantly, operand 2 was classified with a higher accuracy as compared to operand 1 (Figure 4.2 and Figure 4.11), suggesting that more intense and more stable brain activity occurred after operand 2 than after operand 1. This is understandable given that, at this stage subjects were able to start calculating, a process whose duration depends on the size of the *min* operand (or the smallest operand) (Groen & Parkman, 1972; Pinheiro-Chagas, Dotan, et al., 2017; Uittenhove et al., 2016), which in the present experiment is precisely operand 2. These results also fit with recent neurophysiological findings. An ECoG study using an essentially identical verification task (Hermes et al., 2015) showed that neuronal populations in the ventral temporal cortex (VTC) have stronger activity following operand 2 as compared to operand 1, with an averaged time course very similar to our Figure 4.1B. This finding was interpreted as suggesting that the VTC activity is modulated by task demands, in this case the actual manipulation of numbers, which can only happen after operand 2 (Hermes et al., 2015). A more recent ECoG study revealed that in addition to the number form area (NFA) in the ventral temporal cortex (VTC), which selectively responds to numerical digits independently of the presentation context (Shum et al., 2013, for reviews see Hannagan, Amedi, Cohen, Dehaene-Lambertz, & Dehaene, 2015; Price, Yeo, Wilkey, & Cutting, 2016), there are neuronal populations in the posterior inferior temporal gyrus (pITG) (just adjacent to the NFA), that respond slightly later (~10 ms) and exhibit more sustained activity than the NFA. Crucially, these lateral sites respond only when numerals are presented in the context of a calculation or, in the case of the sequentially presented verification task, only for operand 2 and the proposed result, but not for operand 1 (Daitch et al., 2016). Thus, these results provide a plausible psychophysiological basis for our finding that operand 2 can be decoded with a higher accuracy as compared to operand 1.

### **4.6.2 The representational geometries of the operands**

Although those ECoG studies were very informative about the fine-grained spatial-temporal dynamics of calculations, they did not provide any direct indication about the nature of the underlying representations of the operands. Here, to investigate this question, we applied time-resolved representational similarity analysis (RSA). Our results indicated that while for operand 1 the dominant dimension represented was visual, for operand 2 both visual and magnitude dimensions explained unique variance in the MEG signal. A similar conclusion, corroborating this finding, could be drawn from the results of the regression classifier (Figure 4.9), in which only the classifier for operand 2 achieved above chance performance. Although a natural prediction for operand 2 would be that the visual dimension precedes and partially overlaps with the magnitude dimension, we observed an effect of the two dimensions starting practically at the same time, at ~100 ms after stimuli onset, but the magnitude dimension was predominant and lasted longer (Figure 4.2). As ECoG suggested that the difference in latency between NFA and both pITG and IPS is very small (~14 ms), it is possible that we did not have a high enough signal-to-noise ratio to separate in time the visual and magnitude dimensions with MEG. Further ECoG studies specially designed for this purpose could provide a definitive answer. It is also important to note that in our experiment, the magnitude of the operand 2 defines the problem-size, the size of the *min* operand that needs to be added or subtracted, and which is known to be a major determinant of calculation duration and difficulty (Groen & Parkman, 1972; Pinheiro-Chagas, Dotan, et al., 2017). Therefore, the decoding of operand 2 and its correlation with the magnitude model of the RSA could be a combination of the quantity representation and the calculation process itself. Future experiments should aim at disentangling these two processes.

### **4.6.3 Parsing the processing stages of arithmetic decision-making**

At the decision stage (Figure 4.2, time-locked to C), we found a fast and highly overlapping dynamics of identifying the proposed result (from 92 till 400 ms), judging whether it was correct or incorrect (from 172 ms till the end of the trial) and finally pressing the response button (from

196 ms till the end of the trial). The last two stages were better observed when time-locking the signal to the RT. We could see a slow ramping in the decoding of the correctness starting at -428 ms before the RT and persisting until the end of the trial, followed by a fast and sharp increase of classification score for the response button at -212 ms before the RT (Figure 4.2). It is important to highlight that those three features (proposed result, correctness and response button) are orthogonal to each other in our experimental design, so the classifiers could no rely on a single feature to perform above chance level.

The proposed result was transiently decoded after its onset, but we did not observe a distance effect for the incorrect trials (absolute distances = 1 - 4) in both behavioral and electrophysiological levels (no significant decoding scores), which is at odds with previous positive findings (Avancini, Galfano, & Szucs, 2014; Avancini et al., 2015; Dehaene, 1996). We believe that this null finding was probably due to a combination of the small distances used (1 - 4), and the slow pace of our experimental design. As a result, subjects probably had the correct result in mind for at least 1 s before the proposed result appeared, and could perform a fast symbolic same-different judgement without showing any influence of numerical distance.

#### **4.6.4 Temporal dynamics of the decoding patterns**

The decoding patterns of the calculation features observed in this experiment are far from being trivial and deserve attentive consideration. Due to the sequential structure of our task, a series of information had to be maintained in working memory. For example, to correctly perform the task, subjects needed to keep in mind the operand 1 at least until the operand 2 was presented. Yet, surprisingly, the classification score for operand 1 rapidly decreased to chance level after stimulus offset and remained so until the end of the trial. A similar result was observed in a series of working memory studies in which the information could not be decoded in a sustained way during the memory maintenance period, suggesting that, contrary to previous suggestions, working memory may not be encoded by a stable pattern of sustained activity (LaRocque, Lewis-Peacock, Drysdale, Oberauer, & Postle, 2013; Sprague, Ester, & Serences, 2016; Trübutschek et al., 2017; Wolff et al., 2017). A slightly different decoding time course was observed for the operation and

operand 2: both features remained decodable for a much longer time (above 1,000 ms), although again with a drastic drop in accuracy after 800 ms. Finally, remember that we could not the internally generated result, even though subjects were instructed to compute it and keeping it “in mind” during the delay prior to the appearance of the proposed result.

Several theories may explain either the complete absence of decodable sustained activity, or the strong decrease in the decoding performance, during the various delay periods of our arithmetic task. First, instead of stable sustained neural firing, information might be maintained in working memory through occasional gamma and beta bursts (Lundqvist et al., 2016) which would therefore be diluted in time and which our MEG signals might not be sensitive enough to capture. Second, the coding scheme to store information in working memory may not be through persistent neuronal firing, but through short-term synaptic changes (Mongillo, Barak, & Tsodyks, 2008), so called ‘silent states’ (Stokes, 2015; Trübutschek et al., 2017) and therefore may not be directly measurable with conventional neuroimaging methods. Finally, a third possibility is that the neural coding schemes changes across successive stages from an easily decodable spatial code based on large cortical columns in posterior areas, to a more microscopic and sparse code in the prefrontal cortex and other associated areas, based on overlapping neural populations and orthogonal vectors (Mante, Sussillo, Shenoy, & Newsome, 2013), which may therefore not be detectable with MEG. All three possibilities are plausible, and fine-grained electrophysiological recordings will be needed to separate them.

The temporal generalization analysis (King & Dehaene, 2014) revealed that the underlying codes of the main calculation features are highly dynamic along the trial, as indicated by a diagonal generalization-across-time matrix showing that they remained decodable only when train and test time were similar. (Figure 4.7). The sole exception was around 200-400 ms after the presentation of the operation sign and operand 2, where a thicker diagonal, closer to a square pattern of generalization, suggested a more stable neural code. Such a succession of diagonal and then square pattern has been systematically observed in several studies (Crouzet, Busch, & Ohla, 2015; King et al., 2016; Marti, King, & Dehaene, 2015; Stokes, Wolff, & Spaak, 2015; Trübutschek et al., 2017) and has been interpreted (King et al., 2016; Trübutschek et al., 2017) as compatible with

classical cascade models (McClelland, 1979), suggesting that information is encoded by an initial cascade of successive neural codes, followed by a more sustained (though still transient) activity during later decision or working-memory stages. It also corroborates a series of functional and anatomical findings on the highly hierarchical organization of the cortex (Chaudhuri, Knoblauch, Gariel, Kennedy, & Wang, 2015; Cichy & Teng, 2016; Felleman & Van Essen, 1991; King et al., 2016; Rajalingham, Schmidt, & DiCarlo, 2015). Because of the series of mental transformation involved in our task, some of the features could be discarded along the way and substituted by their transformed or combined version. For example, the operands probably underwent a series of visual processing stages before their symbolic identity was established. Similarly, during calculation, operand 1, operand 2 and the operation sign were probably transformed into an internal representation of the computed result after the presentation of operand 2, and from this stage on, the task required only that result to be maintained in working memory for later comparison with the proposed result.

#### **4.6.5 The search for the neural correlates od the internally computed result**

With this idea in mind, we systematically searched for a neural signature of this internally computed result. Surprisingly, however, none of our attempts were successful. Could this finding arise from limitations in our experimental design? One potential weak point is that our task did not allow to establish the precise moment when the calculation was completed, which probably varied on a trial-by-trial basis. Our hypothesis, however, was that the activity induced or evoked by the correct result would last until the proposed result appeared, so that we would decode it without necessarily time-locking the signal to the peak of activation generated by the correct result. For instance, although RT systematically varies across trials, we did not need to time lock the response button press to RT to achieve above-chance classification score when decoding the response side (Figure 4.2). This strategy did not work, however, for the internally computed result. To overcome this potential timing limitation, we tried some decoding models which received as input the induced oscillatory activity in a wide frequency range and one model that used Riemannian geometry (Barachant & Congedo, 2014) and embeds the temporal information of the

signal by concatenating along the sensor axis the averaged ERF (across trial) of each class, and is therefore well suited to capture both evoked and induced responses. Although the latter estimator indeed boosted decoding scores for the other calculation features of interest (operand 1, operation and operand 2), it showed no improvement to decode the correct result. After testing several robust state-of-the-art decoding models, we therefore conclude that the internally computed result of a simple arithmetic calculation is not as easily decodable from MEG signals as the externally presented stimuli. This finding could originate from the same three explanations listed above to account for the vanishing of the codes for operand 1 and 2: brief bursts of gamma or beta activity; short-term synaptic codes; or overlapping neural microcodes.

Additionally, it is also possible that, since we used a verification task, subjects did not need to calculate in every trial. They could use a range of rule-based strategies, such as comparing the parity and size between the operands and the proposed result. However, subjects were explicitly asked to calculate in order to judge as fast as possible the correctness of the proposed result. Moreover, a series of findings indicate that they did indeed engage in calculation. First, we could decode the additions vs. subtractions ~2,000 ms after the onset of the operation sign, overlapping with the decoding of the operand 2 for about 1,000 ms. Second, we found higher classification accuracies for decoding the operand 2 vs. operand 1, and the magnitude model in the RSA was dominant for predicting operand 2. These results suggest that the actual calculation process was initiated after the onset of operand 2 and lasted until the offset of the equal sign (around 1,200 ms), when both operation type and operand 2 could no longer be decoded.

MEG decoding has been successfully applied to characterize the spatial-temporal dynamics of several cognitive functions, such dual-task interference (Marti et al., 2015), attention (Brandman & Peelen, 2017; Kaiser et al., 2016), working memory (King et al., 2016; Trübutschek et al., 2017; Wolff, Jochim, Akyürek, & Stokes, 2017), reward value (Bach et al., 2017), taste perception (Crouzet et al., 2015), object recognition and categorization (Carlson et al., 2011, 2013; Cichy et al., 2014; Isik et al., 2014), written and spoken language (Chan et al., 2011; Kocagoncu et al., 2017), etc. However, virtually all of these studies either used classifiers that could rely on activity evoked by low-level sensory properties of the stimuli (or mental imagery), or probed

classical semantic categories that are known to be anatomically segregated. Therefore, evidence for within category time-resolved decoding at the single-trial level of abstract internally generated mental objects is still lacking. One reason might be that such mental objects, like the result of a calculation, are represented in a highly distributed fashion, difficult to measure with non-invasive methods that have a relatively low signal-to-noise ratio, therefore suggesting the existence of different neural substrates for externally and internally generated codes.

#### **4.6.6 Conclusion**

Despite our inability to decode the internally computed result, our study is the first to directly obtain a comprehensive understanding of the unfolding processing stages and mental transformations during arithmetic calculations at a single-trial level. We could decode a series of calculation features, revealing a highly dynamic coding profile and a cascade of partially overlapping brain states during elementary arithmetic, therefore increasing our understanding of the neurocognitive underpinnings of high level symbolic cognition.

## **4.7 Acknowledgments**

This research was sponsored by INSERM, CEA, and the Bettencourt-Schueller Foundation. Pedro Pinheiro-Chagas gratefully acknowledges a Science Without Borders Fellowship from the Brazilian National Council for Scientific and Technological Development (CNPq) (nr. 246750/2012-0). We are grateful to all subjects who participated in the study and to Veronique Joly-Testault, Laurence Laurier and all the NeuroSpin team who helped recruiting them. We would also like to thank Valentina Borghesani, Marco Buiatti and Darinka Trübtschek for methodological advice. And Sebastian Marti, Fosca Al-Roumi and Maxime Maheu for helpful discussions.

## 4.8 Supplementary Materials

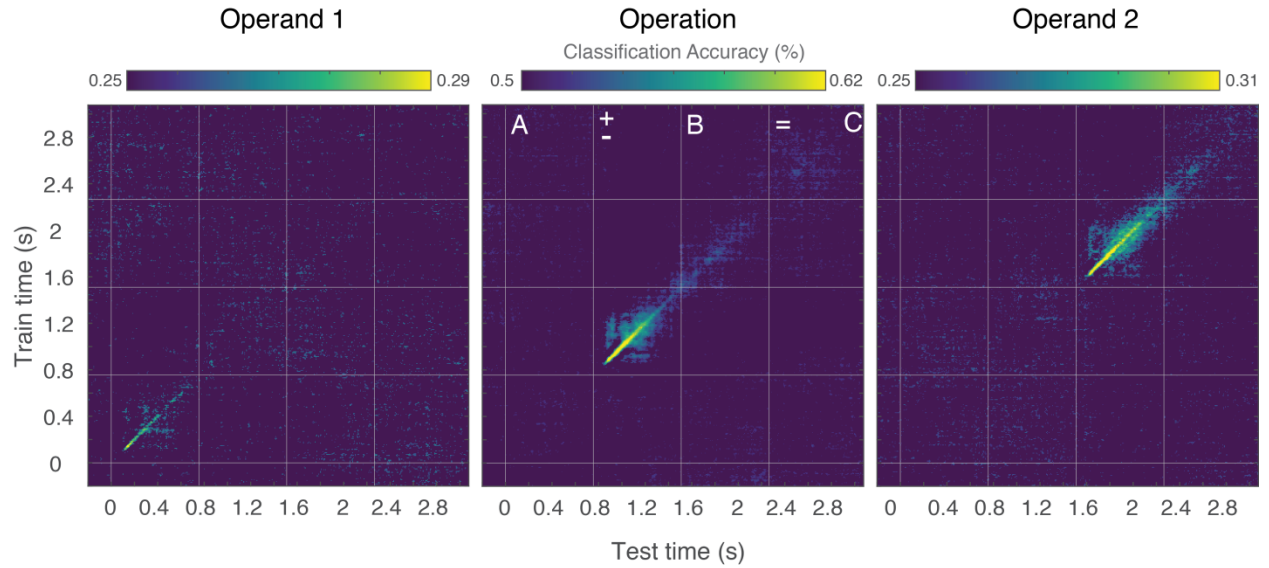
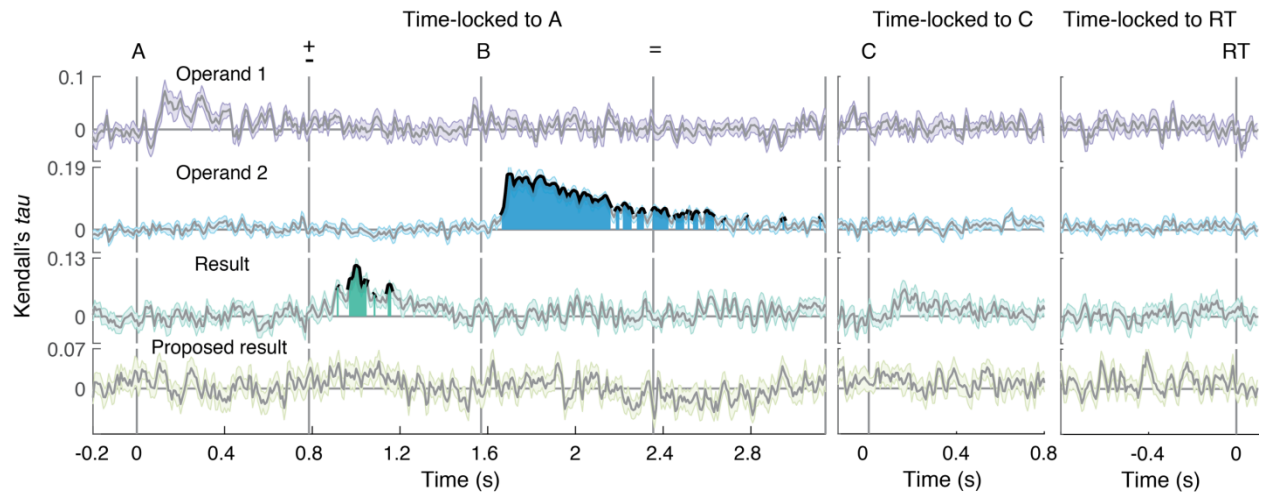


**Figure 4.7 Generalization across time matrices during calculation**

To characterize the dynamics of the mental representations underlying calculation, we tested how the classifiers of the main calculation features generalized in time. Results indicate a succession of dynamical internal codes (diagonal pattern). The plots only show the classification accuracies that were significantly above chance (second-level statistical tests across subjects, with  $p < 0.05$ , not corrected for multiple comparison).

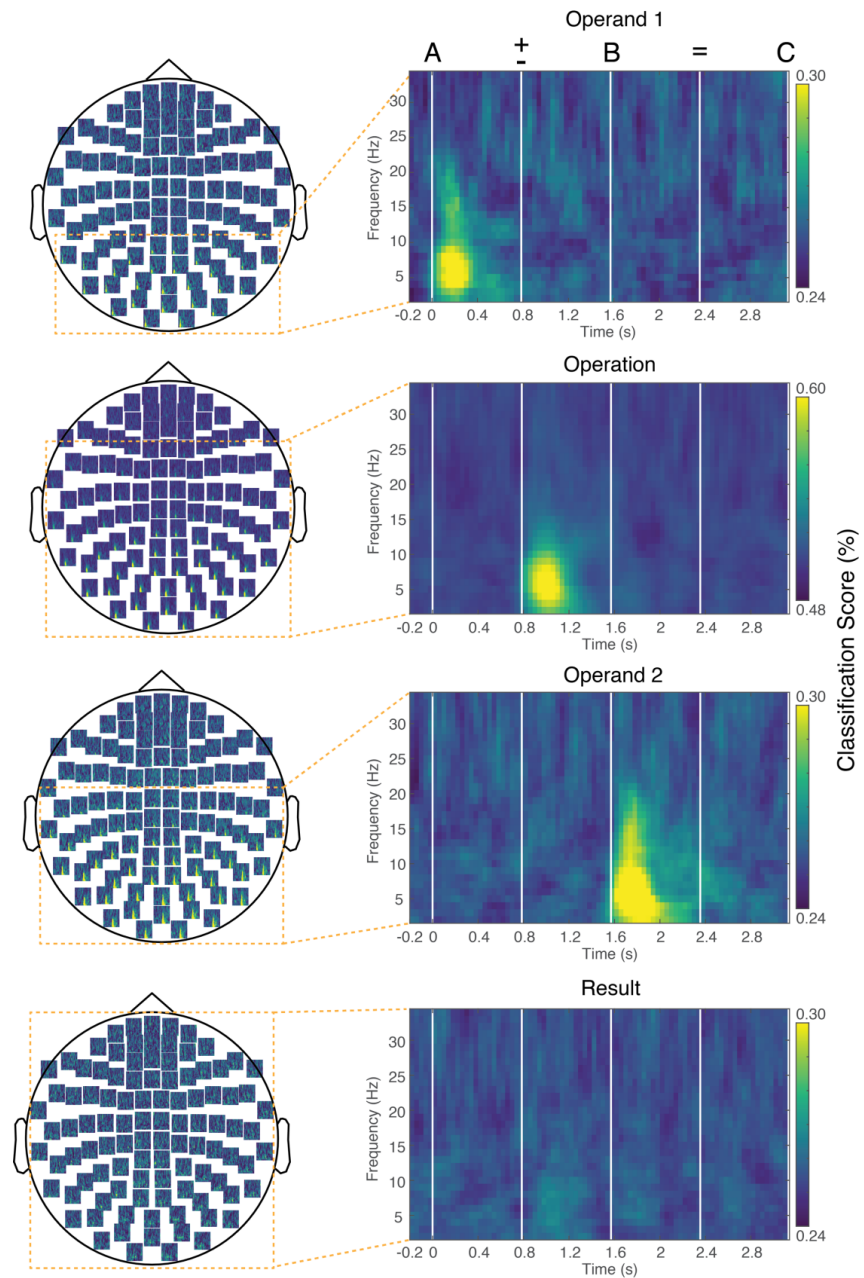
	3+0	3+1	3+2	3+3	3-0	3-1	3-2	3-3	4+0	4+1	4+2	4+3	4-0	4-1	4-2	4-3	5+0	5+1	5+2	5+3	5-0	5-1	5-2	5-3	6+0	6+1	6+2	6+3	6-0	6-1	6-2	6-3
3+0																																
3+1																																
3+2																																
3+3																																
3-0																																
3-1																																
3-2																																
3-3																																
4+0																																
4+1																																
4+2																																
4+3																																
4-0																																
4-1																																
4-2																																
4-3																																
5+0																																
5+1																																
5+2																																
5+3																																
5-0																																
5-1																																
5-2																																
5-3																																
6+0																																
6+1																																
6+2																																
6+3																																
6-0																																
6-1																																
6-2																																
6-3																																

Figure 4.8 Matrix structure used for the RSA



**Figure 4.9 Decoding the calculation features using regression**

Ridge Regression estimators were used to decode main calculation features, thus looking for a monotonic relationship between brain signals and the corresponding numbers. Trials were time-locked to three events of interest: onset of the operand 1 (A), onset of the proposed result (C) and RT. Gray horizontal lines indicate theoretical chance level. Thick lines and filled areas represent time periods in which the second-level statistical tests across subjects revealed a Kendall's *tau* significantly above 0 (cluster corrected for multiple comparison,  $p < 0.05$ ).



**Figure 4.10 Searchlight decoding in time, sensor space and frequency**

To exhaustively explore the decoding of the main calculation features, in time, sensor space and frequency, we fitted a series of linear discriminant analysis (LDA) in a searchlight approach. The topoplots on the left show the classification accuracy (color axis) in each ‘sphere’ of 10 neighbor sensors, for each time (x axis) and low frequency samples (2 - 34 Hz) (y axis). Averaged ‘spheres’ qualitatively chosen after visual inspection are zoomed in the right plots. Operand 1, operation and operand 2 could be generally from occipital-parietal sensors, at a short time window following their respective onsets and mostly between 3 to 20 Hz. For the result, we found no indication of decoding accuracy above chance level in the time window between B and C (when exact calculation is expected to happen).

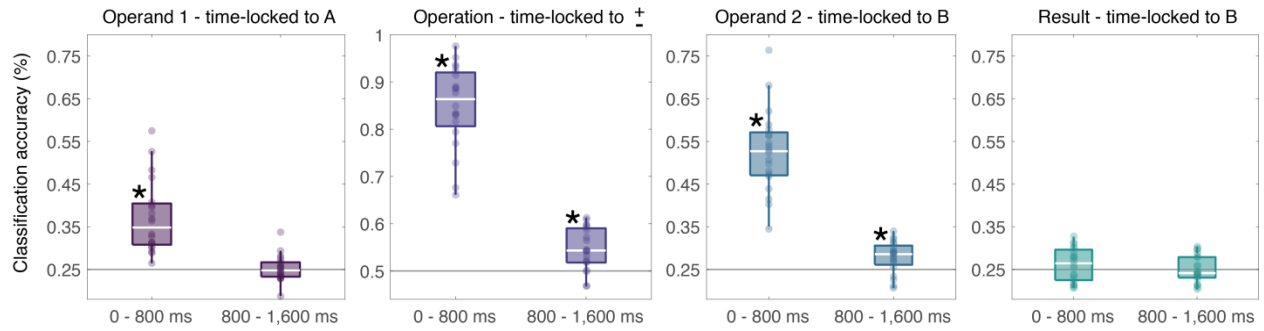


**Figure 4.11 Decoding calculation features with Riemannian geometry**

The ERPCov classifier was used to decode the main calculation features in two time windows (0 – 800 ms and 800 – 1,600). Boxplots represent classification scores across subjects (individual dots). Gray horizontal lines indicate theoretical chance level. (\* =  $p < 0.01$ , second-level 1-sampled t-test). Classification accuracies were highly boosted as compared to time by time SVM, specially for the operation and operand 2 in the time window of 0 – 800 ms. No significant classification accuracy was found for the internally computed result.

# Chapter 5. GENERAL DISCUSSION

---

In the present dissertation, I investigated the neurocognitive mechanisms of arithmetic thinking by using a multimethod approach, which combined continuous behavioral measures, electrocorticography and machine learning applied to magnetoencephalography signals. This methodological toolkit allowed me to parse and characterize a series of processing stages and representational codes underlying numerical computations in the human brain.

Below, I will recapitulate the main findings of each study and discuss them in a broad context, acknowledging the limitations and highlighting some of the outstanding unanswered questions, which constitute the basis for the future directions of my research program.

## 5.1 Simple additions and subtractions rely on quantity manipulation

Over the past four decades, the cognitive arithmetic literature has converged to the hypothesis that elementary arithmetic problems are solved via direct retrieval from verbal long-term memory, with no need for quantity manipulation (Ashcraft, 1992; Campbell, 1987; Siegler, 1987; Zbrodoff & Logan, 2005). However, as discussed in the **Introduction**, the widely replicated problem-size effect and the recently discovered operational momentum (OM) effect, even in small single-digit operations, poses serious challenges to pure fact-retrieval based models (Barrouillet & Thevenot, 2013; Pinhas & Fischer, 2008; Uittenhove et al., 2016). Since most prior studies used *mental chronometry*, which solely relies on summary measures of behavior accumulated over time, it has not been possible to more directly investigate the ongoing processes involved in numerical computations.

In **Chapter 2**, I showed how a novel continuous behavioral method, based on trajectory tracking, can dissect the calculation process and reveal the absolute timing of the covert stages involved in computing single-digit calculations. Subjects solved single-digit additions and subtractions on a tablet computer, and responded by pointing to the position of the result on a

horizontal number line ranging from 0 – 10, while their finger movement was constantly recorded. Next, I applied a series of time-resolved multiple regression models, using the position of the finger projected onto the line (*implied endpoints*) as the dependent variable and different features of the operations as predictors. I found that the two operands were processed serially, both in additions and in subtractions. The finger first pointed to the larger operand, irrespectively of its position, and only then veered towards the correct result. This slow deviation unfolded proportionally to the size of the smaller operand, in such a way that subjects seemed to pass through intermediate results before achieving the final correct location. In the case of additions, movement times (the correspondent of RT in this task) were longer when the smaller operand appeared first, possibly reflecting an additional stage of reordering the operands prior to calculation. Further evidence supporting a model based on quantity manipulation in simple arithmetic comes from the representational similarity analysis (RSA) findings presented in **Chapter 4**, where I showed that the dominant representational code underlying the second operand was based on the magnitude as, opposed to the visual dimension of the stimulus.

I also observed a transient operator effect: a plus sign attracted the finger to the right and a minus sign to the left. Crucially, the timing of transient bias coincided with the timing when the smaller operand affected the finger movement. This suggests that the OM effect is directly related to the calculation procedure and rejects the possibility that it originates solely from post-calculation processes (e.g., that small vs. large computed results attract attention to left vs. right side, respectively). Interestingly, in **Chapter 4** I showed that a classifier trained to discriminate subtractions vs. additions (at the time window when the operation sign appeared on screen) generalized to classify smaller vs. larger values of the second operand. These results are in line with the hypothesis that the representation of the *minus* vs. *plus* operators shares a common code with the representation of smaller vs. larger numbers. Such a shared code could be ultimately grounded in a basic mechanism of reorienting of attention towards the left vs. right side of the space (Fischer et al., 2003; Knops, Viarouge, Dehaene, et al., 2009; Knops, Thirion, et al., 2009; Mathieu, Epinat-duclos, Sigovan, et al., 2017; Mathieu et al., 2016).

Subtractions were solved more serially than additions, even when the operands were the same in both operations. Interestingly, I found that the absolute value of the smaller operand was transiently processed in subtractions. Therefore, a potential explanation of the common findings that subtractions are generally solved slower than additions (Seyler et al., 2003), - and in the present study also more serially – is that one additional processing stage may be required in subtractions: the conversion of the absolute value of the subtrahend into a negative number. It is also possible that the fundamental mechanism of ‘*increment*’ in additions, as opposed to ‘*decrement*’ in subtractions, is implemented in a slightly more efficient way. A hint for this latter hypothesis comes from the recent work by de Hevia et al. (2017): they showed that human infants detect increasing numerical order earlier in life as compared to decreasing order. The authors speculated that this advantage for increasing sequences might have an evolutionary origin (e.g., is more important for survival to sum the numbers of approaching predators than subtracting the number of dispersing ones). Interestingly, as noted by the authors, human infants and other animals have already demonstrated a capacity for perceiving impeding collisions (i.e., stimuli that expands on the screen) by blinking and withdrawing their heads, but show no reaction to objects fading away from the viewer’s location (i.e., stimuli that shrinks on the screen) (Ball & Tronick, 1971). However, the link between these findings and arithmetic calculation is still remote and needs to be empirically tested.

Overall, the results from the present dissertation support a model whereby elementary addition and subtraction rely on quantity manipulation and are computed by a stepwise displacement on the *mental number line*, starting with the larger number and incrementally adding or subtracting the smaller number. This appealing model is compatible with several previously proposed models – counting/summation (Groen & Parkman, 1972), fast automated procedures (Barrouillet & Thevenot, 2013; Uittenhove et al., 2016), and even the retrieval through a tabular search (Ashcraft & Battaglia, 1978). Our model should still be validated using other experimental designs, since it is possible that the finger-tracking task could have particularly encouraged subjects to adopt a quantity-based strategy. However, we believe that this is unlikely, since the analysis of the movement times (this task’s correspondent of RT) replicated several prior studies

that used conventional verbal production or verification tasks (Barrouillet & Thevenot, 2013; Parkman & Groen, 1971; Uittenhove et al., 2016). Finally, the neurophysiological underpinnings of the model still need to be further investigated.

## 5.2 Arithmetic processing is implemented in the dorsal and ventral pathways

Mental calculations engage a complex interplay between several brain regions (Arsalidou & Taylor, 2011). The traditional view, arising from neuropsychological cases and pioneering fMRI studies, is that the lateral parietal cortex (LPC) contains the main hubs engaged in the calculation mechanism *per se*, and that the ventral temporal cortex (VTC) plays a central role in recognizing Arabic numerals. The LPC and VTC are further supported by auxiliary regions, associated with executive functions and working memory (basal ganglia and dorsolateral prefrontal cortex, DLPFC), declarative and semantic memory formation (medial and lateral temporal cortex) and allocation of attentional resources for goal-directed problem solving (PFC) (Dehaene & Cohen, 1995; Menon, 2014).

Although remarkable progress has been made in characterizing a macroscopic functional map of arithmetic processing, the precise role of each brain region and how they communicate with each other still remains elusive. This is because progress in understanding the fine-grained neural correlates of mental calculation has been methodologically impeded by the small degree of specificity of brain lesions, poor temporal resolution of fMRI and coarse spatial resolution of EEG/MEG.

In **Chapter 3**, my goal was to re-evaluate the roles of LPC and VTC regions in arithmetic processing by recording electrophysiological activity directly from the human brain. This goal was inspired by the growing evidence supporting the hypothesis that the VTC might participate in mathematical reasoning beyond merely visual recognition of Arabic numerals (Abboud et al., 2015; Amalric & Dehaene, 2016; Daitch et al., 2016). Subjects implanted with grids of electrodes were asked to verify addition problems in the form of ‘ $15+3 = 18$ ’, in which we systematically varied the magnitude of the operands but preserved the same structure and number of characters, thus

separating numerical from low-level visual features of the stimuli.

Behavioral performance showed a classical problem-size effect and, in line with previous studies and with the results presented in **Chapter 2**, the best predictor of RT was the smaller (*min*) operand. Therefore, I used the *min operand* as the index of problem-size/difficulty and investigated if, how, and when the *min* operand modulated the activity in the math-selective regions. Corroborating prior fMRI findings, I showed that the total high-frequency broadband (HFB) activity in bilateral aIPS and SPL sites increased with problem-size and correlated with RTs. More surprisingly, bilateral pITG sites showed an initial burst of HFB activity that decreased as the operands got larger, yet with a constant integral over the whole trial, and did not correlate with RTs. Crucially, 9 out of 10 math-selective sites in pITG, whose activity decreased as a function of problem-size, did not show any selectivity for Arabic numerals in a second task in which subjects had to identify numbers vs. letters. Only one of these sites could be classified as ‘number form area’ (NFA). Furthermore, even in the subset of pITG sites that significantly, but not exclusively, responded to isolated Arabic numerals, activity was not modulated by the numerical magnitude. This confirms that the pITG modulation by *min operand* was directly dependent on mental calculation, and was not a by-product of putative tuning curves for Arabic numerals in the pITG. Therefore, while parietal sites appear to have a more sustained function in arithmetic computations and decision-making, the pITG may play a role in early identification of the problem difficulty, beyond merely digit recognition.

The role of VTC in mental calculation seems to have been largely underestimated until very recently. This might be explained by several reasons, already discussed in **Chapter 3**. For example, since fMRI is only sensitive to the activity integrated over a temporal window of several seconds, the initial modulation observed in pITG would be undetected. Nevertheless, some previous studies had indeed suspected of this apparent more high-level role of VTC. Delazer, Karner, Zamarian, Donnemiller, & Benke (2006) reported the case of a patient suffering from posterior cortical atrophy (PCA), who had severe cortical reduction in the superior and posterior parietal cortex. Neuropsychological assessment revealed classical parietal dysfunction and severe numerical deficits in counting, number estimation and arithmetic calculations. In a follow-up study,

the authors recorded fMRI activity while the patient solved numerical and linguistic tasks. The contrast between counting and word recitation yield a significant cluster of activity in the inferior temporal cortex, suggesting that the VTC could partially compensate for the impaired numerical functions of the lesioned LPC (Margarete Delazer, Benke, Trieb, Schocke, & Ischebeck, 2006).

Overall, these findings challenge classical neurocognitive models of arithmetic processing (Dehaene & Cohen, 1995; Menon, 2014) and, more broadly, the traditional view of the VTC as the last stage of the ventral stream, associated with object categorization (Grill-Spector & Weiner, 2014). In fact, the radical distinction between the ventral ‘*what*’ and dorsal ‘*where*’ visual pathways might be more blurry (Freud, Culham, Plaut, & Behrmann, 2017) than initially proposed by Goodale and Milner (1992).

The conclusions of **Chapter 3** are restricted by several limitations, and several outstanding questions remain to be addressed. First, the restricted coverage of VTC and LPC regions did not allow us to investigate the role of other regions in mental calculation, such as the PFC and subcortical structures. Secondly, the number of trials was relatively low (~40) and the stimuli were not optimally balanced across different relevant factors of the calculations, such as the incorrect proposed result. Therefore, we could not model the entire activity to unambiguously disentangle some of the processes involved in the verification task, e.g., the addition of the two operands and the comparison between the correct and proposed result. Thirdly, we just had one subject with simultaneous coverage of VTC and LPC who also had sites with both increased IPS total activity and decreased pITG initial activity as a function of problem-size. Consequently, we could not systematically investigate how these two mechanisms interact. Lastly, and perhaps most importantly, it is to determine the causal roles of the specific neuronal populations within the VTC and LPC during arithmetic processing. One fascinating avenue is to use electric brain stimulation in ECoG patients to induce virtual lesions and investigate how it affects behavior. This approach has been successfully applied to characterize causal relationships between face perception and the fusiform gyrus (Parvizi et al., 2012), as well as the ‘*will to persevere*’ and the cingulate gyrus (Parvizi, Rangarajan, Shirer, Desai, & Greicius, 2013). I plan to investigate these

exciting issues during my post-doctoral research in Josef Parvizi's Lab at Stanford University from early 2018.

### 5.3 Decoding the processing stages of mental calculations

The results presented in **Chapters 2** and **3** offer several new insights on the neurocognitive mechanisms of mental calculations. However, they did not provide evidence about the nature of the underlying neural codes of the operands, neither a comprehensive picture of the series of unfolding computations in the brain. Previous studies have shown that it is possible to decode the identity of numbers and even the operator (additions vs. subtractions) from fMRI activity (Bulthé, De Smedt, & Op de Beeck, 2014, 2015; Eger, Sterzer, Russ, Giraud, & Kleinschmidt, 2003; Knops, Thirion, et al., 2009). However, because of the slow signal recorded in fMRI, it has not been possible to investigate the temporal dynamics of the representational codes.

To answer these fundamental questions, in **Chapter 4**, I combined state-of-the-art machine learning techniques with multivariate pattern analysis (MVPA) applied to magnetoencephalography (MEG) signals. Subjects were asked to verify sequentially presented single-digit additions and subtractions, such as ' $3+2=7$ '. This allowed me to partially segregate and investigate in detail the temporal evolution of the main components of mental arithmetic: encoding of the operands, processing of the operation sign, calculation, decision of correctness, and response preparation and execution.

By fitting a series of time-resolve classifiers, I could decode several of calculation features, revealing a cascade of partially overlapping brain states. First, I could transiently decode the identity of the operand 1 from shortly after its onset until  $\sim 250$  ms after its offset. Next, the operation (addition vs. subtraction) could be decoded from shortly after the presentation of the operator sign until the offset of operand 2, with a subsequent transient recovery after the onset of the equal sign (i.e., significant decoding for  $\sim 2,000$  ms). The high initial classification score of the operator is most likely due to the visual difference between the plus and minus signs, but, as discussed before, it might also reflect the pre-activation of subtractions vs. addition calculation

procedures (Fayol & Thevenot, 2012; Fischer et al., 2003; Mathieu, Epinat-duclos, Sigovan, et al., 2017; see **Section 5.1**). Importantly, the classification scores for operand 2 were much higher than operand 1 and overlapped with the decoding of the operation for ~1,000 ms. These results suggest that a more intense brain activity occurred after operand 2, since at this stage subjects can start calculating, a process that depends on the size of the *min operand* (in this case, operand 2 itself; see **Chapter 2** and **Section 5.1**) A possible neurophysiological basis for this result is that, additionally to the NFA, which responds whenever an Arabic numeral appears on the screen, there are some neuronal populations in the IPS and pITG that respond exclusively when numbers have to be manipulated in the context of a calculation, and this is precisely the case for operand 2, but not for operand 1 (Daitch et al., 2016). Also in line with this hypothesis, time-resolved representational similarity analyses (RSA) revealed that while for operand 1 the dominant representational geometry was based on the visual features of the stimuli, for operand 2 the representational geometry correlated both with visual and magnitude features, and the magnitude dimension was the dominant one. Finally, at the decision-making stage, when subjects had to compare the internally computed with the proposed result, I found a fast and highly overlapping dynamics of identifying the proposed result, followed by judging whether it was correct or incorrect and finally by pressing the response button.

Overall, the results of **Chapter 4** provide a first comprehensive description of processing stages underlying arithmetic calculation and decision-making in the brain at a single-trial level. To our surprise, however, I could not decode or find the neural signatures of the internally computed result, which remains an interesting and mysterious problem to be solved. In the following section, I recapitulate some possible explanations to this null finding, and briefly present potential solutions.

## 5.4 Searching for neural signatures of the internally computed result

Throughout the present dissertation, I have presented several new contributions to our understanding of how the brain combines two numbers into a third. However, a fundamental

question remained unsolved: when and where is this *third* number, the *internally computed result*, finally represented? I specifically investigated this question in **Chapter 4**, by designing a carefully controlled arithmetic verification task, in which each element of the operation appeared sequentially. I expected to find a neural signature of the *internally computed result* somewhere between the onset of operand 2, when subjects can initiate the calculation procedure, and the onset of the proposed result, when subjects had to make a comparison to judge the correctness of the problem. However, even after applying an army of state-of-the-art machine learning techniques and using a searchlight approach in time, space and frequency, I was unable to decode the *internally computed result*.

As discussed in **Chapter 4**, this null finding could have resulted from a combination of possible caveats in our experimental design (i.e., not time-stamping the moment of calculation and the relative small number of trials per class of result) and limitations of MEG recordings. Time-resolved MVPA applied to MEG signals has been mostly successful in cases in which decoding models could rely on the activity evoked by low-level sensory properties of the stimuli or when probing classical semantic categories that are known to be anatomically segregated at the macroscopically level (Carlson et al., 2013; Cichy et al., 2014; King et al., 2016). However, internally generated objects that must be maintained in working memory for relatively long periods of time have posed a serious challenge for EEG/MEG decoding (Trübtschek et al., 2017; Wolff et al., 2017), and this is precisely the case of the *internally generated result* of arithmetic calculations. Three main reasons may explain this decoding challenge. First, information could be maintained in working memory through rare gamma and beta bursts (Lundqvist et al., 2016). Secondly, the coding scheme to store information in working memory may not require persistent neuronal firing, but rather that of short-term synaptic changes (Mongillo et al., 2008). Lastly, the mental objects could have a more microscopic and sparse code in associative regions, based on overlapping neural populations and orthogonal vectors (Mante et al., 2013). Therefore, MEG recordings might have a very limited sensitivity, thus requiring a massive amount of experimental trials, to capture the neural correlates of internally generated representations.

My future plans to keep searching for the neural correlates of the *internally computed result* include two projects. The first one is a collaboration with Lina Teichmann, Dror Dotan, Leila Azizi, Thomas Carlson, Anina Rich and Stanislas Dehaene. We are going to simultaneously record MEG signals and finger trajectories (using a similar method used in **Chapter 2**) while subjects solve additions and subtractions. Since the two operands will be presented at once, we could increase the number of trials by a factor of five (as compared to **Chapter 4**) and still fit the task in a single MEG session. Furthermore, the trajectory data will hopefully provide critical information about the temporal evolution of the covert processing stages, which could be then used to inform the multivariate analyses of the MEG signals. This is an ambitious project, and we are still developing the most suited methods to optimally deal with MEG artifacts and possible confounds due to the movement. If this project is successful, we may have detailed information about the temporal dynamics of the result computation. Nevertheless, even in this optimistic scenario, we will only have a very coarse idea of where in the brain it was generated and maintained.

To investigate both the temporal and spatial dynamics of the emergence of the *internally computed result*, I will use the same experimental procedures and analytical tools developed in **Chapter 4**, now applied to intracranial signals. I am especially interested in recording from a handful of subjects who are implanted with high density grids of electrodes, ideal for MVPA.

## 5.5 Beyond numbers: the syntactic structure of arithmetic expressions

So far, I have only discussed the neurocognitive mechanism of elementary arithmetic, in the form of simple calculations involving two operands. However, mathematics, similarly to natural language and music, has a generative structure, organized through a process of embedding constituents inside each other. This recursive way of representing information seems to be a uniquely human capacity (Chomsky, 1957; Dehaene, Meyniel, Wacongne, Wang, & Pallier, 2015; Hauser, Chomsky, & Fitch, 2002).

Few eye-tracking studies suggested that subjects can rapidly extract the hierarchy of the arithmetic expressions constituents (Landy, Jones, & Goldstone, 2008; Schneider, Maruyama, Dehaene, & Sigman, 2012). Inspired by these results, I conducted a study aimed to go a step further in dissecting the covert processing stages involved in syntactic arithmetic reasoning. For that, I adapted the trajectory tracking method used in **Chapter 2** to investigate multi-digit and multi-operation arithmetic expressions of the form ‘ $2+(5\times 2)$ ’. The included one addition outside the parenthesis and either one addition or one multiplication inside the parenthesis, which could be in either side.

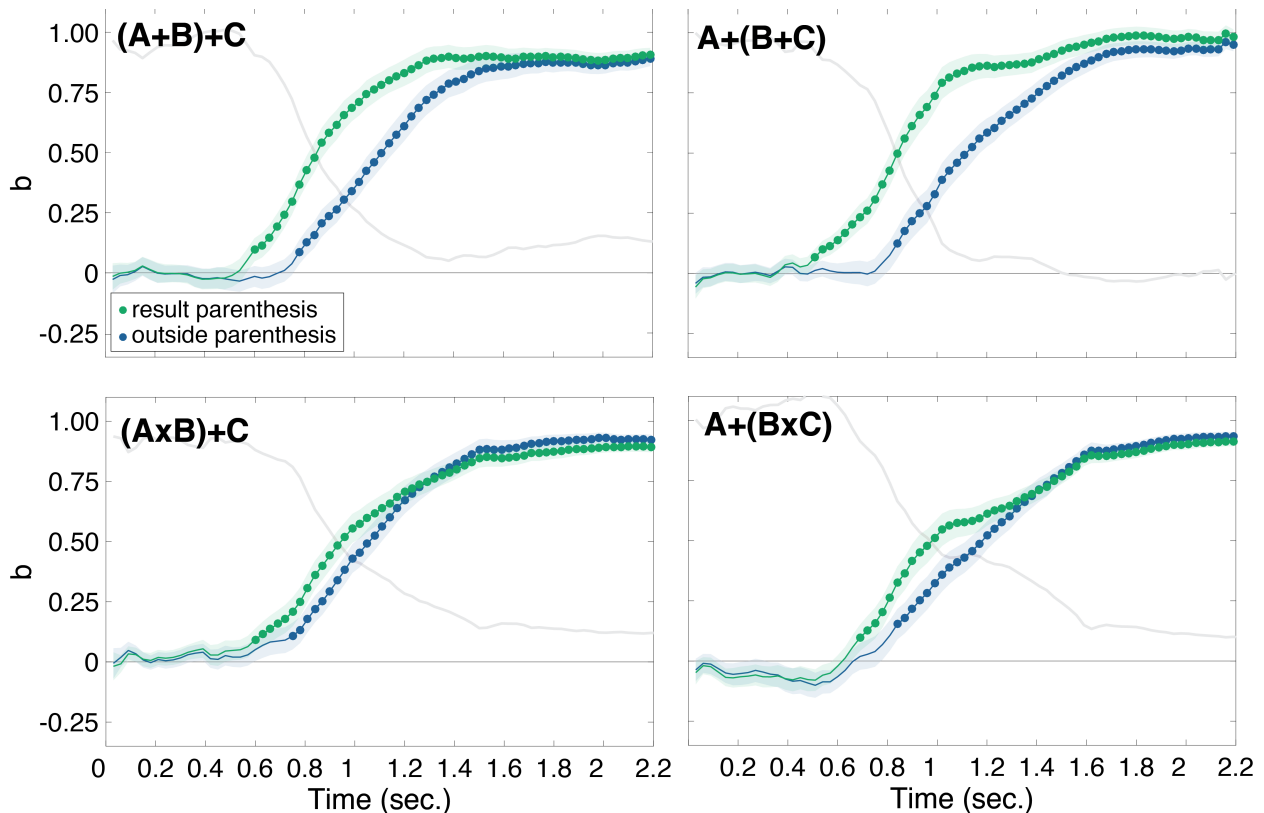


**Figure 5.1 Time course of the regression effects for each type of expression**

Averaged b values across subjects, plotted as a function of time. Filled dots denote  $p < .05$ .

The preliminary findings are promising. The time-resolved regression analysis indicates that the arithmetic expressions are processed serially: subjects first point towards the result of the parenthesis, irrespectively of the order in which the parenthesis appear, and then gradually deviate

towards the overall result. The gradual deviation unfolds proportionally to the size of the number outside of parenthesis (Figure 5.1). These results are in line with the model proposed in **Chapter 2**. Methodologically, they show that the finger-tracking method is sensitive to capture the covert stages during tasks that involve more than a single decision.

## 5.6 Conclusion

Arithmetic is one of the most remarkable human inventions and, since the Paleolithic, it has been a fundamental tool in most societies throughout the history. In our increasingly technological culture, low numeracy represents a dramatic handicap for an individual's life, consequently causing detrimental effects to the wealth of nations (Butterworth, Varma, & Laurillard, 2011).

Until very recently, we had no means of understanding how mental calculation is implemented in the brain. But over the past few decades, with the rise of cognitive neuroscience, a huge progress has been achieved. This dissertation offers a modest contribution to our current knowledge, delineates some of the outstanding questions that still need to be addressed and, more broadly, shows how a multimethod approach including continuous behavioral measures and time-resolved neuroimaging can help us to identify and characterize the mental processes of high-level symbolic cognition.

I hope that some of the discoveries presented in this dissertation will contribute to building a bridge between cognitive neuroscience and education (Bruer, 1997; Sigman, Peña, Goldin, & Ribeiro, 2014), with the ultimate goal of understanding the mechanisms of learning disabilities and improving pedagogical practices.

## REFERENCES

---

- Abboud, S., Maidenbaum, S., Dehaene, S., & Amedi, A. (2015). A number-form area in the blind. *Nature Communications*, 6. <http://doi.org/10.1038/ncomms7026>
- Abrahamse, E., Van Dijck, J. P., & Fias, W. (2016). How does working memory enable number-induced spatial biases? *Frontiers in Psychology*, 7(JUN). <http://doi.org/10.3389/fpsyg.2016.00977>
- Agrillo, C., Piffer, L., Bisazza, A., & Butterworth, B. (2012). Evidence for two numerical systems that are similar in humans and guppies. *PLoS ONE*, 7(2). <http://doi.org/10.1371/journal.pone.0031923>
- Al-Roumi, F., Dotan, D., Yang, T., Wang, L., & Dehaene, S. (2017). Acquisition and processing of an artificial mini-language combining semantic and syntactic elements. *Manuscript in Preparation*.
- Amalric, M., & Dehaene, S. (2016). Origins of the brain networks for advanced mathematics in expert mathematicians. *Proceedings of the National Academy of Sciences of the United States of America*, 113(18), 4909–4917. <http://doi.org/10.1073/pnas.1603205113>
- Anderson, J. R. (1983). *The Architecture of Cognition*. Harvard University Press Cambridge, MA.
- Anobile, G., Cicchini, G. M., & Burr, D. C. (2016). Number As a Primary Perceptual Attribute: A Review. *Perception*. <http://doi.org/10.1177/0301006615602599>
- Arsalidou, M., & Taylor, M. J. (2011). Is  $2+2=4$ ? Meta-analyses of brain areas needed for numbers and calculations. *NeuroImage*, 54(3), 2382–2393. <http://doi.org/10.1016/j.neuroimage.2010.10.009>
- Ashcraft, M. H. (1992). Cognitive arithmetic: a review of data and theory. *Cognition*, 44(1–2), 75–106.
- Ashcraft, M. H., & Battaglia, J. (1978). Cognitive arithmetic: Evidence for retrieval and decision processes in mental addition. *Journal of Experimental Psychology: Human Learning & Memory*, 4(5), 527–538. <http://doi.org/10.1037/0278-7393.4.5.527>

- Ashida, H. (2004). Action-specific extrapolation of target motion in human visual system. *Neuropsychologia*, 42(11), 1515–1524. <http://doi.org/10.1016/j.neuropsychologia.2004.03.003>
- Avancini, C., Galfano, G., & Szucs, D. (2014). Dissociation between arithmetic relatedness and distance effects is modulated by task properties: An ERP study comparing explicit vs. implicit arithmetic processing. *Biological Psychology*, 103, 305–316. <http://doi.org/10.1016/j.biopspsycho.2014.10.003>
- Avancini, C., Soltész, F., & Szucs, D. (2015). Separating stages of arithmetic verification: An ERP study with a novel paradigm. *Neuropsychologia*, 75, 322–329. <http://doi.org/10.1016/j.neuropsychologia.2015.06.016>
- Bach, D. R., Symmonds, M., Barnes, G., & Dolan, R. J. (2017). Whole-Brain Neural Dynamics of Probabilistic Reward Prediction. *The Journal of Neuroscience*, 37(14), 3789–3798. <http://doi.org/10.1523/JNEUROSCI.2943-16.2017>
- Ball, W., & Tronick, E. (1971). Infant responses to impending collision: optical and real. *Science (New York, N.Y.)*, 171(3973), 818–820. <http://doi.org/10.1126/science.171.3973.818>
- Barachant, A., & Congedo, M. (2014). A plug & play P300 BCI using information geometry. Retrieved from <http://arxiv.org/abs/1409.0107>
- Baroody, A. J. (1983). The development of procedural knowledge: An alternative explanation for chronometric trends of mental arithmetic. *Developmental Review*, 3(2), 225–230. [http://doi.org/10.1016/0273-2297\(83\)90031-X](http://doi.org/10.1016/0273-2297(83)90031-X)
- Barrouillet, P., & Thevenot, C. (2013). On the problem-size effect in small additions: Can we really discard any counting-based account? *Cognition*, 128(1), 35–44. <http://doi.org/10.1016/j.cognition.2013.02.018>
- Barth, H., La Mont, K., Lipton, J., Dehaene, S., Kanwisher, N., & Spelke, E. (2006). Non-symbolic arithmetic in adults and young children. *Cognition*, 98(3), 199–222. <http://doi.org/10.1016/j.cognition.2004.09.011>
- Berthier, N. E. (1996). Learning to reach: A mathematical model. *Developmental Psychology*, 32(5), 811–823. <http://doi.org/10.1037/0012-1649.32.5.811>
- Brainard, D. H. (1997). The Psychophysics Toolbox. *Spatial Vision*, 10(4), 433–436.

<http://doi.org/10.1163/156856897X00357>

Brandman, T., & Peelen, M. V. (2017). Interaction between scene and object processing revealed by human fMRI and MEG decoding. *The Journal of Neuroscience*, 582–17.

<http://doi.org/10.1523/JNEUROSCI.0582-17.2017>

Britten, K. H., Shadlen, M. N., Newsome, W. T., & Movshon, J. A. (1993). Responses of neurons in macaque MT to stochastic motion signals. *Visual Neuroscience*, 10(6), 1157–1169.

Bruer, J. T. (1997). Education and the Brain: A Bridge Too Far. *Educational Researcher*, 26(8), 4–16. <http://doi.org/10.3102/0013189X026008004>

Buc Calderon, C., Dewulf, M., Gevers, W., & Verguts, T. (2017). Continuous track paths reveal additive evidence integration in multistep decision making. *Proceedings of the National Academy of Sciences*, 114(40), 10618–10623. <http://doi.org/10.1073/pnas.1710913114>

Buc Calderon, C., Verguts, T., & Gevers, W. (2015). Losing the boundary: Cognition biases action well after action selection. *Journal of Experimental Psychology: General*, 144(4), 737–743. <http://doi.org/10.1037/xge0000087>

Bulthé, J., De Smedt, B., & Op de Beeck, H. P. (2014). Format-dependent representations of symbolic and non-symbolic numbers in the human cortex as revealed by multi-voxel pattern analyses. *NeuroImage*, 87, 311–322. <http://doi.org/10.1016/j.neuroimage.2013.10.049>

Bulthé, J., De Smedt, B., & Op de Beeck, H. P. (2015). Visual Number Beats Abstract Numerical Magnitude: Format-dependent Representation of Arabic Digits and Dot Patterns in Human Parietal Cortex. *Journal of Cognitive Neuroscience*, 27(7), 1376–1387. <http://doi.org/10.1162/jocn>

Butterworth, B., Varma, S., & Laurillard, D. (2011). Dyscalculia: From brain to education. *Science*, 332(6033), 1049–1053. <http://doi.org/10.1126/science.1201536>

Butterworth, B., Zorzi, M., Girelli, L., & Jonckheere, A. R. (2001). Storage and retrieval of addition facts: the role of number comparison. *The Quarterly Journal of Experimental Psychology. A, Human Experimental Psychology*, 54(4), 1005–1029. <http://doi.org/10.1080/713756007>

Campbell, J. I. D. (1987). Network interference and mental multiplication. *Journal of*

- Experimental Psychology: Learning, Memory, and Cognition*, 13(1), 109–123.  
<http://doi.org/10.1037/0278-7393.13.1.109>
- Campbell, J. I. D. (1994). Architectures for numerical cognition. *Cognition*, 53(1), 1–44.  
[http://doi.org/10.1016/0010-0277\(94\)90075-2](http://doi.org/10.1016/0010-0277(94)90075-2)
- Cantlon, J. F., & Brannon, E. M. (2006). Shared System for Ordering Small and Large Numbers in Humans and Monkeys. *Psychological Science*, 17(5), 401–406.  
<http://doi.org/10.1111/j.1467-9280.2006.01719.x>
- Cantlon, J. F., & Brannon, E. M. (2007). Basic math in monkeys and college students. *PLoS Biology*, 5(12), e328. <http://doi.org/10.1371/journal.pbio.0050328>
- Cantlon, J. F., Brannon, E. M., Carter, E. J., & Pelpfrey, K. A. (2006). Functional imaging of numerical processing in adults and 4-y-old children. *PLoS Biology*, 4(5), 844–854.  
<http://doi.org/10.1371/journal.pbio.0040125>
- Cantlon, J. F., Merritt, D. J., & Brannon, E. M. (2016). Monkeys display classic signatures of human symbolic arithmetic. *Animal Cognition*, 19(2), 405–415.  
<http://doi.org/10.1007/s10071-015-0942-5>
- Cappelletti, M. (2015). The Neuropsychology of Acquired Number and Calculation Disorders. In R. Cohen-Kadosh & A. Dowker (Eds.), *The Oxford Handbook of Numerical Cognition* (pp. 808–836). Oxford University Press.
- Carazo, P., Font, E., Forteza-Behrendt, E., & Desfilis, E. (2009). Quantity discrimination in *Tenebrio molitor*: evidence of numerosity discrimination in an invertebrate? *Animal Cognition*, 12(3), 463–470. <http://doi.org/10.1007/s10071-008-0207-7>
- Carey, S. (2009). *The Origin of Concepts*. Oxford University Press.
- Carlson, T. A., Hogendoorn, H., Kanai, R., Mesik, J., & Turret, J. (2011). High temporal resolution decoding of object.pdf. *Journal of Vision*, 11(2011), 1–17.  
<http://doi.org/10.1167/11.10.9.Introduction>
- Carlson, T. A., Tovar, D. A., Alink, A., & Kriegeskorte, N. (2013). Representational dynamics of object vision: The first 1000 ms. *Journal of Vision*, 13(10), 1–1.  
<http://doi.org/10.1167/13.10.1>

- Chan, A. M., Halgren, E., Marinkovic, K., & Cash, S. S. (2011). Decoding word and category-specific spatiotemporal representations from MEG and EEG. *NeuroImage*, 54(4), 3028–3039. <http://doi.org/10.1016/j.neuroimage.2010.10.073>
- Chaudhuri, R., Knoblauch, K., Gariel, M. A., Kennedy, H., & Wang, X. J. (2015). A Large-Scale Circuit Mechanism for Hierarchical Dynamical Processing in the Primate Cortex. *Neuron*, 88(2), 419–431. <http://doi.org/10.1016/j.neuron.2015.09.008>
- Chochon, F., Cohen, L., van de Moortele, P. F., & Dehaene, S. (1999). Differential contributions of the left and right inferior parietal lobules to number processing. *Journal of Cognitive Neuroscience*, 11(6), 617–30. <http://doi.org/10.1162/089892999563689>
- Chomsky, N. (1957). *Syntactic Structures*. Mouton.
- Cichy, R. M., Pantazis, D., & Oliva, A. (2014). Resolving human object recognition in space and time. *Nature Neuroscience*, 17(3), 455–62. <http://doi.org/10.1038/nn.3635>
- Cichy, R. M., & Teng, S. (2016). Resolving the neural dynamics of visual and auditory scene processing in the human brain : a methodological approach. *Philos. Trans. R. Soc. B*, 372, 1–11. <http://doi.org/10.1098/rstb.2016.0108>
- Cohen Kadosh, R., & Walsh, V. (2009). Numerical representation in the parietal lobes: abstract or not abstract? *The Behavioral and Brain Sciences*, 32(3–4), 313-28-73. <http://doi.org/10.1017/S0140525X09990938>
- Crouzet, S. M., Busch, N. A., & Ohla, K. (2015). Taste quality decoding parallels taste sensations. *Current Biology*, 25(7), 890–896. <http://doi.org/10.1016/j.cub.2015.01.057>
- d'Errico, F. (1998). Palaeolithic Origins of Artificial Memory Systems: an Evolutionary Perspective. In C. Renfrew & C. Scarre (Eds.), *Cognition and Material Culture: the Archaeology of Symbolic Storage* (pp. 19–50). McDonald Institute for Archaeological Research - University of Cambridge, Cambridge - UK.
- d'Errico, F., Backwell, L., Villa, P., Degano, I., Lucejko, J. J., Bamford, M. K., ... Beaumont, P. B. (2012). Early evidence of San material culture represented by organic artifacts from Border Cave, South Africa. *Proceedings of the National Academy of Sciences*, 109(33), 13214–13219. <http://doi.org/10.1073/pnas.1204213109>

- Daitch, A. L., Foster, B. L., Schrouff, J., Rangarajan, V., Kasikci, I., Gattas, S., ... Parvizi, J. (2016). Mapping human temporal and parietal neuronal population activity and functional coupling during mathematical cognition. *Proceedings of the National Academy of Sciences*, 113(46), 201608434. <http://doi.org/10.1073/pnas.1608434113>
- Daitch, A. L., Sharma, M., Roland, J. L., Astafiev, S. V., Bundy, D. T., Gaona, C. M., ... Corbetta, M. (2013). Frequency-specific mechanism links human brain networks for spatial attention. *Proceedings of the National Academy of Sciences*, 110(48), 19585–19590. <http://doi.org/10.1073/pnas.1307947110>
- Dantzig, T. (1967). *Number: The Language of Science* (4th ed.). New York: The Free Press.
- Dastjerdi, M., Ozker, M., Foster, B. L., Rangarajan, V., & Parvizi, J. (2013). Numerical processing in the human parietal cortex during experimental and natural conditions. *Nature Communications*, 4. <http://doi.org/10.1038/ncomms3528>
- de Hevia, M. D., Addabbo, M., Nava, E., Croci, E., Girelli, L., & Macchi Cassia, V. (2017). Infants' detection of increasing numerical order comes before detection of decreasing number. *Cognition*, 158, 177–188. <http://doi.org/10.1016/j.cognition.2016.10.022>
- de Hevia, M. D., Izard, V., Coubart, A., Spelke, E. S., & Streri, A. (2014). Representations of space, time, and number in neonates. *Proceedings of the National Academy of Sciences*, 111(13), 4809–4813. <http://doi.org/10.1073/pnas.1323628111>
- De Smedt, B., Holloway, I. D., & Ansari, D. (2011). Effects of problem size and arithmetic operation on brain activation during calculation in children with varying levels of arithmetical fluency. *NeuroImage*, 57(3), 771–781. <http://doi.org/10.1016/j.neuroimage.2010.12.037>
- Dehaene, S. (1992). Varieties of numerical abilities. *Cognition*. [http://doi.org/10.1016/0010-0277\(92\)90049-N](http://doi.org/10.1016/0010-0277(92)90049-N)
- Dehaene, S. (1996). The Organization of Brain Activations in Number Comparison: Event-Related Potentials and the Additive-Factors Method. *Journal of Cognitive Neuroscience*, 8(1), 47–68. <http://doi.org/10.1162/jocn.1996.8.1.47>
- Dehaene, S. (1999). *The number sense. How the mind creates mathematics*. *Science Spectra*. <http://doi.org/10.2307/2589308>

- Dehaene, S. (2007). Symbols and Quantities in Parietal Cortex: Elements of a Mathematical Theory of Number Representation and Manipulation. In P. Haggard, Y. Rossetti, & M. Kawato (Eds.), *Attention & Performance XXII: Sensorimotor Foundations of Higher Cognition*. (pp. 527–574). Cambridge (UK): Oxford University Press.
- Dehaene, S., Bossini, S., & Giraux, P. (1993). The mental representation of parity and number magnitude. *Journal of Experimental Psychology: General*, 122(3), 371.
- Dehaene, S., & Brannon, E. M. (2010). Space, time, and number: a Kantian research program. *Trends in Cognitive Sciences*. <http://doi.org/10.1016/j.tics.2010.09.009>
- Dehaene, S., & Changeux, J. P. (1993). Development of elementary numerical abilities: a neuronal model. *Journal of Cognitive Neuroscience*, 5(4), 390–407. <http://doi.org/10.1162/jocn.1993.5.4.390>
- Dehaene, S., & Cohen, L. (1995). Towards an anatomical and functional model of number processing. *Mathematical Cognition*.
- Dehaene, S., & Cohen, L. (2007). Cultural recycling of cortical maps. *Neuron*, 56(2), 384–98. <http://doi.org/10.1016/j.neuron.2007.10.004>
- Dehaene, S., Dehaene-Lambertz, G., & Cohen, L. (1998). Abstract representations of numbers in the animal and human brain. *Trends in Neurosciences*, 21(8), 355–61. Retrieved from <http://www.ncbi.nlm.nih.gov/pubmed/9720604>
- Dehaene, S., & Mehler, J. (1992). Cross-linguistic regularities in the frequency of number words. *Cognition*, 43(1), 1–29.
- Dehaene, S., Meyniel, F., Wacongne, C., Wang, L., & Pallier, C. (2015). The Neural Representation of Sequences: From Transition Probabilities to Algebraic Patterns and Linguistic Trees. *Neuron*. <http://doi.org/10.1016/j.neuron.2015.09.019>
- Dehaene, S., Piazza, M., Pinel, P., & Cohen, L. (2003). Three Parietal Circuits for Number Processing. *Cognitive Neuropsychology*, 20(3–6), 487–506. <http://doi.org/10.1080/02643290244000239>
- Dehaene, S., Spelke, E., Pinel, P., Stanescu, R., & Tsivkin, S. (1999). Sources of mathematical thinking: behavioral and brain-imaging evidence. *Science (New York, N.Y.)*, 284(5416), 970–151

974. <http://doi.org/10.1126/science.284.5416.970>
- Delazer, M., Benke, T., Trieb, T., Schocke, M., & Ischebeck, A. (2006). Isolated numerical skills in posterior cortical atrophy-An fMRI study. *Neuropsychologia*, 44(10), 1909–1913. <http://doi.org/10.1016/j.neuropsychologia.2006.02.007>
- Delazer, M., Karner, E., Zamarian, L., Donnemiller, E., & Benke, T. (2006). Number processing in posterior cortical atrophy - A neuropsychological case study. *Neuropsychologia*, 44(1), 36–51. <http://doi.org/10.1016/j.neuropsychologia.2005.04.013>
- Diedrichsen, J., & Kriegeskorte, N. (2017). *Representational models: A common framework for understanding encoding, pattern-component, and representational-similarity analysis*. *PLoS Computational Biology* (Vol. 13). <http://doi.org/10.1371/journal.pcbi.1005508>
- Ding, N., Melloni, L., Zhang, H., Tian, X., & Poeppel, D. (2015). Cortical tracking of hierarchical linguistic structures in connected speech. *Nature Neuroscience*, 19(1), 158–64. <http://doi.org/10.1038/nn.4186>
- Donders, F. C. (1969). On the speed of mental processes. *Acta Psychologica*, 30, 412–431. [http://doi.org/10.1016/0001-6918\(69\)90065-1](http://doi.org/10.1016/0001-6918(69)90065-1)
- Dotan, D., & Dehaene, S. (2013). How do we convert a number into a finger trajectory? *Cognition*, 129(3), 512–529. <http://doi.org/10.1016/j.cognition.2013.07.007>
- Dotan, D., & Dehaene, S. (2015). The origins of logarithmic number-to-position mapping. *In Press*, 123(6), 1–52. <http://doi.org/10.1037/rev0000038>
- Dotan, D., & Dehaene, S. (2016). On the origins of logarithmic number-to-position mapping. *Psychological Review*, 123(6), 637–666. <http://doi.org/10.1037/rev0000038>
- Dotan, D., Friedmann, N., & Dehaene, S. (2014). Breaking down number syntax: Spared comprehension of multi-digit numbers in a patient with impaired digit-to-word conversion. *Cortex*, 59, 62–73. <http://doi.org/10.1016/j.cortex.2014.07.005>
- Dotan, D., Meyniel, F., & Dehaene, S. (2017). On-line confidence monitoring during decision making. *Submitted for Publication*.
- Dotan, D., Pinheiro-Chagas, P., & Dehaene, S. (2017). Track it to crack it: revealing the succession of processing stages with pointing trajectories. *Manuscript in Preparation*.

- Drucker, C. B., & Brannon, E. M. (2014). Rhesus monkeys (*Macaca mulatta*) map number onto space. *Cognition*, 132(1), 57–67. <http://doi.org/10.1016/j.cognition.2014.03.011>
- Eger, E., Michel, V., Thirion, B., Amadon, A., Dehaene, S., & Kleinschmidt, A. (2009). Deciphering cortical number coding from human brain activity patterns. *Current Biology: CB*, 19(19), 1608–15. <http://doi.org/10.1016/j.cub.2009.08.047>
- Eger, E., Pinel, P., Dehaene, S., & Kleinschmidt, A. (2015). Spatially invariant coding of numerical information in functionally defined subregions of human parietal cortex. *Cerebral Cortex*, 25(5), 1319–1329. <http://doi.org/10.1093/cercor/bht323>
- Eger, E., Sterzer, P., Russ, M. O., Giraud, A.-L., & Kleinschmidt, A. (2003). A supramodal number representation in human intraparietal cortex. *Neuron*, 37(4), 719–25. Retrieved from <http://www.ncbi.nlm.nih.gov/pubmed/12597867>
- Erb, C. D., Moher, J., Sobel, D. M., & Song, J.-H. (2016). Reach tracking reveals dissociable processes underlying cognitive control. *Cognition*, 152, 114–126. <http://doi.org/10.1016/j.cognition.2016.03.015>
- Faulkenberry, T. J., Cruise, A., Lavro, D., & Shaki, S. (2016). Response trajectories capture the continuous dynamics of the size congruity effect. *Acta Psychologica*, 163, 114–123. <http://doi.org/10.1016/j.actpsy.2015.11.010>
- Fayol, M., & Thevenot, C. (2012). The use of procedural knowledge in simple addition and subtraction problems. *Cognition*, 123(3), 392–403. <http://doi.org/10.1016/j.cognition.2012.02.008>
- Feigenson, L., Dehaene, S., & Spelke, E. (2004). Core systems of number. *Trends in Cognitive Sciences*, 8(7), 307–314. <http://doi.org/10.1016/j.tics.2004.05.002>
- Felleman, D. J., & Van Essen, D. C. (1991). Distributed hierarchical processing in the primate cerebral cortex. *Cerebral Cortex*, 1(1), 1–47. <http://doi.org/10.1093/cercor/1.1.1-a>
- Ferrand, L., Brysbaert, M., Keuleers, E., New, B., Bonin, P., Méot, A., ... Pallier, C. (2011). Comparing word processing times in naming, lexical decision, and progressive demasking: Evidence from Chronolex. *Frontiers in Psychology*, 2(NOV). <http://doi.org/10.3389/fpsyg.2011.00306>

- Fias, W., Lammertyn, J., Reynvoet, B., Dupont, P., & Orban, G. A. (2003). Parietal Representation of Symbolic and Nonsymbolic Magnitude. *Journal of Cognitive Neuroscience*, 15(1), 47–56. <http://doi.org/10.1162/089892903321107819>
- Finkbeiner, M., Song, J.-H., Nakayama, K., & Caramazza, A. (2008). Engaging the motor system with masked orthographic primes: A kinematic analysis. *Visual Cognition*, 16(1), 11–22. <http://doi.org/10.1080/13506280701203838>
- Fischer, M. H., Castel, A. D., Dodd, M. D., & Pratt, J. (2003). Perceiving numbers causes spatial shifts of attention. *Nature Neuroscience*, 6(6), 555–556. <http://doi.org/10.1038/nn1066>
- Fitts, P. M. (1954). The information capacity of the human motor system in controlling the amplitude of movement. *Journal of Experimental Psychology*, 47(6), 381–391. <http://doi.org/10.1037/h0055392>
- Fonken, Y. M., Rieger, J. W., Tzvi, E., Crone, N. E., Chang, E., Parvizi, J., ... Krämer, U. M. (2016). Frontal and motor cortex contributions to response inhibition: evidence from electrocorticography. *Journal of Neurophysiology*, 115(4), 2224–2236. <http://doi.org/10.1152/jn.00708.2015>
- Foster, B. L., Dastjerdi, M., & Parvizi, J. (2012). Neural populations in human posteromedial cortex display opposing responses during memory and numerical processing. *Proceedings of the National Academy of Sciences*, 109(38), 15514–15519. <http://doi.org/10.1073/pnas.1206580109>
- Foster, B. L., Rangarajan, V., Shirer, W. R., & Parvizi, J. (2015). Intrinsic and task-dependent coupling of neuronal population activity in human parietal cortex. *Neuron*, 86(2), 578–590. <http://doi.org/10.1016/j.neuron.2015.03.018>
- Freeman, J. B., & Ambady, N. (2010). MouseTracker: software for studying real-time mental processing using a computer mouse-tracking method. *Behavior Research Methods*, 42(1), 226–241. <http://doi.org/10.3758/BRM.42.1.226>
- Freud, E., Culham, J. C., Plaut, D. C., & Behrmann, M. (2017). The large-scale organization of shape processing in the ventral and dorsal pathways. *eLife*, 6, e27576. <http://doi.org/10.7554/eLife.27576>

- Freyd, J. J., & Finke, R. a. (1984). Representational momentum. *Journal of Experimental Psychology: Learning, Memory, and Cognition*, 10(1), 126–132. <http://doi.org/10.1037/0278-7393.10.1.126>
- Freyd, J. J., Kelly, M. H., & DeKay, M. L. (1990). Representational momentum in memory for pitch. *Journal of Experimental Psychology. Learning, Memory, and Cognition*, 16(6), 1107–17. <http://doi.org/10.1037/0278-7393.16.6.1107>
- Friedman, J., Brown, S., & Finkbeiner, M. (2013). Linking cognitive and reaching trajectories via intermittent movement control. *Journal of Mathematical Psychology*, 57(3–4), 140–151. <http://doi.org/10.1016/j.jmp.2013.06.005>
- Gallistel, C. R. (1990). *The Organization of Learning*. Bradford Books/MIT Press, Cambridge, MA.
- Galton, F. (1881). Visualised numerals. *Journal of the Anthropological Institute*, 10, 85–102. <http://doi.org/doi:10.2307/2841651>
- Gold, J. I., & Shadlen, M. N. (2007). The neural basis of decision making. *Annual Review of Neuroscience*, 30, 535–574. <http://doi.org/10.1146/annurev.neuro.29.051605.113038>
- Gonzalez, A., Hutchinson, J. B., Uncapher, M. R., Chen, J., LaRocque, K. F., Foster, B. L., ... Wagner, A. D. (2015). Electrocorticography reveals the temporal dynamics of posterior parietal cortical activity during recognition memory decisions. *Proceedings of the National Academy of Sciences of the United States of America*, 112(35), 11066–11071. <http://doi.org/10.1073/pnas.1510749112>
- Goodale, M. A., & Milner, A. D. (1992). Separate visual pathways for perception and action. *Trends in Neurosciences*. [http://doi.org/10.1016/0166-2236\(92\)90344-8](http://doi.org/10.1016/0166-2236(92)90344-8)
- Gramfort, A., Luessi, M., Larson, E., Engemann, D. A., Strohmeier, D., Brodbeck, C., ... Hämäläinen, M. (2013). MEG and EEG data analysis with MNE-Python. *Frontiers in Neuroscience*, (7 DEC). <http://doi.org/10.3389/fnins.2013.00267>
- Grill-Spector, K., & Weiner, K. S. (2014). The functional architecture of the ventral temporal cortex and its role in categorization. *Nature Reviews. Neuroscience*, 15(8), 536–548. <http://doi.org/10.1038/nrn3747>

- Groen, G. J., & Parkman, J. M. (1972). A chronometric analysis of simple addition. *Psychological Review*, 79(4), 329–343. <http://doi.org/10.1037/h0032950>
- Halberda, J., Mazzocco, M. M. M., & Feigenson, L. (2008). Individual differences in non-verbal number acuity correlate with maths achievement. *Nature*, 455(7213), 665–668. <http://doi.org/10.1038/nature07246>
- Hamann, M. S., & Ashcraft, M. H. (1986). Textbook Presentations of the Basic Addition Facts. *Cognition and Instruction*, 3(3), 173–192.
- Hannagan, T., Amedi, A., Cohen, L., Dehaene-Lambertz, G., & Dehaene, S. (2015). Origins of the specialization for letters and numbers in ventral occipitotemporal cortex. *Trends in Cognitive Sciences*. <http://doi.org/10.1016/j.tics.2015.05.006>
- Hartmann, M., Mast, F. W., & Fischer, M. H. (2015). Spatial biases during mental arithmetic: Evidence from eye movements on a blank screen. *Frontiers in Psychology*, 6(JAN). <http://doi.org/10.3389/fpsyg.2015.00012>
- Harvey, B. M., & Dumoulin, S. O. (2017). A network of topographic numerosity maps in human association cortex. *Nature Human Behaviour*, 1(2), 36. <http://doi.org/10.1038/s41562-016-0036>
- Harvey, B. M., Ferri, S., & Orban, G. A. (2017). Comparing Parietal Quantity- Processing Mechanisms between Humans and Macaques Two Quantity-Processing Networks in Human Parietal Cortex: a Proposal, 21(10), 779–793. <http://doi.org/10.1016/j.tics.2017.07.002>
- Harvey, B. M., Klein, B. P., Petridou, N., & Dumoulin, S. O. (2013). Topographic Representation of Numerosity in the Human Parietal Cortex. *Science*, 341(6150), 1123–1126. <http://doi.org/10.1126/science.1239052>
- Hauser, M. D., Chomsky, N., & Fitch, W. T. (2002). The faculty of language: what is it, who has it, and how did it evolve? *Science (New York, N.Y.)*, 298(5598), 1569–79. <http://doi.org/10.1126/science.298.5598.1569>
- Hermes, D., Miller, K. J., Noordmans, H. J., Vansteensel, M. J., & Ramsey, N. F. (2010). Automated electrocorticographic electrode localization on individually rendered brain surfaces. *Journal of Neuroscience Methods*, 185(2), 293–298.

<http://doi.org/10.1016/j.jneumeth.2009.10.005>

Hermes, D., Rangarajan, V., Foster, B. L., King, J.-R., Kasikci, I., Miller, K. J., & Parvizi, J. (2015). Electrophysiological Responses in the Ventral Temporal Cortex During Reading of Numerals and Calculation. *Cerebral Cortex (New York, N.Y.: 1991)*.

<http://doi.org/10.1093/cercor/bhv250>

Hubbard, E. M., Piazza, M., Pinel, P., & Dehaene, S. (2005). Interactions between number and space in parietal cortex. *Nature Reviews Neuroscience*, 6(6), 435–448.

<http://doi.org/10.1038/nrn1684>

Huth, A. G., de Heer, W. A., Griffiths, T. L., Theunissen, F. E., & Gallant, J. L. (2016). Natural speech reveals the semantic maps that tile human cerebral cortex. *Nature*, 532(7600), 453–458. <http://doi.org/10.1038/nature17637>

Isik, L., Meyers, E. M., Leibo, J. Z., & Poggio, T. (2014). The dynamics of invariant object recognition in the human visual system. *Journal of Neurophysiology*, 111(1), 91–102.

<http://doi.org/10.1152/jn.00394.2013>

Izard, V., Sann, C., Spelke, E. S., & Streri, A. (2009). Newborn infants perceive abstract numbers. *Proceedings of the National Academy of Sciences*, 106(25), 10382–10385.

<http://doi.org/10.1073/pnas.0812142106>

Jevons, S. (1871). The power of numerical discrimination. *Nature*, 3, 281–282.

<http://doi.org/10.1038/003281a0>

Kaiser, D., Azzalini, D. C., & Peelen, M. V. (2016). Shape-independent object category responses revealed by MEG and fMRI decoding. *Journal of Neurophysiology*, jn.01074.2015.

<http://doi.org/10.1152/jn.01074.2015>

Kanjlia, S., Lane, C., Feigenson, L., & Bedny, M. (2016). Absence of visual experience modifies the neural basis of numerical thinking. *Proceedings of the National Academy of Sciences*, 113(40), 201524982. <http://doi.org/10.1073/pnas.1524982113>

Kay, K. N., Naselaris, T., Prenger, R. J., & Gallant, J. L. (2008). Identifying natural images from human brain activity. *Nature*, 452(7185), 352–355. <http://doi.org/10.1038/nature06713>

King, J.-R., & Dehaene, S. (2014). Characterizing the dynamics of mental representations: the

- temporal generalization method. *Trends in Cognitive Sciences*, 18(4), 203–210.  
<http://doi.org/10.1016/j.tics.2014.01.002>
- King, J.-R., Pescetelli, N., & Dehaene, S. (2016). Brain Mechanisms Underlying the Brief Maintenance of Seen and Unseen Sensory Information. *Neuron*, 92(5), 1122–1134.  
<http://doi.org/10.1016/j.neuron.2016.10.051>
- Knops, A., Thirion, B., Hubbard, E. M., Michel, V., & Dehaene, S. (2009). Recruitment of an area involved in eye movements during mental arithmetic. *Science (New York, N.Y.)*, 324(5934), 1583–5. <http://doi.org/10.1126/science.1171599>
- Knops, A., Viarouge, A., & Dehaene, S. (2009). Dynamic representations underlying symbolic and nonsymbolic calculation: evidence from the operational momentum effect. *Attention Perception Psychophysics*, 71(4), 803–821. Retrieved from <http://app.psychonomic-journals.org/content/71/4/803.full.pdf>
- Knops, A., Viarouge, A., Dehaene, S., Cea, F., Universit, F., & When, F. (2009). Dynamic representations underlying symbolic and nonsymbolic calculation: evidence from the operational momentum effect. *Attention Perception Psychophysics*, 71(4), 803–821.  
<http://doi.org/10.3758/APP>
- Kocagoncu, E., Clarke, A., Devereux, B. J., & Tyler, L. K. (2017). Decoding the Cortical Dynamics of Sound-Meaning Mapping. *The Journal of Neuroscience*, 37(5), 1312–1319.  
<http://doi.org/10.1523/JNEUROSCI.2858-16.2016>
- Krakauer, J. W., Ghazanfar, A. A., Gomez-Marin, A., MacIver, M. A., & Poeppel, D. (2017). Neuroscience Needs Behavior: Correcting a Reductionist Bias. *Neuron*.  
<http://doi.org/10.1016/j.neuron.2016.12.041>
- Krause, J., & Godin, J.-G. J. (1995). Predator preferences for attacking particular prey group sizes: consequences for predator hunting success and prey predation risk. *Anim. Behav*, 50, 465–473. <http://doi.org/10.1006/anbe.1995.0260>
- Kriegeskorte, N., & Kievit, R. A. (2013). Representational geometry: Integrating cognition, computation, and the brain. *Trends in Cognitive Sciences*.  
<http://doi.org/10.1016/j.tics.2013.06.007>

- Kriegeskorte, N., Mur, M., Ruff, D. D. A., Kiani, R., Bodurka, J., Esteky, H., ... Bandettini, P. A. (2008). Matching categorical object representations in inferior temporal cortex of mand and monkey. *Neuron*, 60(6), 1126–1141.  
<http://doi.org/10.1016/j.neuron.2008.10.043>.Matching
- Laird, A. R., Fox, P. M., Price, C. J., Glahn, D. C., Uecker, A. M., Lancaster, J. L., ... Fox, P. T. (2005). ALE meta-analysis: Controlling the false discovery rate and performing statistical contrasts. In *Human Brain Mapping* (Vol. 25, pp. 155–164).  
<http://doi.org/10.1002/hbm.20136>
- Landauer, T. K. (1962). Rate of implicit speech. *Perceptual and Motor Skills*, 15(3), 646.  
<http://doi.org/http://dx.doi.org/10.2466/pms.1962.15.3.646>
- Landy, D. H., Jones, M. N., & Goldstone, R. L. (2008). How the Appearance of an Operator Affects its Formal Precedence. *Proceedings of the Thirtieth Annual Conference of the Cognitive Science Society*, 2109–2114.
- LaRocque, J. J., Lewis-Peacock, J. A., Drysdale, A. T., Oberauer, K., & Postle, B. R. (2013). Decoding Attended Information in Short-term Memory: An EEG Study. *Journal of Cognitive Neuroscience*, 25(1), 127–142. [http://doi.org/10.1162/jocn\\_a\\_00305](http://doi.org/10.1162/jocn_a_00305)
- LeFevre, J.-A., Sadesky, G. S., & Bisanz, J. (1996). Selection of procedures in mental addition: Reassessing the problem size effect in adults. *Journal of Experimental Psychology: Learning, Memory, and Cognition*, 22(1), 216–230. <http://doi.org/10.1037/0278-7393.22.1.216>
- Lefevre, J. A., & Kulak, A. G. (1994). Individual differences in the obligatory activation of addition facts. *Memory & Cognition*, 22(2), 188–200.
- Lehmann, D., & Skrandies, W. (1980). Reference-free identification of components of checkerboard-evoked multichannel potential fields. *Electroencephalography and Clinical Neurophysiology*, 48(6), 609–621. [http://doi.org/10.1016/0013-4694\(80\)90419-8](http://doi.org/10.1016/0013-4694(80)90419-8)
- Lepora, N. F., & Pezzulo, G. (2015). Embodied choice: How action influences perceptual decision making. *PLOS Computational Biology*, 11(4), e1004110.  
<http://doi.org/10.1371/journal.pcbi.1004110>
- Livingstone, M. S., Pettine, W. W., Srihasam, K., Moore, B., Morocz, I. A., & Lee, D. (2014).

- Symbol addition by monkeys provides evidence for normalized quantity coding. *Proceedings of the National Academy of Sciences*, 111(18), 6822–6827.  
<http://doi.org/10.1073/pnas.1404208111>
- Logothetis, N. K., Pauls, J., Augath, M., Trinath, T., & Oeltermann, A. (2001). Neurophysiological investigation of the basis of the fMRI signal. *Nature*, 412(6843), 150–157.  
<http://doi.org/10.1038/35084005>
- Lundqvist, M., Rose, J., Herman, P., Brincat, S. L. L., Buschman, T. J. J., & Miller, E. K. K. (2016). Gamma and Beta Bursts Underlie Working Memory. *Neuron*, 90(1), 152–164.  
<http://doi.org/10.1016/j.neuron.2016.02.028>
- Manning, J. R., Jacobs, J., Fried, I., & Kahana, M. J. (2009). Broadband shifts in local field potential power spectra are correlated with single-neuron spiking in humans. *The Journal of Neuroscience : The Official Journal of the Society for Neuroscience*, 29(43), 13613–13620.  
<http://doi.org/10.1523/JNEUROSCI.2041-09.2009>
- Mante, V., Sussillo, D., Shenoy, K. V., & Newsome, W. T. (2013). Context-dependent computation by recurrent dynamics in prefrontal cortex. *Nature*, 503(7474), 78–84.  
<http://doi.org/10.1038/nature12742>
- Marghetis, T., Núñez, R., & Bergen, B. K. (2014). Doing arithmetic by hand: Hand movements during exact arithmetic reveal systematic, dynamic spatial processing. *The Quarterly Journal of Experimental Psychology*, 67(8), 1579–1596. <http://doi.org/10.1080/17470218.2014.897359>
- Marti, S., King, J.-R., & Dehaene, S. (2015). Time-Resolved Decoding of Two Processing Chains during Dual-Task Interference. *Neuron*, 88(6), 1297–1307.  
<http://doi.org/10.1016/j.neuron.2015.10.040>
- Masson, N., & Pesenti, M. (2014). Attentional bias induced by solving simple and complex addition and subtraction problems. *The Quarterly Journal of Experimental Psychology*, 67(8), 1514–1526. <http://doi.org/10.1080/17470218.2014.903985>
- Mathieu, R., Epinat-duclos, J., Léone, J., Fayol, M., & Thevenot, C. (2017). Developmental Cognitive Neuroscience Hippocampal spatial mechanisms relate to the development of arithmetic symbol processing in children. *Developmental Cognitive Neuroscience*, (August 160

- 2016), 0–1. <http://doi.org/10.1016/j.dcn.2017.06.001>
- Mathieu, R., Epinat-duclos, J., Sigovan, M., Breton, A., Cheylus, A., Fayol, M., ... Prado, J. (2017). What ' s Behind a “ + ” Sign ? Perceiving an Arithmetic Operator Recruits Brain Circuits for Spatial Orienting. *Cerebral Cortex*, 1–12. <http://doi.org/10.1093/cercor/bhx064>
- Mathieu, R., Gourjon, A., Couderc, A., Thevenot, C., & Prado, J. (2016). Running the number line: Rapid shifts of attention in single-digit arithmetic. *Cognition*, 146, 229–239. <http://doi.org/10.1016/j.cognition.2015.10.002>
- McClelland, J. L. (1979). On the time relations of mental processes: An examination of systems of processes in cascade. *Psychol Rev*, 86(4), 287–330. <http://doi.org/10.1037/0033-295X.86.4.287>
- McComb, K., Packer, C., & Pusey, A. (1994). Roaring and numerical assessment in contests between groups of female lions, *Panthera leo*. *Animal Behaviour*, 47(2), 379–387. <http://doi.org/10.1006/anbe.1994.1052>
- McCrink, K., Dehaene, S., & Dehaene-Lambertz, G. (2007). Moving along the number line: operational momentum in nonsymbolic arithmetic. *Perception & Psychophysics*, 69(8), 1324–33. Retrieved from <http://www.ncbi.nlm.nih.gov/pubmed/18078224>
- McCrink, K., & Wynn, K. (2004). Large-number addition and subtraction by 9-month-old infants. *Psychological Science*, 15(11), 776–781. <http://doi.org/10.1111/j.0956-7976.2004.00755.x>
- Menon, V. (2014). Arithmetic in the Child and Adult Brain. In *The Oxford Handbook of Mathematical Cognition* (Vol. 1, pp. 1–23). <http://doi.org/10.1093/oxfordhb/9780199642342.013.041>
- Menon, V., Rivera, S. M., White, C. D., Glover, G. H., & Reiss, A. L. (2000). Dissociating Prefrontal and Parietal Cortex Activation during Arithmetic Processing. *NeuroImage*, 12(4), 357–365. <http://doi.org/10.1006/nimg.2000.0613>
- Molko, N., Cachia, A., Bruandet, M., Bihan, D. Le, Cohen, L., & Dehaene, S. (2003). Functional and Structural Alterations of the Intraparietal Sulcus in a Developmental Dyscalculia of Genetic Origin. *Neuron*, 40, 847–858.
- Mongillo, G., Barak, O., & Tsodyks, M. (2008). Synaptic Theory of Working Memory. *Science*, 161

- 319(5869), 1543–1546. <http://doi.org/10.1126/science.1150769>
- Moyer, R. S., & Landauer, T. K. (1967). Time required for judgements of numerical inequality. *Nature*, 215(5109), 1519–1520.
- Naccache, L., & Dehaene, S. (2001). The priming method: imaging unconscious repetition priming reveals an abstract representation of number in the parietal lobes. *Cerebral Cortex (New York, N.Y.: 1991)*, 11(10), 966–974.
- Nieder, A. (2012). Supramodal numerosity selectivity of neurons in primate prefrontal and posterior parietal cortices. *Proceedings of the National Academy of Sciences*, 109(29), 11860–11865. <http://doi.org/10.1073/pnas.1204580109>
- Nieder, A. (2016). The neuronal code for number. *Nature Reviews Neuroscience*, 17(6), 366–382. <http://doi.org/10.1038/nrn.2016.40>
- Nieder, A., & Miller, E. K. (2004). A parieto-frontal network for visual numerical information in the monkey, 101(19).
- Nuerk, H. C., Wood, G., & Willmes, K. (2005). The universal SNARC effect: The association between number magnitude and space is amodal. *Experimental Psychology*, 52(3), 187–194. <http://doi.org/10.1027/1618-3169.52.3.187>
- Oostenveld, R., Fries, P., Maris, E., & Schoffelen, J. M. (2011). FieldTrip: Open source software for advanced analysis of MEG, EEG, and invasive electrophysiological data. *Computational Intelligence and Neuroscience*, 2011. <http://doi.org/10.1155/2011/156869>
- Oosterhof, N. N., Connolly, A. C., & Haxby, J. V. (2016). CoSMoMVPA: Multi-Modal Multivariate Pattern Analysis of Neuroimaging Data in Matlab/GNU Octave. *Frontiers in Neuroinformatics*, 10, 27. <http://doi.org/10.3389/fninf.2016.00027>
- Pallier, C., Devauchelle, A., & Dehaene, S. (2010). Cortical representation of the constituent structure of sentences. *PNAS*. <http://doi.org/10.1073/pnas.1018711108/-/DCSupplemental.www.pnas.org/cgi/doi/10.1073/pnas.1018711108>
- Pantazis, D., Fang, M., Qin, S., Mohsenzadeh, Y., Li, Q., & Cichy, R. M. (2017). Decoding the orientation of contrast edges from MEG evoked and induced responses. *NeuroImage*, 1–31. <http://doi.org/10.1016/j.neuroimage.2017.07.022>

- Parkman, J. M., & Groen, G. J. (1971). Temporal aspects of simple addition and comparison. *Journal of Experimental Psychology*, 89(2), 335–342. <http://doi.org/10.1037/h0031198>
- Parvizi, J., Jacques, C., Foster, B. L., Witthoft, N., Rangarajan, V., Weiner, K. S., & Grill-Spector, K. (2012). Electrical stimulation of human fusiform face-selective regions distorts face perception. *The Journal of Neuroscience: The Official Journal of the Society for Neuroscience*, 32(43), 14915–14920. <http://doi.org/10.1523/JNEUROSCI.2609-12.2012>
- Parvizi, J., Rangarajan, V., Shirer, W. R., Desai, N., & Greicius, M. D. (2013). The will to persevere induced by electrical stimulation of the human cingulate gyrus. *Neuron*, 80(6), 1359–1367. <http://doi.org/10.1016/j.neuron.2013.10.057>
- Pashler, H. (1984). Processing stages in overlapping tasks: Evidence for a central bottleneck. *Journal of Experimental Psychology: Human Perception and Performance*, 10(3), 358–377. <http://doi.org/10.1037/0096-1523.10.3.358>
- Pedregosa, F., Varoquaux, G., Gramfort, A., Michel, V., Thirion, B., Grisel, O., ... Duchesnay, É. (2011). Scikit-learn: Machine Learning in Python. *Journal of Machine Learning Research*, 12, 2825–2830. <http://doi.org/10.1007/s13398-014-0173-7.2>
- Peirce, J. W. (2007). PsychoPy-Psychophysics software in Python. *Journal of Neuroscience Methods*, 162(1–2), 8–13. <http://doi.org/10.1016/j.jneumeth.2006.11.017>
- Piantadosi, S. T., & Cantlon, J. F. (2017). True Numerical Cognition in the Wild. *Psychological Science*, 28(4), 462–469. <http://doi.org/10.1177/0956797616686862>
- Piazza, M. (2010). Neurocognitive start-up tools for symbolic number representations. *Trends in Cognitive Sciences*, 14(12), 542–551. <http://doi.org/10.1016/j.tics.2010.09.008>
- Piazza, M., Facoetti, A., Trussardi, A. N., Berteletti, I., Conte, S., Lucangeli, D., ... Zorzi, M. (2010). Developmental trajectory of number acuity reveals a severe impairment in developmental dyscalculia. *Cognition*, 116(1), 33–41. <http://doi.org/10.1016/j.cognition.2010.03.012>
- Piazza, M., Izard, V., Pinel, P., Le Bihan, D., & Dehaene, S. (2004). Tuning curves for approximate numerosity in the human intraparietal sulcus. *Neuron*, 44(3), 547–555. <http://doi.org/10.1016/j.neuron.2004.10.014>

- Piazza, M., Pinel, P., Le Bihan, D., & Dehaene, S. (2007). A Magnitude Code Common to Numerosities and Number Symbols in Human Intraparietal Cortex. *Neuron*, 53(2), 293–305. <http://doi.org/10.1016/j.neuron.2006.11.022>
- Pinel, P., Dehaene, S., Rivie, D., & Lebihan, D. (2001). Modulation of Parietal Activation by Semantic Distance in a Number Comparison Task. *Stimulus*, 1026, 1013–1026. <http://doi.org/10.1006/nimg.2001.0913>
- Pinhas, M., & Fischer, M. H. (2008). Mental movements without magnitude? A study of spatial biases in symbolic arithmetic. *Cognition*, 109(3), 408–415. <http://doi.org/10.1016/j.cognition.2008.09.003>
- Pinhas, M., Shaki, S., & Fischer, M. H. (2014). Heed the signs: Operation signs have spatial associations. *Quarterly Journal of Experimental Psychology* (2006), 67(8), 1527–1540. <http://doi.org/10.1080/17470218.2014.892516>
- Pinheiro-Chagas, P., Daitch, A., Parvizi, J., & Dehaene, S. (2017). Brain mechanisms of arithmetic: a crucial role for ventral temporal cortex. *Submitted*.
- Pinheiro-Chagas, P., Dotan, D., Piazza, M., & Dehaene, S. (2017). Finger tracking reveals the covert processing stages of mental arithmetic. *Open Mind: Discoveries in Cognitive Science*, 1–12. [http://doi.org/10.1162/OPMI\\_a\\_00003](http://doi.org/10.1162/OPMI_a_00003)
- Pinheiro-Chagas, P., Wood, G., Knops, A., Krinzinger, H., Lonnemann, J., Starling-Alves, I., ... Haase, V. G. (2014). In how many ways is the approximate number system associated with exact calculation? *PLoS ONE*, 9(11). <http://doi.org/10.1371/journal.pone.0111155>
- Posner, M. I. (1980). Orienting of attention. *Quarterly Journal of Experimental Psychology*, 32(1), 3–25. <http://doi.org/10.1080/00335558008248231>
- Pouget, A., Deneve, S., & Duhamel, J.-R. (2002). A computational perspective on the neural basis of multisensory spatial representations. *Nature Reviews Neuroscience*, 3(9), 741–747. <http://doi.org/10.1038/nrn914>
- Price, G. R., Yeo, D. J., Wilkey, E. D., & Cutting, L. E. (2016). Prospective relations between resting-state connectivity of parietal subdivisions and arithmetic competence. *Developmental Cognitive Neuroscience*. <http://doi.org/10.1016/j.dcn.2017.02.006>

- Rajalingham, R., Schmidt, K., & DiCarlo, J. J. (2015). Comparison of Object Recognition Behavior in Human and Monkey. *Journal of Neuroscience*, 35(35), 12127–12136. <http://doi.org/10.1523/JNEUROSCI.0573-15.2015>
- Ray, S., & Maunsell, J. H. R. (2011). Different origins of gamma rhythm and high-gamma activity in macaque visual cortex. *PLoS Biology*, 9(4), e1000610. <http://doi.org/10.1371/journal.pbio.1000610>
- Restle, F. (1970). Speed of Adding and Comparing Numbers. *Journal of Experimental Psychology*, 83(2p1), 274.
- Resulaj, A., Kiani, R., Wolpert, D. M., & Shadlen, M. N. (2009). Changes of mind in decision-making. *Nature*, 461(7261), 263–266. <http://doi.org/10.1038/nature08275>
- Rickard, T. ., Romero, S. ., Basso, G., Wharton, C., Flitman, S., & Grafman, J. (2000). The calculating brain: an fMRI study. *Neuropsychologia*, 38(3), 325–335. [http://doi.org/10.1016/S0028-3932\(99\)00068-8](http://doi.org/10.1016/S0028-3932(99)00068-8)
- Riès, S. K., Dhillon, R. K., Clarke, A., King-Stephens, D., Laxer, K. D., Weber, P. B., ... Knight, R. T. (2017). Spatiotemporal dynamics of word retrieval in speech production revealed by cortical high-frequency band activity. *Proceedings of the National Academy of Sciences*, 114(23), E4530–E4538. <http://doi.org/10.1073/pnas.1620669114>
- Roitman, J. D., Brannon, E. M., & Platt, M. L. (2007). Monotonic Coding of Numerosity in Macaque Lateral Intraparietal Area. *Trials*, 5(8). <http://doi.org/10.1371/journal.pbio.0050208>
- Rugani, R., & de Hevia, M.-D. (2017). Number-space associations without language: Evidence from preverbal human infants and non-human animal species. *Psychonomic Bulletin & Review*, 24(2). <http://doi.org/10.3758/s13423-016-1126-2>
- Rugani, R., Vallortigara, G., Priftis, K., & Regolin, L. (2015). Animal cognition. Number-space mapping in the newborn chick resembles humans' mental number line. *Science (New York, N.Y.)*, 347(6221), 534–536. <http://doi.org/10.1126/science.aaa1379>
- Santens, S., Goossens, S., & Verguts, T. (2011). Distance in motion: response trajectories reveal the dynamics of number comparison. *PloS One*, 6(9), Article ID e25429.

<http://doi.org/10.1371/journal.pone.0025429>

Scherbaum, S., Dshemuchadse, M., Fischer, R., & Goschke, T. (2010). How decisions evolve: The temporal dynamics of action selection. *Cognition*, 115(3), 407–416.

<http://doi.org/10.1016/j.cognition.2010.02.004>

Schleger, F., Landerl, K., Muenssinger, J., Draganova, R., Reinl, M., Kiefer-Schmidt, I., ... Preissl, H. (2014). Magnetoencephalographic signatures of numerosity discrimination in fetuses and neonates. *Developmental Neuropsychology*, 39(4), 316–329.

<http://doi.org/10.1080/87565641.2014.914212>

Schneider, E., Maruyama, M., Dehaene, S., & Sigman, M. (2012). Eye gaze reveals a fast, parallel extraction of the syntax of arithmetic formulas. *Cognition*, 125(3), 475–490.

<http://doi.org/10.1016/j.cognition.2012.06.015>

Sergent, C., Baillet, S., & Dehaene, S. (2005). Timing of the brain events underlying access to consciousness during the attentional blink. *Nature Neuroscience*, 8(10), 1391–1400.

<http://doi.org/10.1038/nn1549>

Seyler, D. J., Kirk, E. P., & Ashcraft, M. H. (2003). Elementary Subtraction. *Journal of Experimental Psychology: Learning, Memory, and Cognition*, 29(6), 1339–1352.

<http://doi.org/10.1037/0278-7393.29.6.1339>

Shum, J., Hermes, D., Foster, B. L., Dastjerdi, M., Rangarajan, V., Winawer, J., ... Parvizi, J. (2013). A brain area for visual numerals. *The Journal of Neuroscience : The Official Journal of the Society for Neuroscience*, 33(16), 6709–6715.

<http://doi.org/10.1523/JNEUROSCI.4558-12.2013>

Siegler, R. S. (1987). The perils of averaging data over strategies: An example from children's addition. *Journal of Experimental Psychology: General*, 116(3), 250.

Siegler, R. S., & Jenkins, E. A. (1989). *How children discover new strategies*. Hillsdale, NJ: Erlbaum.

Siegler, R. S., & Shrager, J. (1984). Strategy choices in addition and subtraction: How do children know what to do? In C. Sophian (Ed.), *Origins of cognitive skills* (pp. 229–293). Hillsdale, NJ: Erlbaum.

- Sigman, M., & Dehaene, S. (2005). Parsing a cognitive task: a characterization of the mind's bottleneck. *PLoS Biology*, 3(2), e37. <http://doi.org/10.1371/journal.pbio.0030037>
- Sigman, M., Peña, M., Goldin, A. P., & Ribeiro, S. (2014). Neuroscience and education: prime time to build the bridge. *Nature Neuroscience*, 17(4), 497–502. <http://doi.org/10.1038/nn.3672>
- Song, J.-H., & Nakayama, K. (2008). Numeric comparison in a visually-guided manual reaching task. *Cognition*, 106(2), 994–1003. <http://doi.org/10.1016/j.cognition.2007.03.014>
- Song, J.-H., & Nakayama, K. (2009). Hidden cognitive states revealed in choice reaching tasks. *Trends in Cognitive Sciences*, 13(8), 360–366. <http://doi.org/10.1016/j.tics.2009.04.009>
- Spelke, E. S., & Kinzler, K. D. (2007). Core knowledge. *Developmental Science*. <http://doi.org/10.1111/j.1467-7687.2007.00569.x>
- Sprague, T. C., Ester, E. F., & Serences, J. T. (2016). Restoring Latent Visual Working Memory Representations in Human Cortex. *Neuron*, 91(3), 694–707. <http://doi.org/10.1016/j.neuron.2016.07.006>
- Stanescu-Cosson, R., Pinel, P., van De Moortele, P. F., Le Bihan, D., Cohen, L., & Dehaene, S. (2000). Understanding dissociations in dyscalculia: a brain imaging study of the impact of number size on the cerebral networks for exact and approximate calculation. *Brain: A Journal of Neurology*, 123 (Pt 1), 2240–55. Retrieved from <http://www.ncbi.nlm.nih.gov/pubmed/11050024>
- Starr, A., Libertus, M. E., & Brannon, E. M. (2013). Number sense in infancy predicts mathematical abilities in childhood. *Proceedings of the National Academy of Sciences*, 110(45), 18116–18120. <http://doi.org/10.1073/pnas.1302751110>
- Stazyk, E. H., Ashcraft, M. H., & Hamann, M. S. (1982). A network approach to mental multiplication. *Journal of Experimental Psychology: Learning, Memory, and Cognition*, 8(4), 320–335. <http://doi.org/10.1037/0278-7393.8.4.320>
- Sternberg, S. (1969). The discovery of processing stages: Extensions of Donders' method. *Acta Psychologica*, 30, 276–315. Retrieved from <http://www.sciencedirect.com/science/article/pii/0001691869900559>

- Sternberg, S. (2013). The meaning of additive reaction-time effects: some misconceptions. *Frontiers in Psychology*, 4. <http://doi.org/10.3389/fpsyg.2013.00744>
- Stoianov, I., & Zorzi, M. (2012). Emergence of a “visual number sense” in hierarchical generative models. *Nature Neuroscience*, 15(2), 194–196. <http://doi.org/10.1038/nn.2996>
- Stokes, M. G. (2015). “Activity-silent” working memory in prefrontal cortex: A dynamic coding framework. *Trends in Cognitive Sciences*. <http://doi.org/10.1016/j.tics.2015.05.004>
- Stokes, M. G., Wolff, M. J., & Spaak, E. (2015). Decoding Rich Spatial Information with High Temporal Resolution. *Trends in Cognitive Sciences*. <http://doi.org/10.1016/j.tics.2015.08.016>
- Tanenhaus, M. K., Spivey-Knowlton, M. J., Eberhard, K. M., & Sedivy, J. C. (1995). Integration of visual and linguistic information in spoken language comprehension. *Science (New York, N.Y.)*, 268(5217), 1632–1634.
- Tang, C., Hamilton, L. S., & Chang, E. F. (2017). Intonational speech prosody encoding in the human auditory cortex. *Science*, 355(801)(August), 797–801. <http://doi.org/10.1126/science.aam8577>
- Taulu, S., & Simola, J. (2006). Spatiotemporal signal space separation method for rejecting nearby interference in MEG measurements. *Physics in Medicine and Biology*, 51(7), 1759–1768. <http://doi.org/10.1088/0031-9155/51/7/008>
- Thomas, H. B. G. (1963). Communication theory and the constellation hypothesis of calculation. *Quarterly Journal of Experimental Psychology*, 15(3), 173–191. <http://doi.org/http://dx.doi.org/10.1080/17470216308416323>
- Tomonaga, M., & Matsuzawa, T. (2002). Enumeration of briefly presented items by the chimpanzee (*Pan troglodytes*) and humans (*Homo sapiens*). *Animal Learning & Behavior*, 30(2), 143–157. <http://doi.org/10.3758/BF03192916>
- Tosoni, A., Galati, G., Romani, G. L., & Corbetta, M. (2008). Sensory-motor mechanisms in human parietal cortex underlie arbitrary visual decisions. *Nature Neuroscience*, 11(12), 1446–1453. <http://doi.org/10.1038/nn.2221>
- Trübutschek, D., Marti, S., Ojeda, A., King, J.-R., Mi, Y., Tsodyks, M., & Dehaene, S. (2017). A

- theory of working memory without consciousness or sustained activity. *eLife*, 6, 1–46. <http://doi.org/10.7554/eLife.23871>
- Uittenhove, K., Thevenot, C., & Barrouillet, P. (2016). Fast automated counting procedures in addition problem solving: When are they used and why are they mistaken for retrieval? *Cognition*, 146, 289–303. <http://doi.org/10.1016/j.cognition.2015.10.008>
- Van Den Berg, R., Anandalingam, K., Zylberberg, A., Kiani, R., Shadlen, M. N., & Wolpert, D. M. (2016). A common mechanism underlies changes of mind about decisions and confidence. *eLife*, 5(FEBRUARY2016). <http://doi.org/10.7554/eLife.12192>
- Varoquaux, G. (2017). Cross-validation failure: Small sample sizes lead to large error bars. *NeuroImage*. <http://doi.org/10.1016/j.neuroimage.2017.06.061>
- Verguts, T., & Fias, W. (2004). Representation of Number in Animals and Humans: A Neural Model. *Journal of Cognitive Neuroscience*, 16(9), 1493–1504. <http://doi.org/10.1162/0898929042568497>
- Visscher, A. De, Berens, S. C., Keidel, J. L., Noël, M., Bird, C. M., De Visscher, A., ... Bird, C. M. (2015). The interference effect in arithmetic fact solving: An fMRI study. *NeuroImage*, 116, 92–101. <http://doi.org/10.1016/j.neuroimage.2015.04.063>
- Viswanathan, P., & Nieder, A. (2013). Neuronal correlates of a visual “sense of number” in primate parietal and prefrontal cortices. *Proceedings of the National Academy of Sciences*, 110(27), 11187–11192. <http://doi.org/10.1073/pnas.1308141110>
- Voytek, B., Kayser, A. S., Badre, D., Fegen, D., Chang, E. F., Crone, N. E., ... D'Esposito, M. (2015). Oscillatory dynamics coordinating human frontal networks in support of goal maintenance. *Nature Neuroscience*, 18(9), 1318–1324. <http://doi.org/10.1038/nn.4071>
- Walsh, V. (2003). A theory of magnitude : common cortical metrics of time , space and quantity. *Trends in Cognitive Sciences*, 7(11), 483–488. <http://doi.org/10.1016/j.tics.2003.09.002>
- Wolff, M. J., Jochim, J., Akyürek, E. G., & Stokes, M. G. (2017). Dynamic hidden states underlying working-memory-guided behavior. *Nature Neuroscience*, 20(6), 864–871. <http://doi.org/10.1038/nn.4546>
- Wynn, K. (1992). Addition and subtraction by human infants. *Nature*, 358(6389), 749–750.

<http://doi.org/10.1038/358749a0>

Yeo, D. J., Wilkey, E. D., & Price, G. R. (2017). The search for the number form area: A functional neuroimaging meta-analysis. *Neuroscience and Biobehavioral Reviews*.

<http://doi.org/10.1016/j.neubiorev.2017.04.027>

Zbrodoff, J. N., & Logan, G. D. (2005). What everyone finds: the problem size effect. In J. I. D. Campbell (Ed.), *The Handbook of Mathematical Cognition* (pp. 331–345). New York: Psychology Press.

Zgonnikov, A., Aleni, A., Piironen, P., O'Hora, D., & di Bernardo, M. (2017). Visualising decision landscapes using mouse-tracking data. *PsyArXiv*.

Zimmerman, F., Shalom, D., Gonzalez, P. A., Garrido, J. M., Heduan, F. A., Dehaene, S., ... Rieznik, A. (2016). Arithmetic on your phone: A large scale investigation of simple additions and multiplications. *PLoS ONE*, 11(12), 1–15. <http://doi.org/10.1371/journal.pone.0168431>

Zorzi, M., Priftis, K., & Umiltà, C. (2002). Brain damage: Neglect disrupts the mental number line. *Nature*, 417(6885), 138–139. <http://doi.org/10.1038/417138a>